



UiT The Arctic University of Norway

Department of Chemistry

Computer Simulation of Antimicrobial Agents

-

Tonje Reinholdt Haugen

KJE-3900 Master's Thesis in Molecular Science, October 2021

Abstract

The last 18 months has shown the impact a single microorganism can have on society with the SARS-CoV-2 virus. This is not the only global threat on our health, with the World Health Organisation and other government agencies warning against the increase in antimicrobial resistance today. Antimicrobial peptides have been seen as a possible solution, as they are known to fight bacteria as a part of the immune system and there is a high variety of molecules.

This thesis uses molecular dynamic simulation to look into two different cyclic peptides, mrs-002 and tkbs-013, as possible antimicrobial peptides to determine their interactions and effects on a POPE:POPG lipid bilayer membrane. Different systems were set up for this thesis for conformational analysis of the peptides and to investigate the peptide-membrane interactions and their effect on the membrane themselves.

It was found that the mrs-002 and tkbs-013 was most likely biologically active from their interactions and the effects than had, with mrs-002 having stronger interactions and effects overall. Visual analysis of the interactions and positions of the peptides suggested the mrs-002 peptide either using the barrel-stave or the toroidal method as mode of attack, while the tkbs-013 peptide seemed to suggest a combination of the carpet and the barrel-stave or toroidal method against the lipid bilayer. Their conformational analysis showed that the mrs-002 had some sterical hindrance compared to tkbs-013, but that none of the peptides seem to favour any secondary structure.

Acknowledgements

I would first like to thank my supervisor Bjørn Olav Brandsdal for support and guidance writing this thesis and during my 5 years of education. I would also like to thank my co-supervisor Laura Liikanen for your guidance and help I have received.

I would also like to thank my parents, Ann Kristin and Tore for believing and supporting me.

Last, but certainly not least I would like to thank my friends, Marte, Martine, Siri and Veronica. Thank you for interesting discussion, encouragements and support you have given me.

Contents

Abstract	i
Acknowledgements	iii
1 Introduction	1
1.1 Antimicrobial resistance	1
1.2 Antimicrobial peptides	2
1.2.1 Cyclic antimicrobial peptides	4
1.3 Biological Membranes	6
1.4 Force fields	8
1.5 Statistical mechanics	10
1.6 Molecular Dynamics	12
1.7 Biological simulations	14
1.7.1 Simulation of lipid bilayer	15
2 Method	17
2.1 Preparation of the peptide molecules and the membrane	17
2.2 Simulation of the systems	18
2.3 Analysis of the systems	19
3 Results and Discussion	21
3.1 Peptide conformation	21
3.2 Peptide interaction	23
3.3 Peptide effect on membrane	34

4 Conclusion	45
4.1 Future work	46
Bibliography	47
A Conformation of peptide in end of peptide-only simulations	53
B Position and orientation of peptide in membrane	55
C Position of peptide in xy-plane during simulation	57
D Area per lipid	61
E Calculated average membrane thickness during simulation	67
F Calculated variance of membrane thickness for peptide+membrane and membrane-only systems.	73
G Calculated S_{CD} for peptide+membrane and membrane-only systems	79

List of Figures

1.1	<i>Different modes of attack from antibacterial peptides on a lipid bilayer. The figure is adapted from Brodgen [5]</i>	3
1.2	<i>Two cyclic peptides used in the systems for this thesis.</i>	5
1.3	<i>PE and PG lipids, commonly the main components of the inner lipid bilayer found in bacterial membrane. Figure adapted from Spooner [20]</i>	7
1.4	<i>Figure showing how the membrane constructed by Hong et al changed during their simulation with a more uniform distribution of lipids and separated into small areas of certain lipids. Figure taken from Hong [17]</i>	16
3.1	<i>Final conformation on the simulations from one of the parallels run with peptide-only systems.</i>	23
3.2	<i>Comparison of z-coordinates in the lipid bilayer membrane and peptide in the different simulations.</i>	24
3.3	<i>Position of peptide within the membrane showing how the different peptides have inserted themselves into the membrane</i>	26
3.4	<i>Position of the peptide from the third parallel of tkbs-013 in the end of simulation</i>	29
3.5	<i>Plots showing xy-position of the peptide over the simulation, from 0ns to 260ns. Larger versions of these plots for more details can be found with the appendix.</i>	30
3.6	<i>Area per lipid plots for the 1st parallel of the membrane-only and peptide-membrane systems.</i>	36
3.7	<i>Calculated mean thickness for membrane.</i>	40

3.8	<i>Calculated map of average thickness of the membrane during the simulation in the xy-plane with red indicating higher values and blue lower.</i>	41
A.1	<i>Conformation of the different peptides in all peptide-only simulations run. All figures rendered from end of simulation.</i>	54
B.1	<i>Position and orientation of the peptides in the different peptide-membrane simulations. All figures rendered in the end of simulation, at 260ns.</i>	56
C.1	<i>Position of the peptide in the xy-plane for the different peptide-membrane simulations. The overview of the colours corresponding to the time can be seen before the first plot.</i>	60
D.1	<i>Calculated area per lipid for both peptide+membrane and membrane-only systems. This includes calculations for POPE, POPG and for all lipids in the system over the simulation.</i>	66
E.1	<i>Calculated average thickness of the membrane over the simulation period for peptide+membrane and membrane-only systems.</i>	72
F.1	<i>Calculated membrane thickness for simulation period, with variation from average shown in red and blue. The figures are calculated from peptide+membrane and membrane-only system simulations.</i>	78
G.1	<i>Calculated S_{CD} values for the POPE lipid in the membrane for all peptide+membrane and membrane systems.</i>	84
G.2	<i>Calculated S_{CD} values for the POPG lipid in the membrane for all peptide+membrane and membrane systems.</i>	89
G.3	<i>Calculated S_{CD} values for all lipids in the membrane for all peptide+membrane and membrane systems.</i>	94

Chapter 1

Introduction

1.1 Antimicrobial resistance

The SARS-CoV-2 virus has shown how much of an impact microorganisms can have on society when there are no safeguards and the human body is not capable of fighting them properly. Not only was hospitals overrun in several nations with the health care system desperate to get treatment for the patients, there has also been struggles with the worlds supply chain, making everything from electric car production to clothing brands such as Nike struggling to supply consumers [16]. While the Covid-19 pandemic might be an extreme case, the World Health Organisation (WHO) included antimicrobial resistance in a 2020 list of urgent health challenges for this decade, stating that it is a threat to modern medicine [39]. The UN has also made a call on action for antimicrobial resistance, calling it 'the silent tsunami' [34].

There are several ways that antimicrobial resistance can develop and understanding them may help develop novel antibiotics and medicine to help fight against antimicrobial resistance. There are many ways for bacteria to develop antimicrobial resistance, with some bacteria even having the genes for resistance inherently, but using gene amplification they end up with enough of the gene to end up becoming resistant. It can also happen with modification of the RNA, a process that does happen naturally in all cells, including

human cells. Bacteria has also the ability of horizontally transfer genes between different species, meaning if one species ends up resistant against antimicrobes, it can share this to other bacteria as well, not only the 'offspring' [9]. Adding on to the mechanisms of how bacteria naturally form antimicrobial resistance, there are several studies showing that there is a correlation between antibiotics used and the antimicrobial resistance found in bacteria, such as in *E. coli* and *S. pneumoniae* [11]

Selective pressure from medicine use and the host immune systems are ways for the bacteria to develop antimicrobial resistance and it is important to note that these resistant bacteria move between places and species. The usage of antibiotics in livestock not only for treatment, but also as growth promotion, may give unnecessary selective pressure and end up developing more resistant bacteria than necessary. This problem with livestock and antimicrobial resistant bacteria is not only affecting people who eat meat from livestock, as it can easily spread from livestock to farm workers and into society, if the disease is zoonotic [38]. As seen with the SARS-CoV-2 virus, foreign travel can also aid in the spread of antimicrobial resistant strains of bacteria, meaning that this is not only a local problem, but a global one. This means that individual countries cannot do all of the solution solving, but like with global warming, a global solution would be needed to properly combat this problem [32].

1.2 Antimicrobial peptides

Antimicrobial peptides and proteins (AMPs) have been found to be a ubiquitous part of the immune system, found in animals, plants and bacteria [3]. The difference between the antimicrobial peptides and proteins is their size, with antimicrobial peptides historically being characterised with around 12-60 amino acids and under 10 kDa. Proteins on the other hand can be much larger and heavier than peptide, even including several amino acid chains. While this thesis will focus on how AMP, specifically antimicrobial peptides,

impact bacteria, it is important to note that they are a part of the immune system against fungi, virus, yeast and other biological attacks as well [41].

Antimicrobial peptides discovery most likely started with peptides from plants followed by animals in the 1960s, even if the first AMP was reported in 1920 by Sir Alexander Fleming. Several decades of analysing and categorising AMPs has given scientists some characteristics that may help when identifying AMPs. The first as mentioned before, is that the peptides themselves are usually very small, and when they fold they tend to end up in one of three different categories based on their secondary structure, 1) α -helical; 2) β -sheet and 3) extended AMPs. The secondary structures defining the first two categories may not form in aqueous solution, but the folds are adapted in non-polar environments, like in a cell membrane. The third category does not have a secondary structure element in common, but is recognised from having a high content of a specific residue, such as histidine or tryptophan [42]. Most characterised peptides are also cationic and this may be essential to interact with the electronegative membrane in fungi and bacteria [41]. This wide variety and amount of possibilities within AMPs means that there are plenty of possibilities for novel structures and usages.

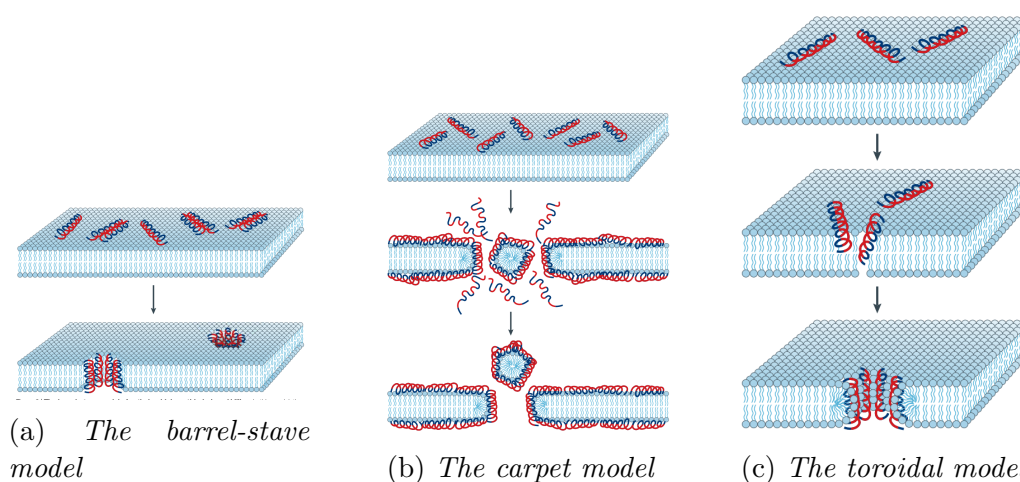


Figure 1.1: *Different modes of attack from antibacterial peptides on a lipid bilayer. The figure is adapted from Brodgen [5]*

Antimicrobial peptides are a diverse group, not only structurally, but also with their modes of action. Antibacterial peptides are cationic and is dependent on cell wall or cell membrane interaction along with a high ratio of hydrophobic amino acids. This combination of hydrophobic amino acids and positive charge(s) makes them ideal for the negative cell membrane that is found in bacteria membrane. This initial interaction with the membrane either leads to the peptide disrupting the cell membrane or the peptides entering the bacteria to act as an inhibitor for a function inside of the cell. [42]. It has been suggested that the disruption of the cell membrane can happen in several different ways as seen in figure 1.1. The barrel-stave model suggests that the peptides aggregate and creates a tunnel through the membrane, with hydrophobic amino acids against the membrane and hydrophilic amino acids in the interior of the tunnel, marked in blue and red respectively. The second model called 'the carpet model' suggests that the peptides 'carpet' the lipid bilayer and can end up isolating smaller regions of the membrane. This isolation of the membrane as seen in figure 1.1b depend on the interactions between the lipids and the peptide as well as how the lipids are structured in the membrane. The third model is 'the toroidal model' and may look similar to the barrel-stave model, however there are some differences. The peptides aggregate to make a 'tunnel' through the membrane, but unlike the first model, the lipid heads follow with, creating a lipid monolayer that bend 180 degrees, with the peptide still inserted in the membrane, instead of acting as a protective layer between the membrane and the interior of the tunnel [5].

1.2.1 Cyclic antimicrobial peptides

While AMP can be of great help within drug design and the development of new drugs such as new antibiotics, there are several problems with AMPs. It has been found that they have low bioavailability with oral ingestion of the peptides and a rapid degradation, making them hard for mass production and for use in prescription drugs [24]. One possible solution to this has been cyclic peptides as some have been known to have a stronger secondary structure with higher biological activity [8]. It is also known that some cyclic

peptides such as cyclic lipopeptides have shown to be more stable than their linear counterparts [7].

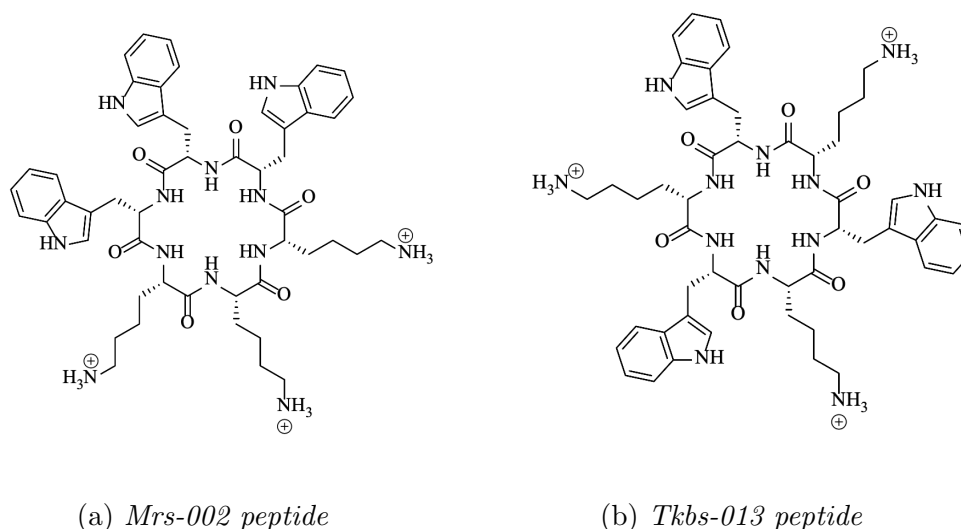


Figure 1.2: Two cyclic peptides used in the systems for this thesis.

The two AMPs used in this thesis are two cyclic peptides with the same amino acids, but in different configurations as seen in figure 1.2. They both consists of 6 residues, three tryptophan and three ionised lysine. The first structure, *mrs-002* has one 'side' of lysine and another of tryptophan, meaning they are concentrated on each side. The other structure, called *tkbs-013*, has an even spread of the two amino acids and both of the peptides has a net +3 charge from the +1 charge for each ionised lysine. This means that *mrs-002* have a higher concentration of positive charge on one side of the peptide, whilst the positive charge in *tkbs-013* is more in an even ring around the peptide as the lysine is spread evenly. Experimental data from MIC tests shows that *mrs-002* has higher biological activity compared to *tkbs-013* as shown in table 1.1 [31]

Table 1.1: Values from MIC tests for mrs-002 and tkbs-013 against different bacteria. The values are given in $\mu\text{g}/\text{ml}$ and taken from [31]

	S.aureus	E.coli	B.subtilis	P.aeruginosa
mrs-002	32	8	4	32
tkbs-013	128	64	32	NA

1.3 Biological Membranes

Biological membranes can be seen surrounding all cells, and consists mainly of lipids, amphiphatic molecules that form into a bilayer due to the hydrophobic effect. All lipids in such layers has a hydrophilic end and a hydrophobic end, with the hydrophilic ends being on the 'outside' of the membrane and the hydrophobic making the interior of the membrane [1]. The lipid bilayer is a permeable barrier between the cytoplasm inside the cell and the exterior and there are complex reactions with both sides of the membrane, for such things like signalling or making sure only the 'correct' molecules pass the membrane. In the lipid bilayer there has also been found membrane proteins that has many functions, from signalling between the exterior and the interior of the cell and scaffolding to bending and forming the membrane topology along with the lipids [25].

The lipids used in membranes are called phospholipids, lipids with a hydrophilic 'head' which include a phosphate group and two hydrophobic 'tails' that are derived from fatty acids, thus mainly consisting of hydrocarbon chains with single and double bonds. Phospholipids are found to be either neutral or negative in charge at neutral pH, depending on the phosphate acid precursor. There are 5 major headgroups found in biological membranes, with the precursors being choline and ethanolamine forming neutral headgroups and the serine, inositol and glycerol precursors forming negative headgroups, with hundreds of other types of lipids also found in membranes. The combination of the different lipids, plus the difference in the lipid tails makes a big difference for the different membranes and the concentration can help certain interactions happen at certain places at the membrane topology [27]. Approx 50% of mammalian cells consists of lipids

and they are typically a combination of several different lipids and the rest of the membranes consisting of proteins, sterols and other molecules. Eukaryotic or bacterial membranes typically consists of mainly one or two types of lipids along with some proteins and other lipids, though not near the variety seen in mammalian membranes. Two important lipids to note in this thesis are phosphatidylglycerols (PGs) and phosphatidylethanolamines (PEs) [29]. PGs are unique as glycerol has structural properties to mimic water and help more than just be a negative charge in the membrane. The combination of these two lipids are common in the inner membrane bilayer of bacteria. [27]

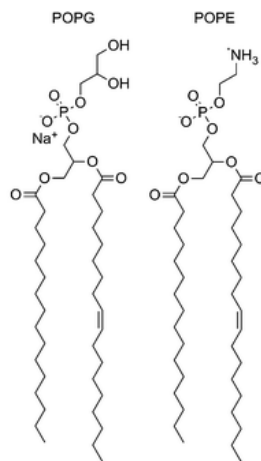


Figure 1.3: *PE and PG lipids, commonly the main components of the inner lipid bilayer found in bacterial membrane. Figure adapted from Spooner [20]*

Not all bacteria has the same structure in their membrane as there are two distinct groups of bacteria that can be differentiated by a Gram test, called Gram-positive and Gram-negative. A Gram-negative bacteria has a membrane consisting of three distinct layers, with an outer and inner lipid bilayer and a peptidoglycan layer between them. It is usually this inner membrane that mainly consists of PG and PE lipids. A Gram-positive membrane does not have the outer lipid bilayer, only the inner one. Usually a Gram-positive cell has a higher concentration of PG-lipids, while PE lipids have been found in higher concentration in Gram-negative membranes [10].

1.4 Force fields

Using computers to calculate and model chemical reactions and interactions can give a new or more detailed perspective on how the mechanisms work compared to traditional analysis methods used. However, it is then important to be familiar with the mathematics, physics and chemistry behind these models to know where the simulations may fail or where one might benefit from using such models. When looking at larger systems, something typical in biological simulations including lipid bilayers and proteins, empirical models called force fields from molecular mechanics are employed. This is a simplification based on the Born-Oppenheimer approximation, making it possible to write the energy of the system as a function of the nuclear coordinates [21].

The force field calculations used in molecular mechanics are based on the nuclear coordinates, with all force fields using the same basic equation and then having different specialisations with different focuses depending on additional terms. The basic equation (equation 1.1), shows different terms describing the chemical bond length, the angles between the bonds, the torsion around the bonds and the non-bonded forces, described using Coulomb's law and a 12-6 Lennard-Jones potential.

$$\begin{aligned}
 U(\mathbf{r}^N) = & \sum_{bonds} \frac{k_i}{2} (l_i - l_{i,0})^2 + \sum_{angles} \frac{k_i}{2} (\theta_i - \theta_{i,0})^2 + \sum_{torsions} \frac{V_n}{2} (1 + \cos(n\omega - \gamma)) \\
 & + \sum_{i=1}^N \sum_{j=i+1}^N (4\epsilon_{ij} [(\frac{\sigma_{ij}}{r_{ij}})^{12} - (\frac{\sigma_{ij}}{r_{ij}})^6] + \frac{q_i q_j}{4\pi\epsilon_0 r_{ij}})
 \end{aligned}
 \tag{1.1}$$

The first term in equation 1.1 explains the chemical bonds of the system and the stretching that happens between two atoms. This form comes from a Taylor series between a reference length ($l_{i,0}$) and the calculated length (l_i) of the bond. It usually only contains the first and second-order from

the series, with the first order term being equal to 0. It also includes a force constant k_i , and is in the form of a harmonic oscillator, meaning the calculated energy will be most realistic with relaxed chemical bonds. This is based on Hooke's law from physics, saying that the force is proportional to the elongation of a spring. While using Hooke's law may not be as accurate as the full Taylor series, it makes the computational power and time needed lower than computations using higher order terms [40].

The second term explains the angles between two bonds, A-B and B-C, again from a Taylor series with only the second-order term in the form of a harmonic oscillator. It includes a reference angle ($\theta_{i,0}$), a calculated angle (θ_i) and a force constant for the angle itself.

The third term describes the torsion around the chemical bonds, with the torsional angle, ω , the 'barrier height' V_n , the multiplicity, n and the phase factor γ . The torsional angle is easy to understand, but the barrier height gives an indication on how 'difficult' it is to rotate the bond. The multiplicity is how many minima there is in a energy function from the bond being rotated 360° with the phase factor describing where the global minima is in the same function. All these variables are expressed in a cosine series expansion as shown in equation 1.1, using only the first term, however there are certain bonds where it is necessary to include higher order terms for a better accuracy, one example being simulation of DNA.

The last term in equation 1.1 tries to describe the non-bonded forces in a molecule, such as the electrostatic effect and the van der Waals forces. In this equation, a combination of Coulombs law and the Lennard-Jones 12-6 potential is used. Coulombs law describes the electrostatic forces between two net atomic charges and it is often only the lowest charge with non-zero moment that is included in this calculation, meaning that an ion such as Na^+ only includes the charge q , but uncharged molecules may have the dipole, μ , in their calculation. The Lennard-Jones 12-6 potential describes the van der Waals interactions and tries to balance the repulsive and attractive forces depending on the distance between the atoms. The collision diameter, σ ,

and well depth, ϵ , are the major variables determining the 'ideal' distance between the atoms and where the attractive and repulsive forces are in a balance with each other.

With the terms not being a strict set, it is possible to specialize certain force fields and the terms included, such as the MM2 force field mostly being used for small organic molecules [2]. Cross terms, a term in the force field that reflects the coupling between the coordinates may also be included if there are certain properties that one wishes to calculate, such as the vibrational frequency of a system or molecule [21].

1.5 Statistical mechanics

While force field calculates the potential energy of the system, this is on a microscopic level, meaning that it does not translate well over to a macroscopic sample and makes it hard to have the system in realistic conditions. Statistical mechanics is a field in physics that makes it possible to connect the microscopic level with the macroscopic and tries to calculate thermodynamic properties of a system. One example in statistical mechanics is the correlation between the average kinetic energy and the temperature seen in equation 1.2 [19].

$$\langle E_k \rangle = \frac{3}{2}RT \quad (1.2)$$

Using statistical mechanics with a probabilistic model makes it possible to calculate thermodynamical properties of a system. Each particle can be described using the position \mathbf{r}^N and momentum \mathbf{p}^N by giving them a defined state $\mathbf{p}^N \mathbf{r}^N$ for the $6N$ space in the system, with N representing each particle in the system. At temperature T , each particle has a certain probability of being in a state with energy ϵ , and this can be seen as a Boltzmann factor $e^{(-\epsilon/kT)}$. A partition function that sums all possible states of the systems as seen in equation 1.3, makes it possible to calculate the macroscopic functions.

$$q = \sum_{k=1}^N e^{(-\epsilon_i/kT)} \quad (1.3)$$

The partition function can be used to normalise the energy distribution of the system, making the function into a Boltzmann distribution. The energy of the system can also be described as dependent on the momentum and position of each particle, meaning that the Boltzmann probability distribution can then be written as:

$$\rho(\mathbf{p}^N, \mathbf{r}^N) = q^{-1} \cdot e^{(-E(\mathbf{p}^N, \mathbf{r}^N)/kT)} \quad (1.4)$$

Calculating the time average of equation 1.4 requires much longer simulations than one can calculate without spending years on said calculations. However in statistical mechanics it is thought that a time average of a property is equal to the ensemble average of the same property at equilibrium. This makes it possible to calculate the average of said property as molecular dynamics simulations produces an ensemble average over time with a certain number of atoms. The time average initially used can then be replaced by the calculated ensemble average by using equation 1.5, a multi-variable integral over the $6N$ space with weighted probabilities for all N particles [19][21].

$$\langle A \rangle = \iint d\mathbf{p}^N d\mathbf{r}^N A(\mathbf{p}^N, \mathbf{r}^N) \rho(\mathbf{p}^N, \mathbf{r}^N) \quad (1.5)$$

Using equation 1.5 to calculate the average for a property in the system, makes it then possible to control the energy, and thus the thermodynamical properties of the system itself. This is because in thermodynamics it is stated that the equation of state of the system can be described by the relationship between thermodynamic parameters in the system. This means if one sets the temperature (T), volume (V), pressure (P) and particles (n) as the fundamental thermodynamical parameters of the system, it then follows

that the relationship can be described as:

$$g(n, P, T, V) = 0 \quad (1.6)$$

Using this relationship between the different parameters and setting the different parameters as constants means that the ensemble calculated can calculate its energy. One example is the NTP ensemble used in this thesis, where the temperature, pressure and particles are constant while the volume can change. This makes it an isothermal-isobaric ensemble and it just one of many types of ensembles found in statistical mechanics [33].

1.6 Molecular Dynamics

While force fields and statistical mechanics can help with simulations in chemistry, it is only computed for that instant, meaning reactions and interactions between molecules over time is not a part of the calculations. Molecular dynamics, the use of successive configurations of the system integrated from Newton's laws of motion can make the simulation happen over time. Newton's laws state [40]:

1. A body acted on by no net force has a constant velocity and zero acceleration

$$\Sigma \mathbf{F} = 0 \rightarrow \frac{d\mathbf{v}}{dt} = 0 \quad (1.7)$$

where \mathbf{v} is the velocity of the particle.

2. The rate of change of a particles linear momentum is directly proportional to the net force acting on said particle.

$$\Sigma \mathbf{F} = \frac{d\mathbf{p}}{dt} = m \frac{d\mathbf{v}}{dt} \quad (1.8)$$

where \mathbf{p} is the momentum of the particle.

3. To every force, there is an equal and opposite directed counterforce.

$$\mathbf{F}_{AB} = -\mathbf{F}_{BA} \quad (1.9)$$

It is especially Newton's second law (equation 1.8) with the use of differential equation that helps with calculating the trajectories of the particles in the simulated system. The simplest molecular dynamics model by Alder and Wainwright in 1957 can be broken into 4 steps.

1. Identifying the spheres that are to collide based on current trajectories and calculate when this collision will occur
2. Calculate the position of all the spheres in the system at time of collision
3. Determine the new velocity of the colliding spheres after the collision
4. Repeat until simulation is complete

While this algorithmic approach can work for simulations, there are more realistic methods including the change in forces on each particle as the positions are changed with the use of continuous potentials, with the equations of motion being integrated using finite difference method. The molecular dynamics algorithms that integrates with the finite difference method, also assumes that the position and dynamics properties such as velocity and acceleration, can be expressed using Taylor series expansions, shown in equations 1.10a - 1.10d, for position, \mathbf{r} , velocity, \mathbf{v} , acceleration, \mathbf{a} , and the third and fourth derivative of position, \mathbf{b} and \mathbf{c} .

$$\mathbf{r}(t + \delta t) = \mathbf{r}(t) + \delta t \mathbf{v}(t) + \frac{1}{2} \delta t^2 \mathbf{a}(t) + \frac{1}{6} \delta t^3 \mathbf{b}(t) + \frac{1}{24} \delta t^4 \mathbf{c}(t) + \dots \quad (1.10a)$$

$$\mathbf{v}(t + \delta t) = \mathbf{v}(t) + \delta t \mathbf{a}(t) + \frac{1}{2} \delta t^2 \mathbf{b}(t) + \frac{1}{6} \delta t^3 \mathbf{c}(t) + \dots \quad (1.10b)$$

$$\mathbf{a}(t + \delta t) = \mathbf{a}(t) + \delta t \mathbf{b}(t) + \frac{1}{2} \delta t^2 \mathbf{c}(t) + \dots \quad (1.10c)$$

$$\mathbf{b}(t + \delta t) = \mathbf{b}(t) + \delta t \mathbf{c}(t) + \dots \quad (1.10d)$$

One of the most used algorithms is the Verlet algorithm that uses the position and acceleration at time, t , plus the positions from the last timestep,

$t - \delta t$ to calculate the positions at the new timestep, $t + \delta t$.

$$\mathbf{r}(t + \delta t) = \mathbf{r}(t) + \delta t \mathbf{v}(t) + \frac{1}{2} \delta t^2 \mathbf{a}(t) + \dots \quad (1.11a)$$

$$\mathbf{r}(t - \delta t) = \mathbf{r}(t) - \delta t \mathbf{v}(t) + \frac{1}{2} \delta t^2 \mathbf{a}(t) - \dots \quad (1.11b)$$

$$\mathbf{r}(t + \delta t) = 2\mathbf{r}(t) - \mathbf{r}(t - \delta t) + \delta t^2 \mathbf{a}(t) \quad (1.11c)$$

Adding equations 1.11a and 1.11b gives equation 1.11c, and to find information on the new velocities for the systems, the difference in positions at the two timesteps if then divided by $2\delta t$.

$$\mathbf{v}(t) = [\mathbf{r}(t + \delta t) - \mathbf{r}(t - \delta t)]/2\delta t \quad (1.12)$$

The Verlet algorithm, does have some flaws, such as adding a small term, $\delta t^2 \mathbf{a}(t)$ and two much larger terms, $\mathbf{r}(t + \delta t)$ and $\mathbf{r}(t - \delta t)$, leading to a possibility of loosing some precision in the calculations, the lack of a velocity term in equation 1.11a and 1.11b makes it hard to obtain the velocity and calculate them. The Verlet algorithm also lack a starting point, the equation relies on a previous step, however this can be solved using Taylor series. The timestep, δt is also important as this is chosen before the simulation can begin. If it is too large one may end up with particles overlapping and too small of a timestep may end up with too long computations, meaning wasted time. However it is important to note that for chemical simulations, operating with timesteps at 10^{-12} s is not too small or too big of a step [21].

1.7 Biological simulations

Simulation of biological systems has a great variety, from small systems like peptides in vacuum to large systems of lipid bilayers in solution. This makes the different techniques used for biological simulations also varied, as one can use quantum mechanics for smaller simulations, while molecular dynamics for larger, more complicated simulations has become prevalent. While MD simulations do work for all different types of biological systems, there are obstacles

such as force field inaccuracies and time consuming computations [4]. This can be seen in this thesis as it includes simulations for a maximum of 260 ns with approx 75 000 atoms, and used a week of cpu-time to complete. To minimise force field inaccuracies, a force field specialised towards biological systems, such as CHARMM is used in this thesis. CHARMM focuses on peptides, proteins and other biological molecules in solvents and membrane environments, making it an ideal force field for such simulations compared to INFF that focuses on organic-inorganic and inorganic-biological system interactions [5] [15]. A problem in general with computational simulations is that while the system may seem to be minimised, it may not be at the global energy minima, but on a local one, 'trapped' in a free energy well that is not representative of how the system would behave in nature [4]

1.7.1 Simulation of lipid bilayer

Simulations of large biological systems may be harder compared to smaller molecules and systems, both in computational time needed to compute the simulations, but also in finding a proper structure that is representative of how it is in nature. Finding a structure of a lipid bilayer that is hydrated and biologically relevant is hard due to the fluctuations of the system that is present in nature. These fluctuations are necessary as they are relevant for structure determination and interactions between the lipids. An alternative for this difficulty is to use simulations of an approximate of the wanted lipid bilayer, constructing it from the start with relevant lipids and lipid concentrations. This do take a lot of time and these structures are no better than the force fields used for the structures [26].

This thesis uses a lipid bilayer that has been constructed by Hong et al [17], where they calibrated two different systems. The one chosen for this thesis was a combination of POPE:POPG (3:1) (figure 1.4) calibrated with a NaCl concentration at 0.15 M as it was seen as most biologically relevant for the human body. They simulated the system for 12 μ s or 12000 ns, much longer than any simulations done in this thesis. This made the lipid bilayer

have a more uniform distribution of the different lipids compared to having concentrated areas of each peptide. It is also known that the inner membrane of bacteria is mainly composed of POPE and POPG, making this membrane system a good representation for real bacteria [17]

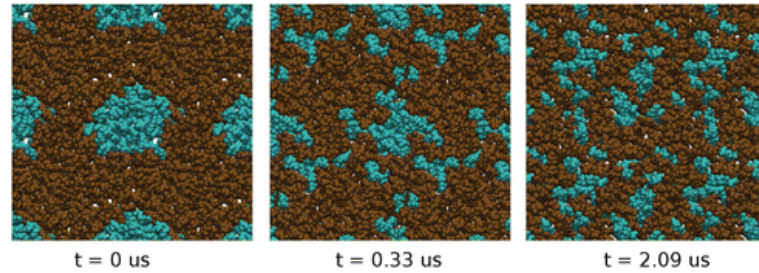


Figure 1.4: *Figure showing how the membrane constructed by Hong et al changed during their simulation with a more uniform distribution of lipids and separated into small areas of certain lipids. Figure taken from Hong [17]*

Chapter 2

Method

2.1 Preparation of the peptide molecules and the membrane

The two peptides used in this thesis, mrs-002 and tkbs-013-2, were constructed in Maestro v.2020-1 and energy minimised using opl-2005 in water with different starting-conformations to find the most stable that was used for the different peptides [30]. The corresponding topology-files for the conformations was made using CGenFF v.4.0 [35]. The lipid bilayer used in this thesis was constructed by Hong et al [17] and was taken from the calibrated model made of POPE and POPG lipids at 0.15 M NaCl concentration. Along with the lipid bilayer, water molecules and ions closer than 4 Å to the lipid bilayer in the original system was extracted along with the lipid bilayer. The combination of the extracted lipid bilayer, water, ions and peptides was done using VMD v.1.9.4a48 [18] and topology files from CHARMM [6] and the generated file from CGenFF. The new system was then re-centered before a layer of water molecules with a width of 20Å in either y-direction of the system was added using tcl-scripting in VMD. The added bulk water molecules was from the TIP3P water model [23] help minimise the computational time needed while still having accurate peptide-water interactions. The water was then ionised using the built-in feature, 'autoionize', in VMD, adding KCl such that the ionic concentration was at approx 0.15 M, getting the system

to correspond to physiological conditions at 315.5 K. Along with the two systems made for each peptide, a system was made with no peptide, only the lipid bilayer, TIP3P water and ions. There was also two systems with peptides, TIP3P water and ions, where the peptides was solvated using 10 Å of TIP3P water in all directions, along with KCl-concentration set at 0.15 M, using the same methods as mentioned with a combination of scripts and VMD.

2.2 Simulation of the systems

5 different systems were simulated, all with 3 parallels each, making it a total of 15 simulations completed for this thesis. The timestep used for all of the simulations was set to 2 fs, making 5 000 000 steps equal to 10 ns real time. When running these systems over all the steps, the output from the simulations was put on 10 ns increments as to prevent too much data being put in a single file. The longest simulations were related to the full systems with both a peptide, the membrane, water and ions, running at a total of 260 ns real time, with the shortest only lasting for 20 ns real time, those being the conformation simulations for the peptides in water as shown in table 2.1. To regulate the total energy of the system, both the pressure and the temperature was kept constant, making use of the isothermal-isobaric ensemble (NPT) known from statistical mechanics. All of the systems was set to use a periodic cell to make sure the peptide could move freely and a cutoff range was set at 12 Å. In the beginning of each calculations, all the systems were also minimised for 10 000 steps to make sure the components put together when preparing the systems was properly behaving and in optimal positions. The simulation was computed using the program NAMD v.2.13[36] sent to a supercomputer because of the high volume of calculations needed for the simulation.

Table 2.1: Overview of how many steps each system was simulated for, they were the same for all parallels for the same system

System	Total steps in simulation	Real time (ns)
mrs-002 w/ lipid bilayer	130 000 000	260
tkbs-013-2 w/ lipid bilayer	130 000 000	260
lipid bilayer	50 000 000	10
mrs-002 w/o lipid bilayer	10 000 000	20
tkbs-013-2	10 000 000	20

2.3 Analysis of the systems

Before the analysis of the systems could begin, wrapping of the trajectory files was done, meaning that the centre of the system was in the same coordinates in all of the saved steps. Only every 500 steps was written in the trajectory files, and when wrapping these trajectory files, only every 5 of the saved steps was wrapped and saved, ending up with 2600 steps in the end. This wrapping and cutting down of frames was completed using CatDCD v4.0 [13] and BigDCD v2 [14].

The analysis of the systems was a bit different depending on what was included in the systems. The systems with only the peptide included only had a visual analysis in VMD to confirm the conformation, whilst calculations of the order parameter of the lipids, area per lipid and the thickness of the membrane was calculated for the systems with a membrane along with a visual analysis. The order parameter, area per lipid and thickness of the membrane was not calculated directly in VMD, but by using an external plugin, called MEMBPLUGIN v1.1 [12]. The systems with both the peptide and the membrane had not only a visual analysis as well as the calculation of order parameter, area per lipid and membrane thickness, but also the z- and xy-position of the peptide compared to the membrane layer was extracted from the trajectory files and plotted using python v3.8.

The order parameter, or S_{CD} calculated is usually derived in NMR analysis of lipids, and calculates the orientational mobility in each C-H bond in the lipid tails, thus giving a measure on the membrane fluidity [37]. MEM-

BPLUGIN calculates the S_{CD} using equation 2.1 with Θ representing the angle between the C-H bond and the reference axis.

$$S_{CD} = \frac{1}{2} \cdot 3\cos^2\Theta - 1 \quad (2.1)$$

The area per lipid calculation in MEMBPLUGIN is both for the individual types of lipids, in this case POPE and POPG, as well as the average for all types of lipids in the membrane. The atoms C2, C21 and C31 was chosen for both lipids, and using these, MEMBPLUGIN uses a Voronoi diagram to calculate the area per lipid. The membrane thickness calculation was a calculation of the average thickness of the membrane over time and a map of the deformation of the membrane in the simulation. This is done measuring the distance between two density points with a plane between them before formalizing them as two mass density profiles of phosphorus. When looking at the deformation of the membrane over the simulation, this is calculated from the lipids head position over the simulation [12].

Chapter 3

Results and Discussion

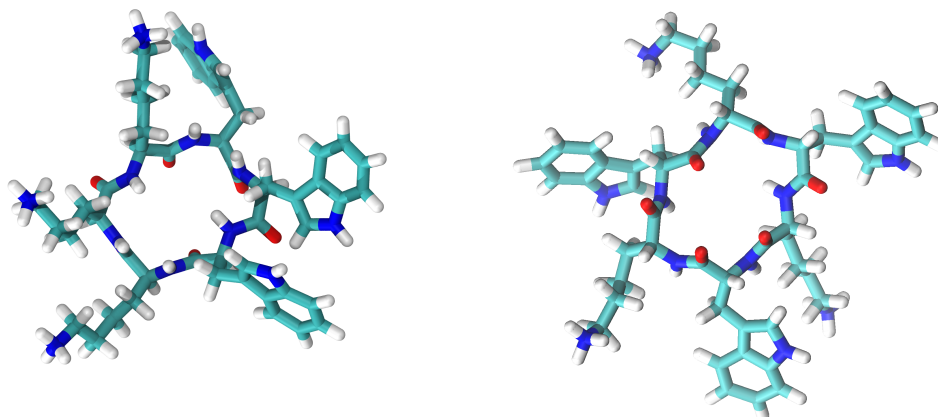
Looking at the systems simulated for this thesis there are many different angles and ways to help determine if the peptides has a possibility of being biologically active. The peptide-only systems may show how the different residues interact with each other and may help to give an indication if the peptides would degrade fast. The interactions between the peptides and lipid bilayer may help see if one can predict if the peptides are biologically active from the simulations and give an indication on their efficiency, at least compared to each other. Looking at the effect of the membrane compared to the membrane-only system may also help discover this.

3.1 Peptide conformation

Before the insertion of the peptides, a minimisation from different starting conformations was done on the peptides. To further make sure that the peptides included into the system was in optimal conformation, two simulations with only water, ions and the peptides was made. The mrs-002 peptides showed in all three parallels that the oxygen on the main chain repelled the side chains of the amino acids, most likely because of the free electrons. This made the tryptophan bend in the other direction and the lysine side chains horizontal compared to the main chain ring. Visual analysis of the simulation for all three parallels showed that the lysine side chains had more freedom

of movement, compared to the tryptophan side chains that had sterical hindrance from their close proximity. The tryptophan could also be prevented from moving too much from the benzene ring, as this may give a small negative charge with the double bonds and thus make the side chains repel each other. Over the course of the simulation, the conformation of the main chain does not change significantly, with mainly the side chains of the amino acids changing, however this is to be expected as they have a higher degree of freedom in the structure itself.

Like the mrs-002 peptide, the tkbs-013 peptide does not undergo any significant change to the peptide that gives an indication that the conformation used in the simulation was disadvantageous for the simulation itself. There were some small changes, such as the main chain changing into a more round frame, but this can also be seen in the peptide-membrane systems as well. One parallel showed 2 possible β -strand with 3 residues each, however this was not seen in the other parallels. Secondary structures does not tend to show up in polar environments and the peptide may end up with a stronger secondary structure when inside the membrane, however for this thesis it is assumed that it is an extended peptide from lack of evidence. Compared to the mrs-002 peptide, the side chains for the tryptophan ends up horizontal compared to the main chain, most likely from the extra space around because of the lysine as the neighbour and other tryptophan. This has given the tryptophan side chains a higher degree of movement compared to the tryptophan in mrs-002 and one can see that the peptide is more flat over time, with some fluctuations up and down. This is also seen in the membrane-peptide system with tkbs-013 with the peptide laying flat on the membrane surface. The structure of tkbs-013 may give all of the side chains a higher degree of freedom as each side chain seem to be pointed in a different direction horizontally as seen in figure 3.1b.



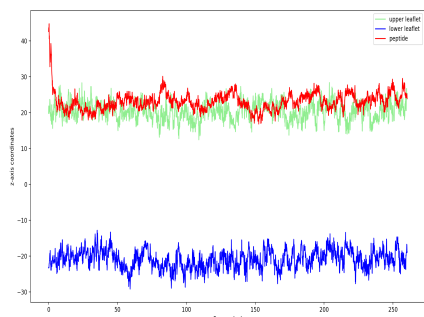
(a) Conformation of *mrs-002* from parallel 3.

(b) Conformation of *tkbs-013* from parallel 3.

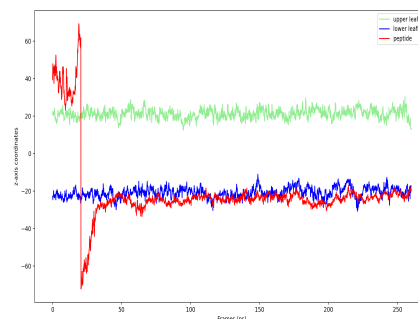
Figure 3.1: Final conformation on the simulations from one of the parallels run with peptide-only systems.

3.2 Peptide interaction

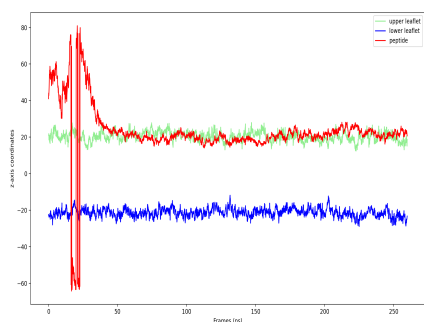
Interactions between the membrane and peptide can be important to help determine if the peptide disrupt the membrane structure. There are several ways of looking into this, such as where along the z-axis the peptide ends up in the simulation compared to the membrane itself, or even how much the peptide moves on the membrane surface or if it end up in one particular spot. This can be done visually, but also with plots showing the data from the simulation giving a overview, and with both types of analysis, this can help determine what types of interactions and how much interactions there is between the membrane itself and the different peptides. This can then further help determine if the peptides may be biologically active and what peptides may be worth continuing in future work. Both lysine and tryptophan are amphiphilic amino acids, however the lysine is in its ionised state in this system, makes it act as positive and polar amino acid. This means that one can expect the lysine to mainly interact with the polar parts of the membrane such as the lipid heads, however the tryptophan can interact with both the lipid heads and the non-polar lipid tails due to its amphiphatic nature.



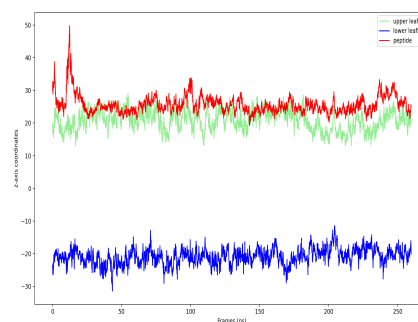
(a) Comparison of z -coordinates in parallel 1 of *mrs-002* simulation



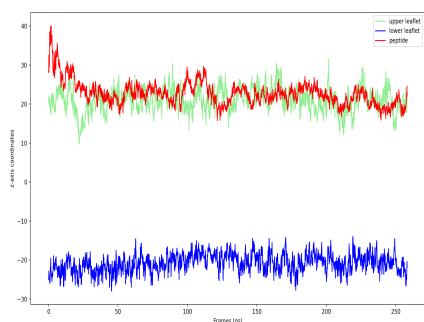
(b) Comparison of z -coordinates in parallel 2 of *mrs-002* system



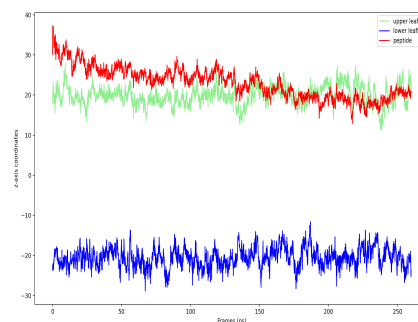
(c) Comparison of z -coordinates in parallel 3 of *mrs-002* system



(d) Comparison of z -coordinates in parallel 1 of *tkbs-013* system



(e) Comparison of z -coordinates in parallel 2 of *tkbs-013* system



(f) Comparison of z -coordinates in parallel 3 of *tkbs-013* system

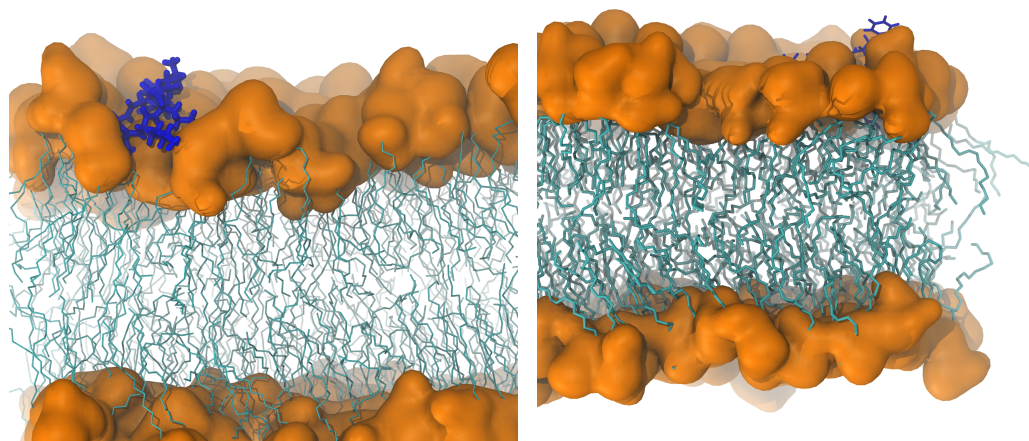
Figure 3.2: Comparison of z -coordinates in the lipid bilayer membrane and peptide in the different simulations.

Looking at figure 3.2a, the mrs-002 peptide seem to move straight down to the membrane itself and mostly surfing on or inserting itself into the membrane. It is important to note that the membrane itself it quite thick compared to the peptide, meaning the plot may not be a completely accurate representation of how deep the peptide itself goes into the membrane. The figures 3.2b and 3.2c show parallel 2 and 3 of the mrs-002 simulations, and here it seems like the peptide suddenly moves through the membrane itself. This comes from the use of a periodic cell, and shows the peptide moving up and out of the cell, thus moving into the cell from the bottom again. This happens once in the 2nd parallel and twice in the 3rd parallel, and may come from how the peptide was inserted with the tryptophan side chains against the membrane before the simulation. This was to prevent the attraction between the positive lysine and the negative membrane surface to interact and help minimise favourable interactions and push the output of the data towards a biologically active peptide artificially.

The parallels for tkbs-013 do have some similarities in how the peptides move compared to the membrane, but there are differences between the different peptides. While an unfavourable position was much easier to find with the uneven distribution of amino acids in mrs-002, this was much harder for tkbs-013, where it ended up in a more horizontal position, making sure no peptide was any closer than the other to the membrane. This may be the reason why all three parallels did not end up going out of the periodic cell like two of the mrs-002 parallels. The 3rd parallel shown in figure 3.2f shows tkbs-013 not really interacting with the membrane itself for almost half the simulation, something that may come from the even distribution of the amino acids in the peptide, making attraction between the membrane and the peptide weaker compared to mrs-002. This weaker attraction between the peptide and the membrane may suggest that the mrs-002 may be more biologically active than tkbs-013. Both peptides seem to have an attraction to the membrane, meaning that while there seem to be a difference, this does not suggest that tkbs-013 is not biologically active. One thing to note for these graphs it that the z-values used for these graphs comes from a single

atom in the peptide and a single atom in the membrane as mentioned in the methods. This may then give a wrong view of how deep the peptide is in the membrane as the membrane does not have an even surface at all times, and the peptide may be a bit deeper into the membrane than it seems.

Visual analysis showing how the peptides interact and inserts themselves into the lipid bilayer, figure 3.3 shows no large difference in how deep the peptides inserts themselves inside the membrane. However, what is not shown in these figures and what can be seen some in figure 3.2, is how the different peptides ended up in the different positions and how much each peptide moved on the membrane surface. This is more clearly shown in figure 3.5, and like figure 3.2, there is a clear difference both peptides and the different parallels.



(a) *Position of parallel 1 of mrs-002 peptide in the end of simulation in membrane*

(b) *Position of parallel 1 of tkbs0-13 peptide in the end of simulation in membrane*

Figure 3.3: *Position of peptide within the membrane showing how the different peptides have inserted themselves into the membrane*

From visual analysis in VMD, the 1st parallel of mrs-002 first interacts with the membrane using two of the lysine side chains. It does not take long before the peptide twists, ending up with all of three tryptophan side chains

interacting with the membrane, and the lysine side chains either laying on the membrane surface or interacting with the water. As this happens, it also shows that the peptide does not move much on the membrane surface, slowly moving from corner to corner as shown in figure 3.5a. Comparing this with figure 3.5b there is a clear difference in how much each of the parallels moving around. The second parallel of mrs-002 moves much more in the beginning of the simulation, and this has several possible explanations. As shown in figure 3.2b, this peptide not only moved in the xy direction of the periodic cell, but also moves up in the z-direction, meaning it interacts with the other leaflet of the membrane than parallel 1. This takes time and when it does interact with the membrane, it is also with two of the lysine side chains. The peptide stays like this for a while, only having two lysine and one tryptophan side chain interacting with the membrane and it does not insert itself into the membrane, only moving on the membrane surface. However, the peptide ends up in a position where the tryptophan ends up inserting itself into the membrane and interacts not only with the lipid heads, but also with the lipid tails. This can also be seen in figure 3.5b where the movement seem to slow down at around 150 ns, and the peptide ends up in the same situation as parallel 1.

Figure 3.5c show that the peptide move in the beginning of the simulation, but this may come from the peptide not interacting with the membrane as it moves in the water shown in figure 3.2c. Comparing the 3rd parallel to the 2nd parallel of mrs-002, the 3rd ends up on the same side of the membrane as it starts at and visual analysis show that the peptides inserts itself much earlier in the simulation, not needing to reorient itself to fit the lower leaf of the lipid bilayer. It also ends up in a similar position as the 1st parallel, including the first interaction being between the membrane and lysine. This may suggest that the peptide needs to be in a certain position with lysine doing the initial interaction followed by tryptophan positioning the side chains down against the membrane to actually insert itself into the membrane. The peptides all started in a position with the tryptophan down as it was expected that the tryptophan would be the least attracted

to the membrane, and while none of the peptides ended up having their first interaction with the membrane with tryptophan, both the 1st and the 3rd parallel did not need to much reorientation before the peptides ended up in the membrane compared to the 2nd parallel. This further suggests that mrs-002 may be biologically active, as all parallels ended up 'attacking' the membrane with the same 'mechanism'.

Figure 3.5d shows that the peptide tkbs-013 interacts with the membrane mainly in the corners of the periodic cell like the 1st parallel of mrs-002. However when comparing it with figure 3.5a, there is more movement of the tkbs-013 peptide, suggesting less or weaker interactions between the peptide and the membrane for tkbs-013 than the mrs-002 peptide. Visual analysis in VMD, shows that it is actually a combination of one lysine and one tryptophan that first interacts with the membrane. After interacting with the membrane, the peptide ends up flat on the membrane surface, moving around and not going any deeper in the membrane itself. As seen in figure ??, the peptide ends up with one tryptophan and two lysine inside the membrane and the other amino acids of the peptide on the membrane surface. The second parallel, shown in figure 3.5e, shows a slightly different picture, with the peptide not ending up only in the corner of the periodic cell, but ends up going back and forth on the x-axis while moving in the negative-y direction. This parallel also has the first interaction between the peptide and the membrane with one tryptophan and one lysine side chain, whilst the rest of the peptide flattens out on the membrane surface. This parallel ends up switching between being horizontal and vertical on the membrane surface, as it moves back and forth on the x-axis. In the end the peptides settles on being flat on the membrane surface, with one tryptophan inside the membrane itself.

In last parallel of tkbs-013 (fig 3.5f) the peptide seems to move less along the membrane surface than the other parallels. Figure 3.5f shows that the peptide staying in the middle of the xy-plane for approximately 70ns, however looking at figure 3.2f, as well as looking at the corresponding trajectory data, the peptide spends these 70ns interacting with water. It also differs in that

in the first membrane interaction it uses only a tryptophan side chain and inserts itself quickly into the membrane compared. Compared to both the other tkbs-013 and the mrs-002 peptide, this parallel seem to insert itself deeper into the membrane as well, as shown in figure 3.4. The 3rd tkbs-013 parallel also stays in the corner of the periodic cell after the first interaction with the membrane like the 1st parallel. Comparing all three parallels, it is clear that the tkbs-013 moves more than the mrs-002 peptide and that it is the tryptophan side chain that inserts itself into the membrane. All three of the parallels ends up with a flat peptide along the membrane surface, with the exception of one tryptophan and lysine that are more inserted into the membrane. The two different ways the peptide ends up interacting with the membrane suggests that the tkbs-013 does have a specific path for interacting with such membranes. It does suggest that it is biologically active, maybe even with different modes of action, depending on how it interacts, as the first two parallels may suggest that a high enough concentration of tkbs-013 may end up carpeting the membrane, while the last parallel shows the peptide inserting itself into the membrane.

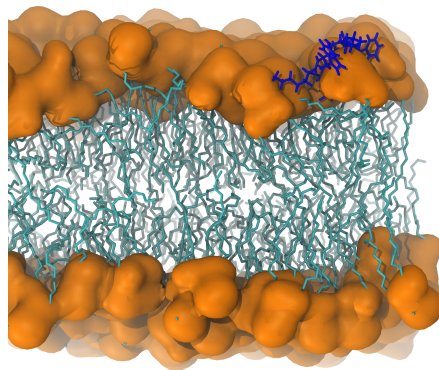
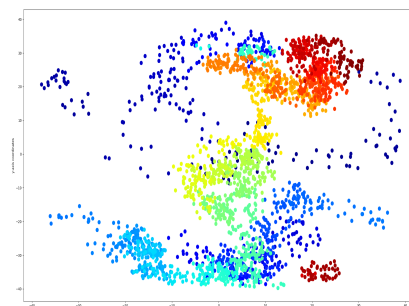
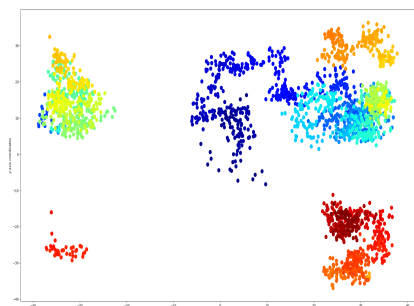
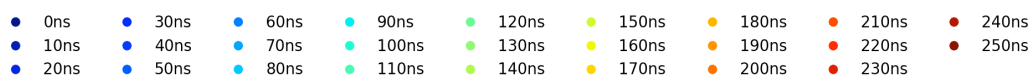
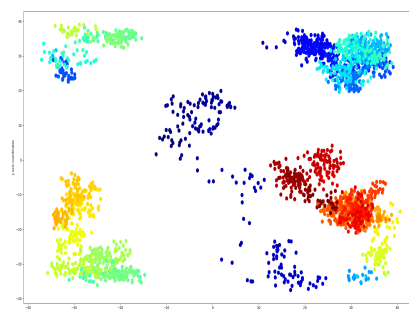
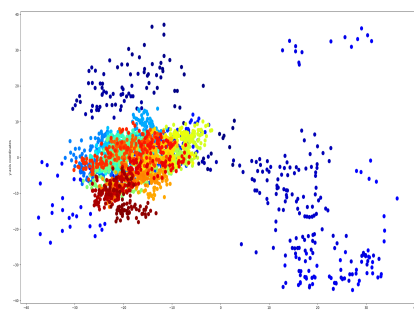


Figure 3.4: *Position of the peptide from the third parallel of tkbs-013 in the end of simulation*



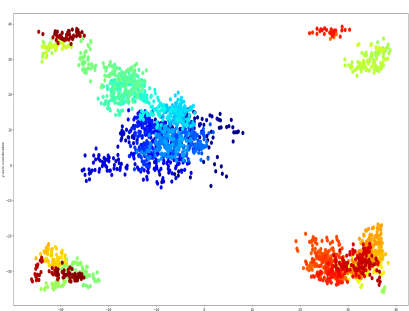
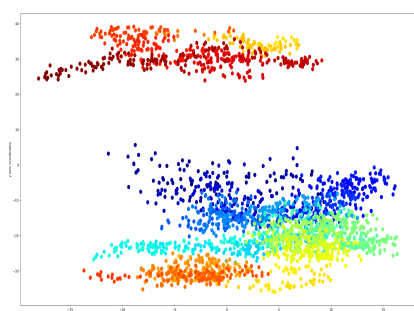
(a) Overview xy -coordinates in parallel 1 of *mrs-002* simulation

(b) Overview xy -coordinates in parallel 2 of *mrs-002* simulation



(c) Overview xy -coordinates in parallel 3 of *mrs-002* simulation

(d) Overview xy -coordinates in parallel 1 of *tkbs-013* simulation



(e) Overview xy -coordinates in parallel 2 of *tkbs-013* simulation

(f) Overview xy -coordinates in parallel 3 of *tkbs-013* simulation

Figure 3.5: Plots showing xy -position of the peptide over the simulation, from 0ns to 260ns. Larger versions of these plots for more details can be found with the appendix.

Comparing the figures in figure 3.5 between the two peptides, it is clear that the tkbs-013 peptides has move movement, but both of the peptides have one outlier that is different from the other two parallels. However, these differences can likely be explained with other figures and visual analysis, with more parallels of these systems along with different starting positions for the peptides in future work something to consider to further understand the differences between the parallels. The 2nd mrs-002 parallel had more movements in the xy-plane, but this was significantly reduced after the first interaction with the membrane and insertion into the membrane as seen with the other mrs-002 parallels. The 3rd tkbs-013 parallel may come from difference in how the tkbs-013 peptide orientation affects the affinity for interacting with the membrane, with the 3rd parallel showing an orientation of the peptide that has a higher affinity for inserting itself into the membrane. Several of the parallels did end up with the peptides along the edge or corners of the periodic cell of the simulation box, and this may have had an affect on the calculations. The calculations of some of the interactions may be a bit different in the border, and might have even been the reason the peptides did stay around the borders of the simulation box, however it may also be how the membrane itself and its lipid concentration affecting where the peptide stayed. The positioning of the peptides did show the difference between them and might help suggest that both of them are biologically active. The mrs-002 peptide seems to be the candidate likely to have an higher activity, as it seems to start making a tunnel to distrust the membrane and in that all three parallels ended up in the same position, suggesting that if the peptide interacts with the membrane, there would not be competing modes of attack. The tkbs-0132 peptide does seem to have two different modes of attack from the positioning of the peptide, both carpeting the membrane and making a tunnel depending on the parallels. The competition of two modes of attack and the higher movement of the peptide before inserting itself into the membrane, suggest that the activity would be lower than the mrs-002 peptide, substantiating experimental data from table 1.1.

So far, only the position of the peptide and the membrane with rough

estimates of possible interactions has been shown. However a more detailed view of these interactions from looking at the peptide and membrane during a visual analysis can give a clearer picture on the differences between the two peptides. Figure 3.3a shows how the 1st parallel from mrs-002 is inserted into the membrane in the last frame of the simulation. This frame was chosen, as all of the parallels was inserted into the membrane at this point in the simulation and in an similar situation with their interactions to the membrane. As stated earlier, it is the tryptophan side chain that is deepest into the membrane in the mrs-002 parallels, and with the lysine interacting with the lipid heads in the membrane. As seen in table 3.1, all three parallels of mrs-002 have both possible hydrogen bonds and van der Waals interactions with the membrane. Some of the possible hydrogen bonds may also be salt bridges, however due to the fluctuations of the membrane and the charge, in this thesis they are mentioned as possible hydrogen bonds. The first parallel shows that the tryptophan has two possible hydrogen bonds, along with the lysine having two possible hydrogen bonds. However, it is important to note that the bonds with the lysine are quite long, meaning that they would most likely not form if the peptide stayed still as seen in frame 260. The second parallel shows one hydrogen bond between the tryptophan and the membrane, and one possible hydrogen bond between the lysine and the membrane. This is also the parallel that has the most movement of the mrs-002 as shown in figure 3.5b, meaning that the lack of interactions may come from the peptide orientation in space and that it has not had enough time to get into an optimal position as parallel 1 has. The 3rd parallel shows 2 possible hydrogen bonds with lysine and 2 possible hydrogen bonds with tryptophan. The hydrogen bonds with lysine are quite long and thus weak, meaning that it is mainly the tryptophan that keeps interacting with the peptide during the membrane fluctuations. The hydrogen bonds with tryptophan comes from the amino acids not being as deep down into the membrane as the 1st parallel, and may come from not enough time interacting with the membrane itself. If this is correct, then the three parallels may show how the interactions between the membrane and the peptide evolves over time, with lysine getting stronger interactions with several possible hydrogen

bonds and the tryptophan ending up with mainly van der Waals and possible non-polar interactions depending on how deep the peptide ends up.

Table 3.1: *Overview over possible hydrogen bonds and other interactions between the different amino acids in the peptides and the membrane. Some of the possible H-bond may be salt bridges, however due to fluctuations in the membrane it was looked as at possible H-bonds instead.*

System	Lysine	Tryptophan
mrs-002-1	3 H-bonds + vdW	vdW
mrs-002-2	1 H-bond + vdW	1 H-bond + vdW
mrs-002-3	2 weak H-bond + vdW	2 H-bond + vdW
tkbs-013-1	5 H-bond + vdW	vdW
tkbs-013-2	5 H-bond + vdW	vdW
tkbs-013-3	2 H-bond + vdW	2 H-bond + vdW

The parallels of tkbs-013 also has several possible hydrogen bonds between the amino acids and the membrane, with the 1st and 2nd parallel having 5 different possible hydrogen bonds between lysine and the membrane. The 3rd parallel shows potential for 2 hydrogen bonds between tryptophan and the membrane and 2 possible hydrogen bonds between lysine and the membrane. This difference in interactions may come from the 3rd parallel being more inserted into the membrane than the first 2 parallels and the different orientation of the peptides. There are also possible hydrogen bonds between the membrane and the main chain of the peptide, however there is not a big difference in the possible interactions for the two peptides. TKBS-013 has 1-2 possible hydrogen bonds with the main chain of the peptide and 2-3 possible hydrogen bonds exists for the main chain of the mrs-002 peptide. There is a difference in how the peptides are oriented on the membrane, with all the parallels for mrs-002 and the 3rd parallel of tkbs-013 being vertical on the xy-plane and at least partially inside the membrane. The other two parallels of tkbs-013 are oriented horizontal on top of the membrane surface, most likely meaning that while there are interactions with the membrane, there are more possibilities for van der Waals and non-polar interactions for mrs-002.

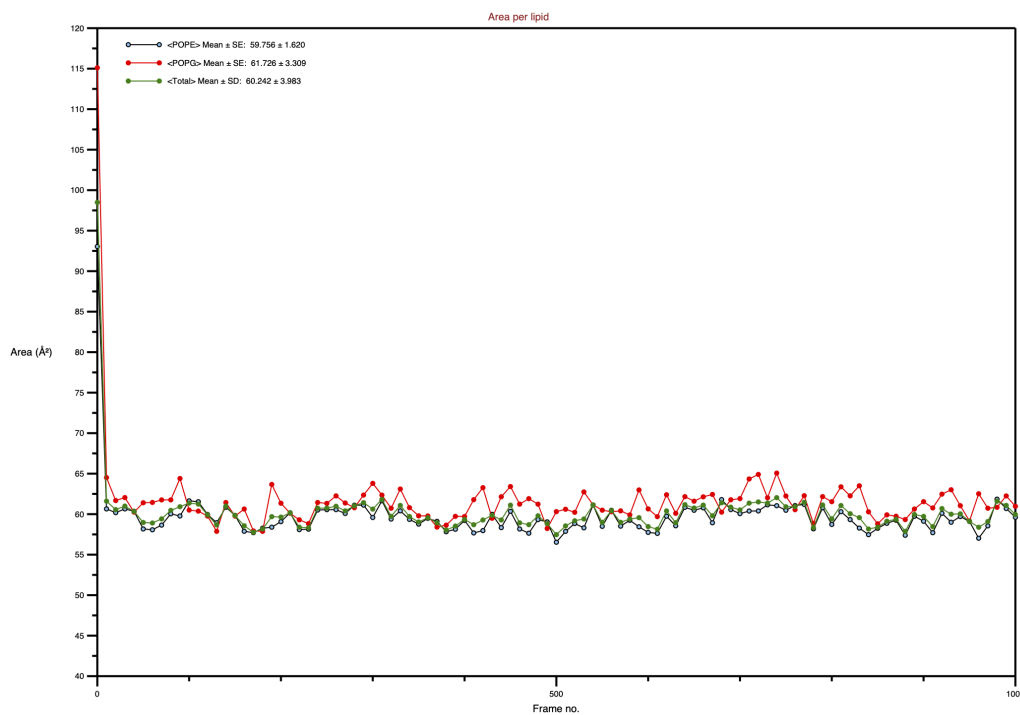
In total, while both the mrs-002 and the tkbs-013 peptide interact with the membrane itself, there were some differences that could have an impact when it comes to how well they interact and how much of an effect these interactions have on the membrane. The parallels in mrs-002 did not show the peptide moving the same way in the space, but they ended up with the peptide in the approximately same orientation in the membrane. The difference in possible hydrogen bond and interactions may come from how long time and how deep the peptides were in the membrane. The parallels of tkbs-013 had also some differences in positions of the peptide, however the 3rd parallel also showed a difference in orientation of the peptide, with it being inserted into the membrane and not ending up on the membrane surface. The difference between the peptides in position suggests that mrs-002 may be the peptide with the highest biological activity, and while there are some differences in amount of possible hydrogen bond interactions, the possible sum of van der Waals and non-polar interactions for mrs-002 may negate this difference.

3.3 Peptide effect on membrane

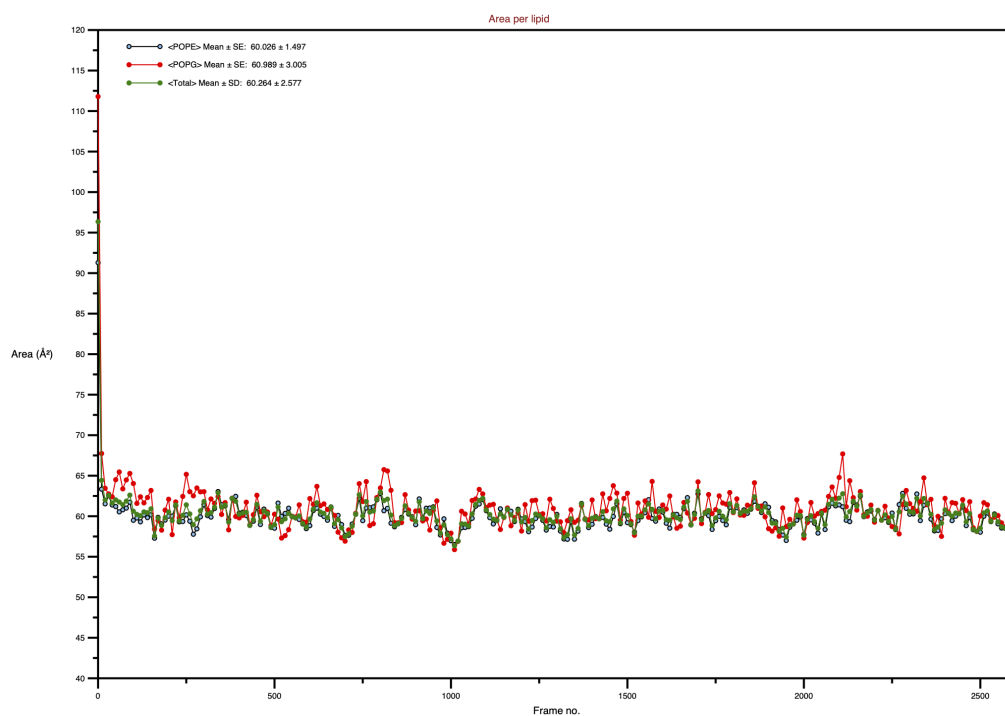
Understanding how the peptide interacts with the membrane is only one view to determine if a peptide is biologically active and often include looking at a system over time. The effect these interactions have on the membrane are equally important and may give a new view or give further proof for what the interactions say. The effects on the membrane may help determine if the peptides disturb the membrane and by how much, both by looking at the different lipids, but also on the membrane as a whole. The peptide-membrane interactions do not only need to affect the nearby lipids, but have consequences seen further away as well. Comparing the peptide-membrane systems with the membrane-only system may give an indication on how the membrane will behave with higher concentrations of peptides and may give proof for or against the peptides being biologically active.

Table 3.2: Calculated area per lipid with standard deviation over the simulations given in \AA^2 for the different systems. The values are the average over the full simulation period, with one value for each lipid type and a mean for all the lipids in the membrane.

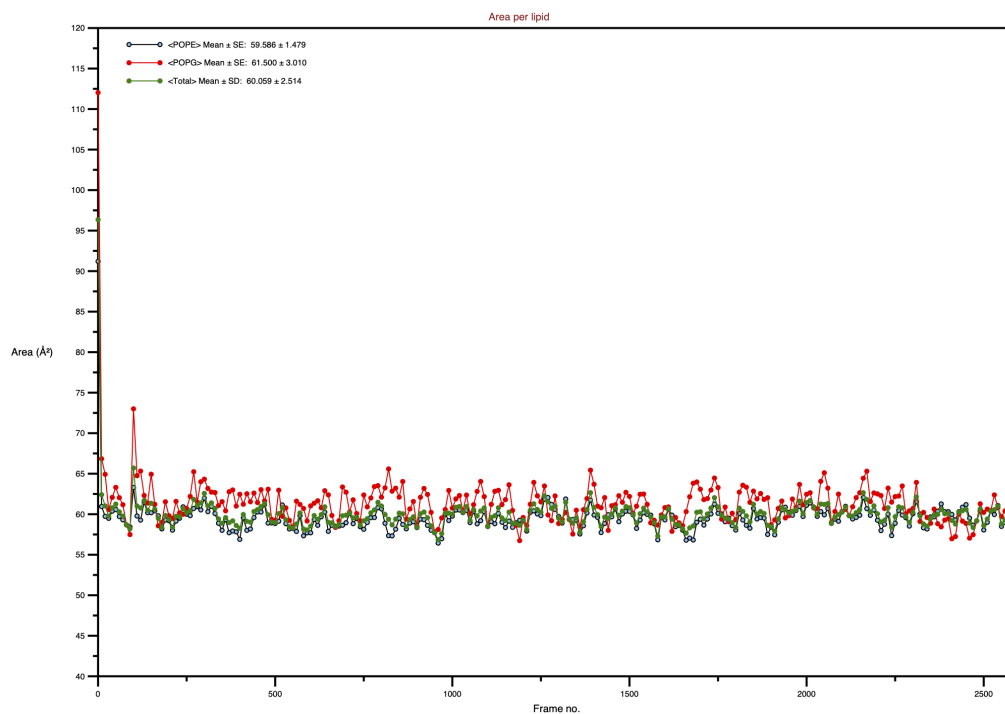
System	POPE	POPG	Mean
membrane - 1	59.756 ± 1.620	61.726 ± 3.309	60.242 ± 3.983
membrane - 2	59.730 ± 1.644	61.567 ± 3.334	60.184 ± 3.953
membrane - 3	60.066 ± 1.664	61.704 ± 3.391	60.471 ± 3.988
mrs-002 - 1	60.026 ± 1.492	60.989 ± 3.005	60.264 ± 2.577
mrs-002 - 2	59.567 ± 1.467	61.493 ± 3.022	60.043 ± 2.466
mrs-002 - 3	59.699 ± 1.490	61.450 ± 3.022	60.094 ± 2.509
tkbs-013 - 1	59.678 ± 1.479	60.778 ± 2.891	59.950 ± 2.531
tkbs-013 - 2	59.589 ± 1.479	61.500 ± 3.010	60.059 ± 2.514
tkbs-013 - 3	59.730 ± 1.470	60.899 ± 2.907	60.019 ± 2.492



(a) Area per lipid plot for 1st parallel of membrane-only system



(b) Area per lipid plot for 1st parallel of membrane-only system



(c) Area per lipid plot for 1st parallel of membrane-only system

Figure 3.6: Area per lipid plots for the 1st parallel of the membrane-only and peptide-membrane systems.

Calculating the area per lipid for all of the systems in this section may show if there is a development in the membrane density and if the peptide affected the POPE or POPG lipids more than the other. The plot for the area per lipid over the simulation period for the membrane-only systems shows a certain trend that is similar for all 3 parallels, with an example from parallel 1 shown in figure 3.6a. For the first couple of frames, the area per lipid for both the POPE and POPG lipids decrease rapidly, likely from the minimisation of the system before the simulation began. After this change, it is mostly POPG that has the biggest change in area per lipid of the two lipids and this is shown in all three membrane-only parallels. This can be seen when looking at the calculated mean and standard deviation as shown in table 3.2. Here it is shown that the POPG on average uses approximately 1.5\AA^2 more space than the POPE lipid in the membrane-only systems. Looking at the distribution of area per lipid used by the lipids, the lipid distribution looks like a Gaussian distribution, with POPE concentrated around 60\AA^2 and POPG at almost 62\AA^2 . One can see that the highest concentration of lipids at a certain volume is also reflected in their calculated mean value. There are some outlier lipids with area per lipid at around 80-90, however these are most likely lipids at the border of the simulation box. The small amount of them makes it possible to exclude them in the analysis and assume that their effect on the calculated values are negligible.

Including the mrs-002 peptide seem to give small changes in the area per lipid analysis shown in figure 3.6b. For the plots over the simulation, there is still the significant drop from the minimisation at the beginning of the simulation, however there is also more change in between the different frames, suggesting that overall the lipids change their area per lipid more over the simulation compared to the membrane-only system. It is still the POPG that is the lipid with the most change and it has the higher mean of the two lipid types, and the change from the calculated mean area per lipid is a small decrease in the standard deviation shown in table 3.2. The distribution of area per lipids looks still like a Gaussian distribution, however there is also more variety in the lipids for this simulation. This may suggest that some

lipids end up with more space and others end up in a tighter space, most likely from the peptide inserting itself into the membrane. This suggests that the mrs-002 peptide affects both the lipids close and lipids further away.

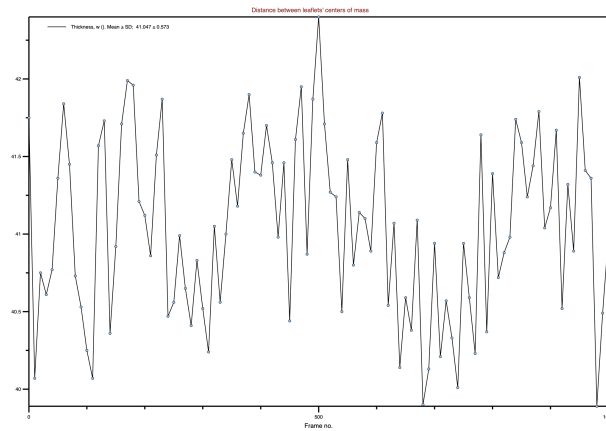
The figures 3.6c and the corresponding mean values in table 3.2 shows a decrease in the area per lipid for both POPE and POPG compared to the membrane-only system and a decrease in the standard deviation from the mean like mrs-002. The lipids change how much space they take more from frame to frame as the mrs-002 system showed, but with not as many values at either end of the 'extreme' values. These frames where the lipids suddenly take more space on average it's the most distinct when looking at the POPG lipid plots, but is still visible in the other plots. The reason the tkbs-013 peptide has less than the mrs-002 system, may come from the difference in how much each peptide inserts itself into the membrane themselves, thus disturbing the membrane. Other literature with POPE/POPG membranes has calculated the area per lipid at $60 \pm 1 \text{ \AA}^2$, 57.7 \AA^2 and $57 \pm 0.7 \text{ \AA}^2$ [22] [28] [17] and with separate area per lipid calculations suggesting that POPG uses more space. While the difference between the values in table 3.2 and the given values most likely be explained by differences in the systems such as ions, peptide-membrane interactions and such, it also suggests that the area per lipid calculations from the peptide-membrane systems was not affected much by the peptides. This could change with an increase of peptide concentration, as a suggested mode of attack for the peptides are tunnelling.

Examining the space the lipids use in the membrane, the average membrane thickness and map of the membrane thickness shown on the xy-plane of the membrane may help indicate how the peptides affect the membrane during the simulations. When looking at the membrane-only systems, figure 3.7a shows the membrane thickness changing during the simulation, with a mean at approx 41 Å for all 3 parallels and figure 3.8a shows that the membrane end up with some areas thicker than others, and this is seen in all 3 parallels. There does not seem to be a pattern to what areas of the membrane that changes in thickness, but all three parallels seem to have one thicker and one thinner area of the membrane, most likely from natural fluctuations. It

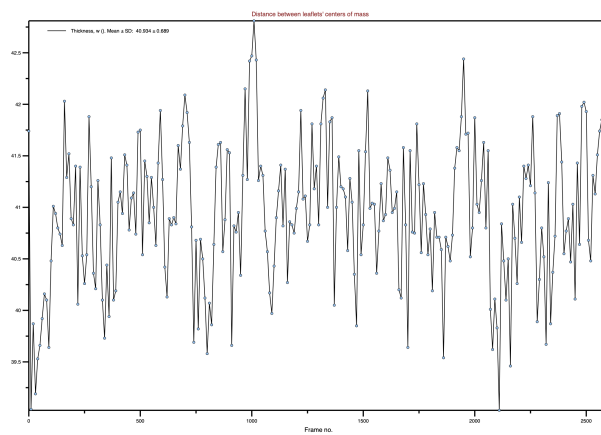
is important to note that the differences between the thinner and the thicker areas for the parallels is a maximum of 2Å in difference, meaning that there are no deep wells in the membrane.

The introduction of mrs-002 does not change the mean thickness of the membrane by any significant amount, but there seems to be more fluctuations during the simulation as seen in figure 3.7b. This may come from the longer simulations, from 100 ns to 260ns, but may also stem from the introduction of a peptide. The membrane does also end up with concentrated areas where the membrane is either thicker or thinner than average, however when looking at them in comparison to where the peptide wanders in the simulation, there do seem to be a correlation as seen between figure 3.8b and 3.5a. This correlation may originate from the mrs-002 peptide inserting itself into the membrane, thus forcing the lipids away and from how the peptide affects the area per lipid for the closest lipids compared to the ones further away. The effect on the lipids may come from the oxygen on the main chain of the peptide repelling the negatively charged lipid heads, creating small 'pockets' of space on the membrane surface.

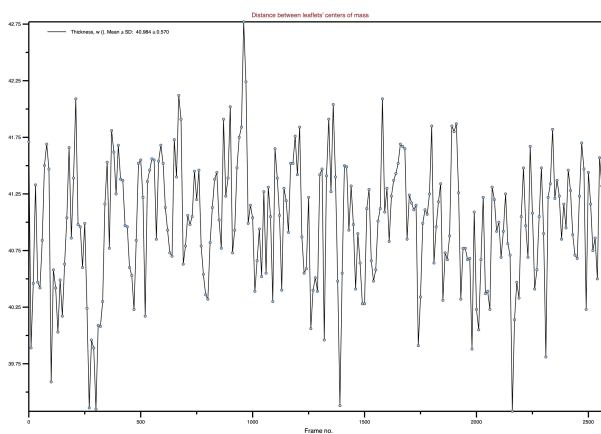
The systems including tkbs-013 peptide shows that the peptide did not have any significant impact on the mean membrane thickness during the simulation. There are a couple of more peaks in the plot, as seen in figure 3.7c, but this may come from the longer simulation like the mrs-002 system. When looking at where the membrane ends up thicker and thinner than the average as in figure 3.8c and comparing them to figure 3.5d, there does to be a correlation between the xy-position of the peptide and where the membrane seems to be thinner as with the mrs-002 systems. Suggesting that the peptide has a small impact on how thin the membrane becomes. This correlation in both peptides suggests that they do affect the membrane thickness and where it changes. A higher concentration may show a greater impact on the membrane as well. However it is likely that the mrs-002 peptides has a higher impact on the membrane thickness compared tkbs-013 when looking at figure 3.8b and 3.8c and this may come from how the peptide interacts with the membrane.



(a) *Calculated mean thickness of membrane over the simulation period for 1st parallel of membrane-only system*



(b) *Calculated mean thickness of membrane over the simulation period for 1st parallel of mrs-002 system*



(c) *Calculated mean thickness of membrane over the simulation period for 1st parallel of tkbs-013 system*

Figure 3.7: *Calculated mean thickness for membrane.*

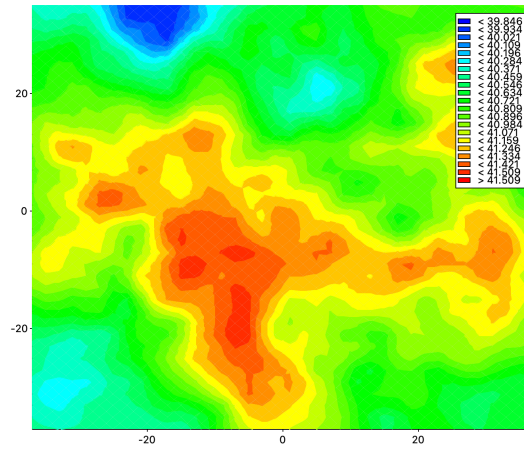
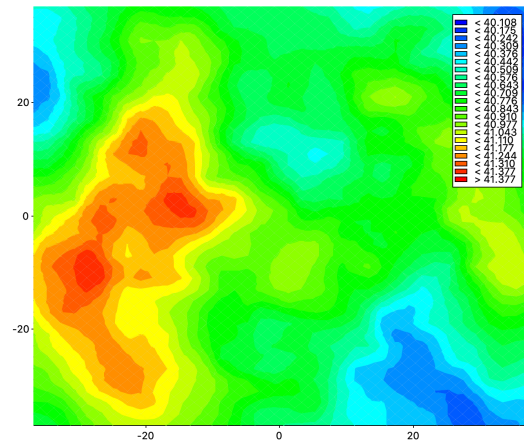
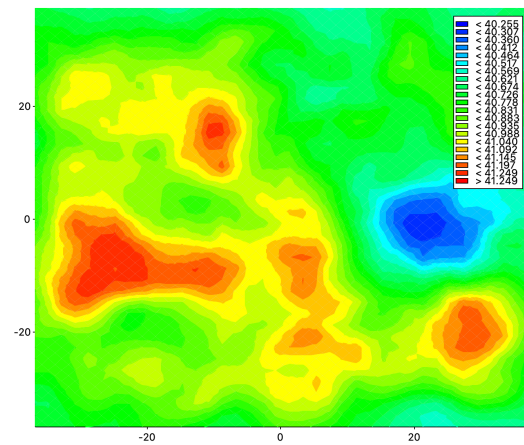
(a) *Parallel 1 of membrane-only system*(b) *Parallel 1 of mrs-002 system*(c) *Parallel 1 of tkbs-013 system*

Figure 3.8: *Calculated map of average thickness of the membrane during the simulation in the xy -plane with red indicating higher values and blue lower.*

Investigating the membrane fluidity and the mobility of the lipid tails can also reveal important information, especially as it seems that at least one of the peptides interacts with the lipid tails in the membrane. S_{CD} analysis was done both separately for the POPE and POPG lipids and for all the lipids in the system. In the membrane-only system, there were differences between the parallels, however like the membrane thickness, it was without any obvious pattern. This may suggest that the change may be from the membrane fluctuation and thus random, however longer or more parallels could help determine this.

The mrs-002 system S_{CD} plots shows more consistent between the three parallels compared to the membrane-only system. It does not seem to be a significant change in the mobility of the C-H bonds, only noting a small decrease, however the standard deviation, especially for the POPG lipid, seem to have decreased compared to the membrane-only. This may show that there might be less mobility in the lipid tails from the peptide interacting with them. The system including tkbs-013 also has a consistency between the parallels that was not seen in the membrane-only system parallels. Compared to the mrs-002 system, there are some small differences, such as the POPG lipids having a greater mobility at C3 and C13 for the tkbs-013 than mrs-002 and the mrs-002 system having greater mobility at C4 and C5. This may come from the interactions between the peptide and the membrane. It is also important to note that the S_{CD} plots are an average between all the lipids in the membrane and this may make any changes seen from the peptide interactions very small in the calculations of mobility.

The membrane-only and the membrane-peptide systems do show some differences during the simulations, most likely coming from how the introduction of a peptide to the systems. Both mrs-002 and tkbs-013 showed differences in area per lipid, membrane thickness and S_{CD} analysis compared to the membrane-only system, however there were also some differences between the peptides themselves. Comparing the two peptides, there were not the biggest differences in some of the different analysis, but in total mrs-002 might be the peptide with the biggest effect on the membrane structure,

suggesting that it is the peptide most biologically active of the two. The difference in biological activity shown in the simulations correspond to difference in MIC tests between the two peptides. There were no data on modes of attack for the peptides and experimental data may substantiate the mechanisms suggested in this thesis. There were no indication that the peptides were biologically inactive against the membrane from the simulation, as seen with the data provided.

Chapter 4

Conclusion

The molecular dynamics simulations of the different systems, including only the two peptides, mrs-002 and tkbs-013, only the lipid bilayer membrane and the combination of the membrane and the peptides, suggests that both peptides are biologically active against a POPE:POPG membrane.

The conformational simulations showed that the peptides did not have a strong secondary structure, most likely from the cyclic structure and being an extended peptide, as they consist of tryptophan and lysine. The interactions between the mrs-002 peptide and the membrane in all three parallels suggests that it is biologically active and most likely makes a tunnel as a mode of attack, a known mechanism for antibacterial peptides. The tkbs-013 peptide was also seen to be biologically active with two possible modes of attack, either carpeting the membrane or making a tunnel, suggesting the orientation of the peptide during the interactions being a determinant for this. The difference between the interactions and effects on the membrane, suggests that it is the mrs-002 peptide that most likely is more active of the two. All analysis of the different systems was completed using VMD, plugins for VMD and extracting and plotting data from the computed trajectory files using python and tcl-scripting.

4.1 Future work

For further studies, other cyclic hexapeptides with different amino acids may be interesting, especially with amino acids close or similar to tryptophan and lysine such as arginine or phenylalanine. Looking at how the linear counterpart of mrs-002 and tkbs-013 interacts with the membrane may also give valuable information.

There are experimental data produced that is not yet published that could be interesting to compare with data from this thesis. Further conformational studies and other biochemical analysis from the lab may also help uncover imperfections with the method or system that may be important for other similar simulations.

Bibliography

- [1] ALBERTS, B., JOHNSON, A., LEWIS, J., RAFF, M., ROBERTS, K., AND WALTER, P. The Lipid Bilayer. In *Molecular Biology of the Cell*, 4th ed. Garland Science, 2002.
- [2] ATKINS, P. *Molecular quantum mechanics*, 5th ed. ed. Oxford University Press, Oxford, 2011.
- [3] BECHINGER, B., AND GORR, S. U. Antimicrobial Peptides: Mechanisms of Action and Resistance. *Journal of Dental Research* 96, 3 (mar 2017), 254–260.
- [4] BERNARDI, R. C., MELO, M. C., AND SCHULTEN, K. Enhanced sampling techniques in molecular dynamics simulations of biological systems. *Biochimica et Biophysica Acta (BBA) - General Subjects* 1850, 5 (may 2015), 872–877.
- [5] BROGDEN, K. A. Antimicrobial peptides: pore formers or metabolic inhibitors in bacteria? *Nature Reviews Microbiology* 2005 3:3 3, 3 (mar 2005), 238–250.
- [6] BROOKS, B. R., BROOKS, C. L., MACKERELL, A. D., NILSSON, L., PETRELLA, R. J., ROUX, B., WON, Y., ARCHONTIS, G., BARTELS, C., BORESCH, S., CAFLISCH, A., CAVES, L., CUI, Q., DINNER, A. R., FEIG, M., FISCHER, S., GAO, J., HODOSCEK, M., IM, W., KUCZERA, K., LAZARIDIS, T., MA, J., OVCHINNIKOV, V., PACI, E., PASTOR, R. W., POST, C. B., PU, J. Z., SCHAEFER, M., TIDOR, B., VENABLE, R. M., WOODCOCK, H. L., WU, X., YANG, W.,

- YORK, D. M., AND KARPLUS, M. CHARMM: The biomolecular simulation program. *Journal of Computational Chemistry* 30, 10 (jul 2009), 1545–1614.
- [7] CHEN, C. H., AND LU, T. K. Development and Challenges of Antimicrobial Peptides for Therapeutic Applications. *Antibiotics* 2020, Vol. 9, Page 24 9, 1 (jan 2020), 24.
- [8] CIRAC, A. D., MOISET, G., MIKA, J. T., KOÇER, A., SALVADOR, P., POOLMAN, B., MARRINK, S. J., AND SENGUPTA, D. The Molecular Basis for Antimicrobial Activity of Pore-Forming Cyclic Peptides. *Biophysical Journal* 100, 10 (may 2011), 2422–2431.
- [9] DAVIES, J. Origins and evolution of antibiotic resistance. *Microbiología (Madrid, Spain)* 12, 1 (1996), 9–16.
- [10] EPAND, R. F., POLLARD, J. E., WRIGHT, J. O., SAVAGE, P. B., AND EPAND, R. M. Depolarization, bacterial membrane composition, and the antimicrobial action of ceragenins. *Antimicrobial Agents and Chemotherapy* 54, 9 (sep 2010), 3708–3713.
- [11] GOOSSENS, H., FERRECH, M., VANDER STICHELE, R., AND ELSEVIERS, M. Outpatient antibiotic use in Europe and association with resistance: a cross-national database study. *The Lancet* 365, 9459 (feb 2005), 579–587.
- [12] GUIXÀ-GONZÁLEZ, R., RODRIGUEZ-ESPIGARES, I., RAMÍREZ-ANGUITA, J. M., CARRIÓ-GASPAR, P., MARTINEZ-SEARA, H., GIORGINO, T., AND SELENT, J. MEMBPLUGIN: studying membrane complexity in VMD. *Bioinformatics* 30, 10 (may 2014), 1478–1480.
- [13] GULLINGSRUD, J. CatDCD - Concatenate DCD files, 2009.
- [14] GULLINGSRUD, J., AND KOHLMAYER, A. Analyze Big DCD Files, 2003.

-
- [15] HEINZ, H., LIN, T.-J., MISHRA, R. K., AND EMAMI, F. S. Thermodynamically Consistent Force Fields for the Assembly of Inorganic, Organic, and Biological Nanostructures: The INTERFACE Force Field. *Langmuir* 29, 6 (feb 2013), 1754–1765.
- [16] HIAR, C. Chip shortage could slow electric vehicle rollouts. *Scientific American* (Aug 2021).
- [17] HONG, C., TIELEMAN, D. P., AND WANG, Y. Microsecond Molecular Dynamics Simulations of Lipid Mixing. *Langmuir* 30, 40 (oct 2014), 11993–12001.
- [18] HUMPHREY, W., DALKE, A., AND SCHULTEN, K. VMD: Visual molecular dynamics. *Journal of Molecular Graphics* 14, 1 (feb 1996), 33–38.
- [19] JENSEN, F. *Introduction to Computational Chemistry*, 3rd ed. 2017.
- [20] J. SPOONER, M., AND A. GALE, P. Anion transport across varying lipid membranes – the effect of lipophilicity. *Chemical Communications* 51, 23 (mar 2015), 4883–4886.
- [21] LEACH, A. R. *Molecular Modelling Principles and Applications*, second ed. Pearson, 2001.
- [22] LYU, Y., XIANG, N., MONDAL, J., ZHU, X., AND NARSIMHAN, G. Characterization of interactions between curcumin and different types of lipid bilayers by molecular dynamics simulation. *The Journal of Physical Chemistry B* 122, 8 (2018), 2341–2354. PMID: 29394060.
- [23] MACKERELL, A. D., BASHFORD, D., BELLOTT, M., DUNBRACK, R. L., EVANSECK, J. D., FIELD, M. J., FISCHER, S., GAO, J., GUO, H., HA, S., JOSEPH-MCCARTHY, D., KUCHNIR, L., KUCZERA, K., LAU, F. T. K., MATTOS, C., MICHNICK, S., NGO, T., NGUYEN, D. T., PRODHOM, B., REIHER, W. E., ROUX, B., SCHLENKRICH, M., SMITH, J. C., STOTE, R., STRAUB, J., WATANABE, M., WIÓRKIEWICZ-KUCZERA, J., YIN, D., AND KARPLUS, M.

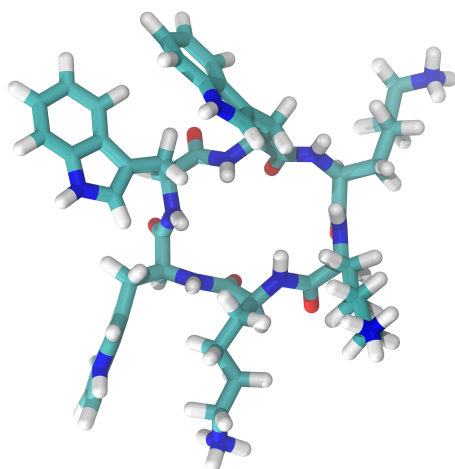
- All-atom empirical potential for molecular modeling and dynamics studies of proteins. *The Journal of Physical Chemistry B* 102, 18 (1998), 3586–3616. PMID: 24889800.
- [24] MAHLAPUU, M., HÅKANSSON, J., RINGSTAD, L., AND BJÖRN, C. Antimicrobial Peptides: An Emerging Category of Therapeutic Agents. *Frontiers in Cellular and Infection Microbiology* 0, DEC (2016), 194.
- [25] MCMAHON, H. T., AND GALLOP, J. L. Membrane curvature and mechanisms of dynamic cell membrane remodelling. *Nature* 2005 438:7068 438, 7068 (nov 2005), 590–596.
- [26] NAGLE, J. F., AND TRISTRAM-NAGLE, S. Structure of lipid bilayers. *Biochimica et Biophysica Acta (BBA) - Reviews on Biomembranes* 1469, 3 (nov 2000), 159–195.
- [27] PAN, J., HEBERLE, F. A., TRISTRAM-NAGLE, S., SZYMANSKI, M., KOEPFINGER, M., KATSARAS, J., AND KUČERKA, N. Molecular structures of fluid phase phosphatidylglycerol bilayers as determined by small angle neutron and X-ray scattering. *Biochimica et Biophysica Acta (BBA) - Biomembranes* 1818, 9 (sep 2012), 2135–2148.
- [28] PANDIT, K. R., AND KLAUDA, J. B. Membrane models of e. coli containing cyclic moieties in the aliphatic lipid chain. *Biochimica et Biophysica Acta (BBA) - Biomembranes* 1818, 5 (2012), 1205–1210.
- [29] SARRE, B. R. MD simulations reveal how synthetic antimicrobial peptides interact with membrane models.
- [30] SCHRÖDINGER. Maestro, 2020.
- [31] SVENDSEN ET AL. Unpublished data. 2021.
- [32] TÄNGDÉN, T., CARS, O., MELHUS, Å., AND LÖWDIN, E. Foreign travel is a major risk factor for colonization with *Escherichia coli* producing CTX-M-type extended-spectrum β -lactamases: A prospective study with Swedish volunteers. *Antimicrobial Agents and Chemotherapy* 54, 9 (sep 2010), 3564–3568.

-
- [33] TUCKERMAN, M. E. Statistical mechanics : theory and molecular simulation. 696.
- [34] UNITED NATIONS. Call to Action on Antimicrobial Resistance (AMR) - 2021. Tech. rep.
- [35] VANOMMESLAEGHE, K., HATCHER, E., ACHARYA, C., KUNDU, S., ZHONG, S., SHIM, J., DARIAN, E., GUVENCH, O., LOPES, P., VOROBYOV, I., MACKERELL, A. D., AND JR. CHARMM General Force Field (CGenFF): A force field for drug-like molecules compatible with the CHARMM all-atom additive biological force fields. *Journal of computational chemistry* 31, 4 (mar 2010), 671.
- [36] VENTOLA, C. L. The Antibiotic Resistance Crisis: Part 1: Causes and Threats. *Pharmacy and Therapeutics* 40, 4 (2015), 277.
- [37] VERMEER, L. S., DE GROOT, B. L., RÉAT, V., MILON, A., AND CZAPLICKI, J. Acyl chain order parameter profiles in phospholipid bilayers: Computation from molecular dynamics simulations and comparison with ²H NMR experiments. *European Biophysics Journal* 36, 8 (2007), 919–931.
- [38] WOOLHOUSE, M., WARD, M., VAN BUNNIK, B., AND FARRAR, J. Antimicrobial resistance in humans, livestock and the wider environment. *Philosophical Transactions of the Royal Society B: Biological Sciences* 370, 1670 (2015).
- [39] WORLD HEALTH ORGANIZATION (WHO). Urgent health challenges for the next decade, 2020.
- [40] YOUNG, H., AND FREEDMAN, R. *University physics with modern physics*, 14th ed. Pearson Education Limited, 2007.
- [41] YOUNT, N. Y., BAYER, A. S., XIONG, Y. Q., AND YEAMAN, M. R. Advances in antimicrobial peptide immunobiology. *Peptide Science* 84, 5 (jan 2006), 435–458.

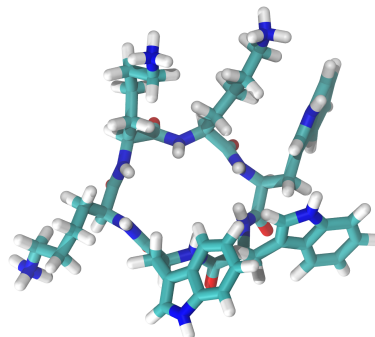
- [42] ZHANG, L. J., AND GALLO, R. L. Antimicrobial peptides. *Current Biology* 26, 1 (jan 2016), R14–R19.

Appendix A

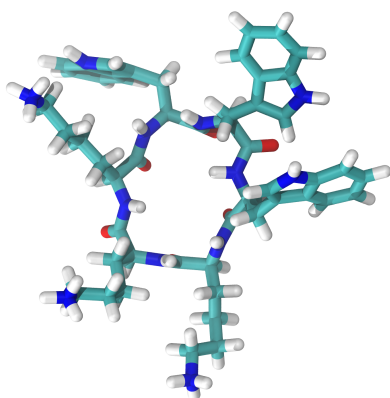
Conformation of peptide in end of peptide-only simulations



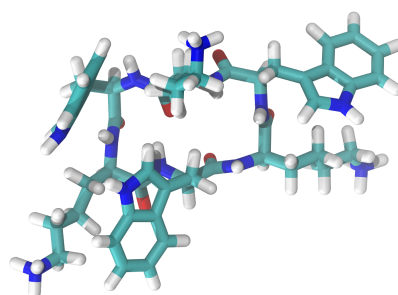
(a) *Parallel 1 of mrs-002 only system*



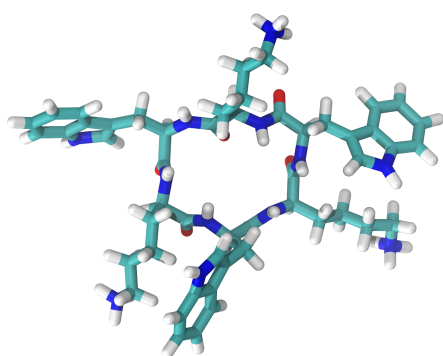
(b) *Parallel 2 of mrs-002 only system*



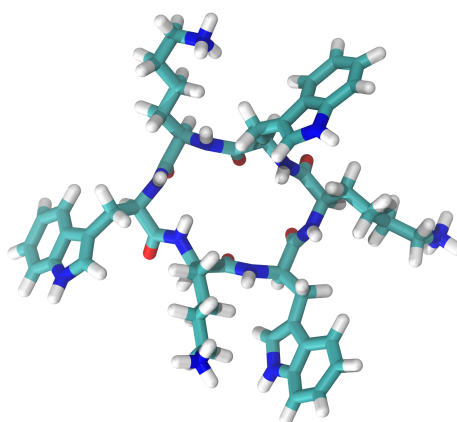
(c) *Parallel 3 of mrs-002 only system*



(d) *Parallel 1 of tkbs-013 only system*



(e) *Parallel 2 of tkbs-013 only system*

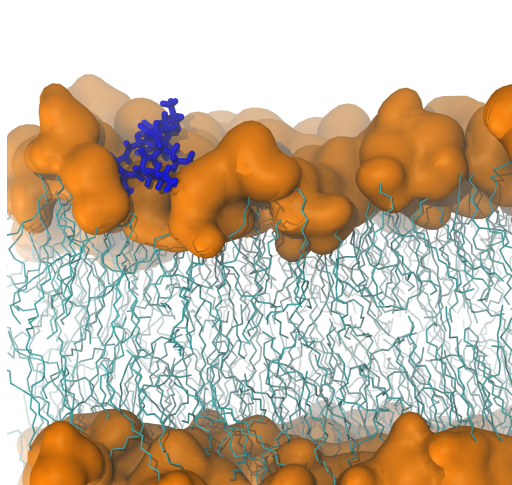


(f) *Parallel 3 of tkbs-013 only system*

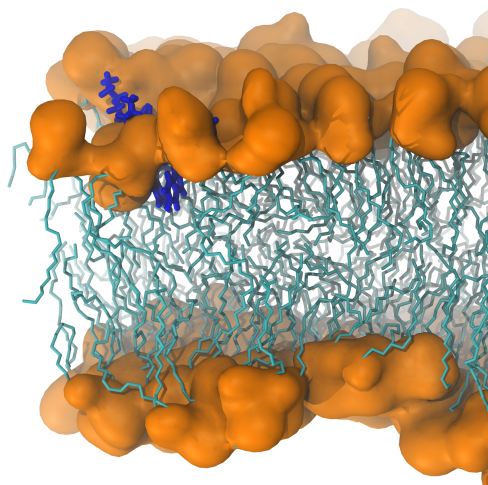
Figure A.1: *Conformation of the different peptides in all peptide-only simulations run. All figures rendered from end of simulation.*

Appendix B

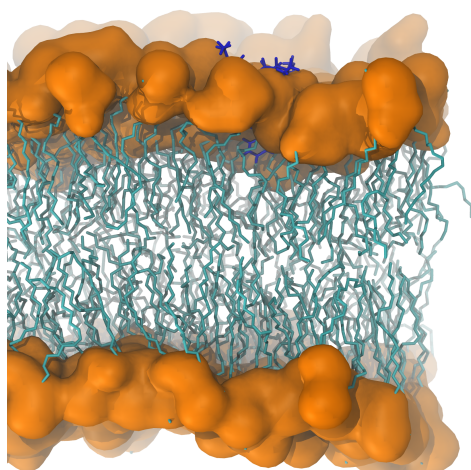
Position and orientation of peptide in membrane



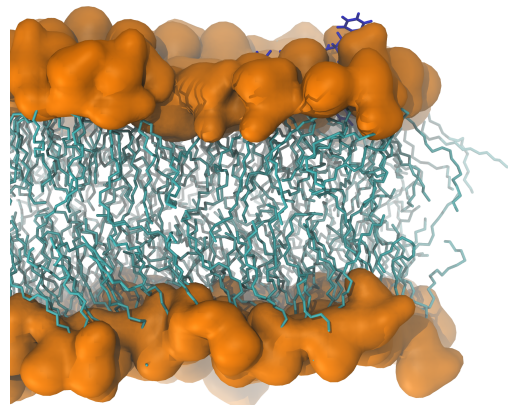
(a) *Parallel 1 of mrs-002 and membrane system*



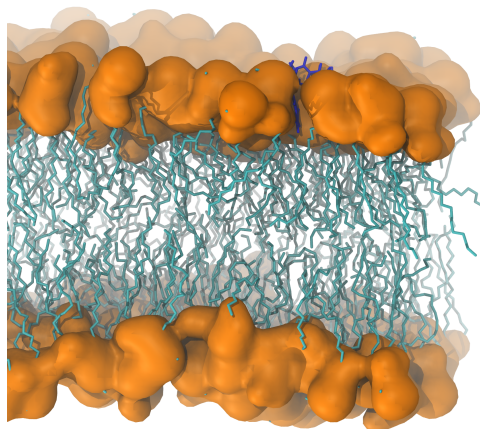
(b) *Parallel 2 of mrs-002 and membrane system*



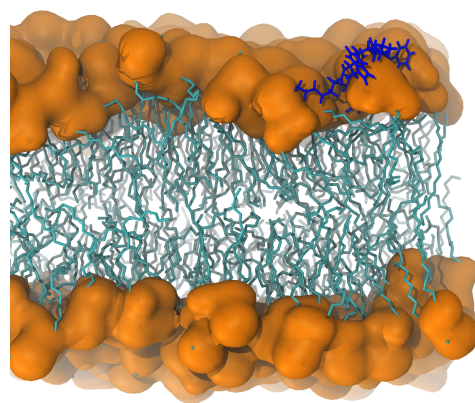
(c) *Parallel 3 of mrs-002 and membrane system*



(d) *Parallel 1 of tkbs-013 and membrane system*



(e) *Parallel 2 of tkbs-013 and membrane system*

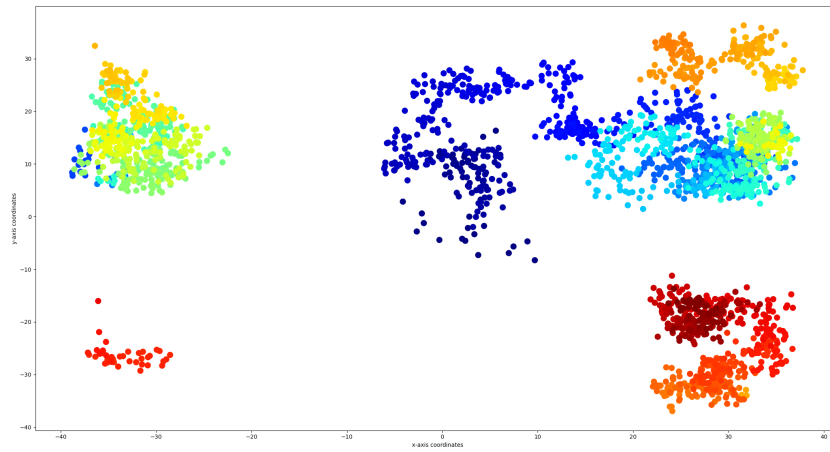
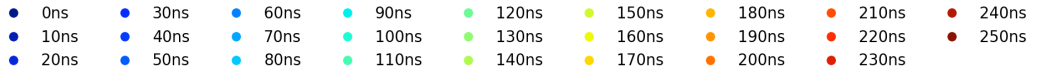


(f) *Parallel 3 of tkbs-013 and membrane system*

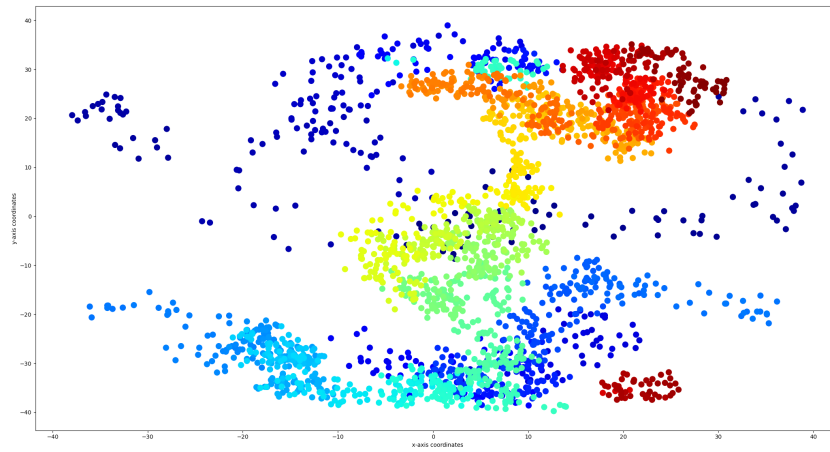
Figure B.1: *Position and orientation of the peptides in the different peptide-membrane simulations. All figures rendered in the end of simulation, at 260ns.*

Appendix C

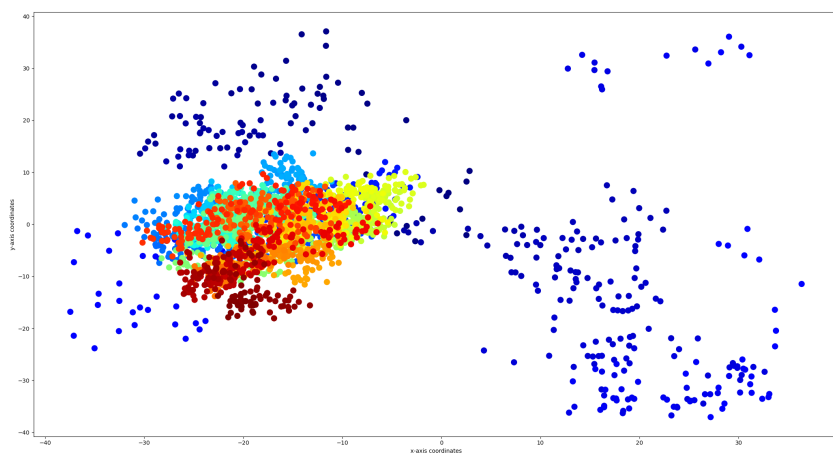
Position of peptide in xy-plane during simulation



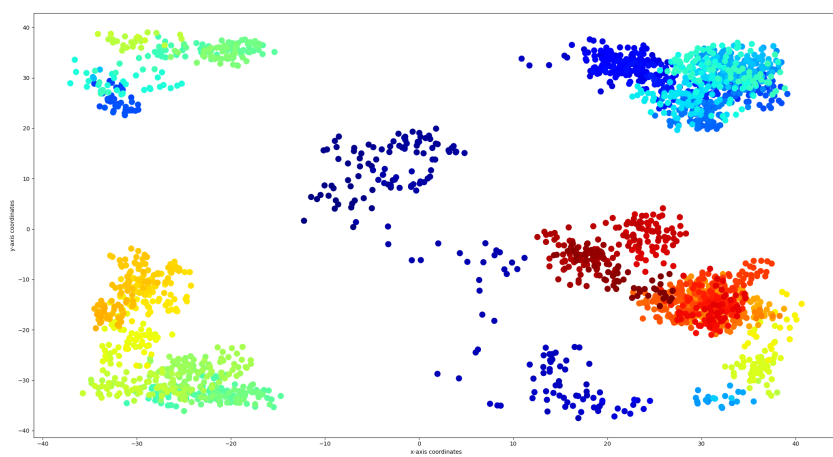
(a) *Parallel 1 of mrs-002 + membrane*



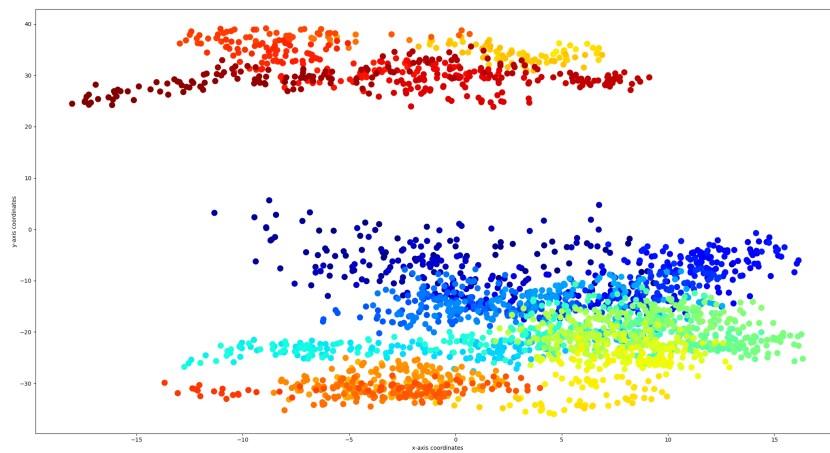
(b) *Parallel 2 of mrs-002 + membrane*



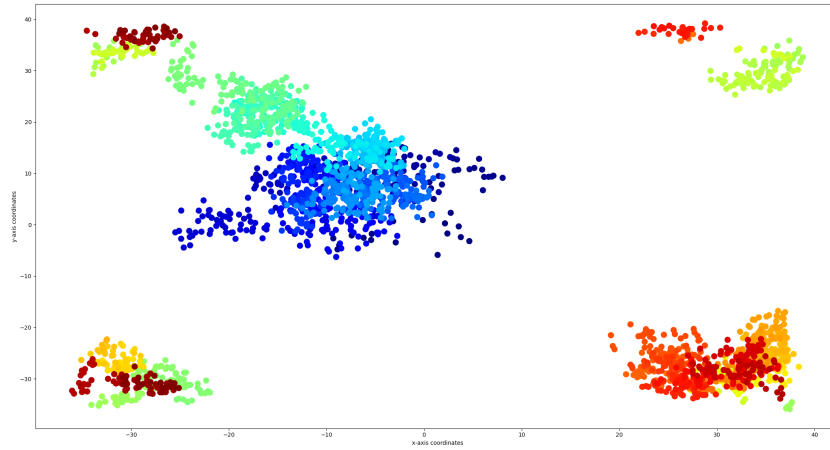
(c) *Parallel 3 of mrs-002 + membrane*



(d) *Parallel 1 of tkbs-013 + membrane*



(e) *Parallel 2 of tkbs-013 + membrane*

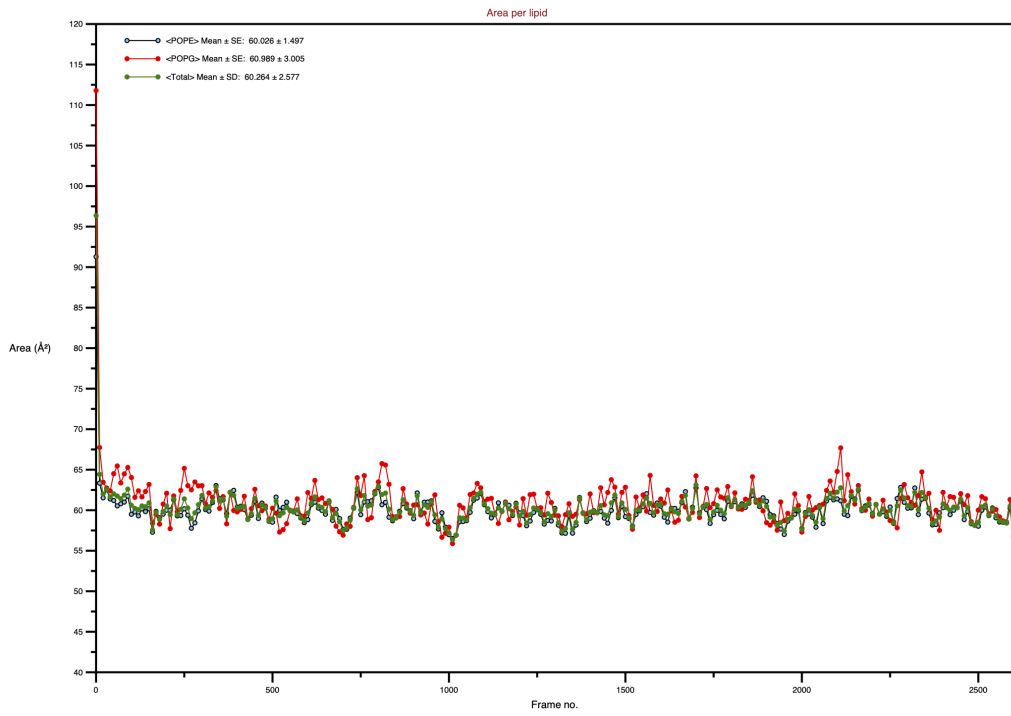
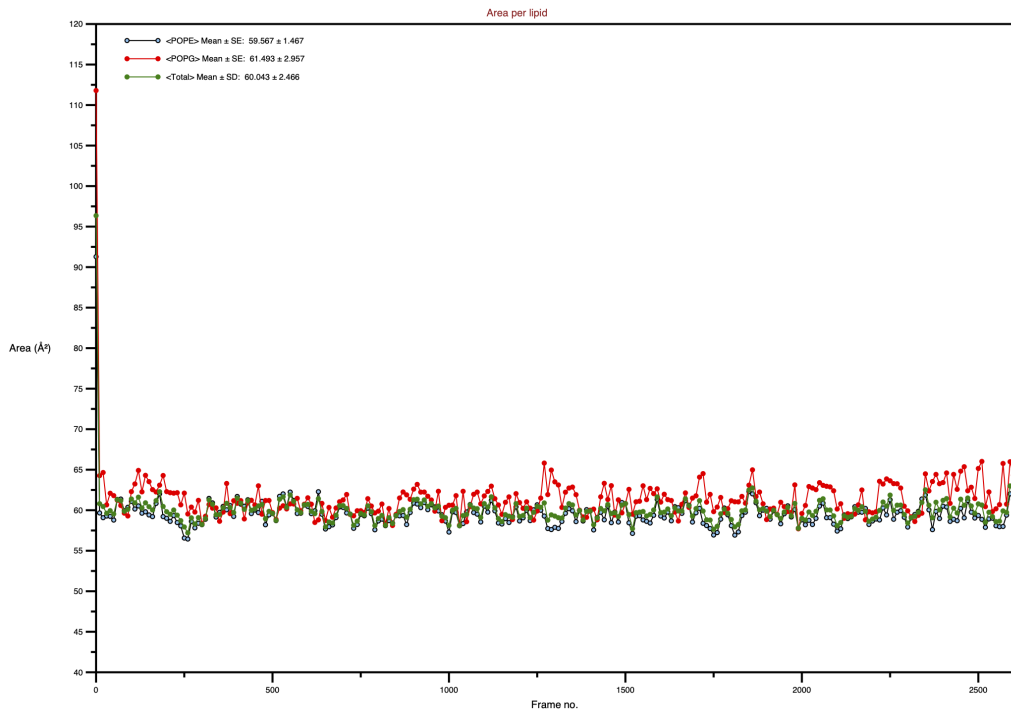


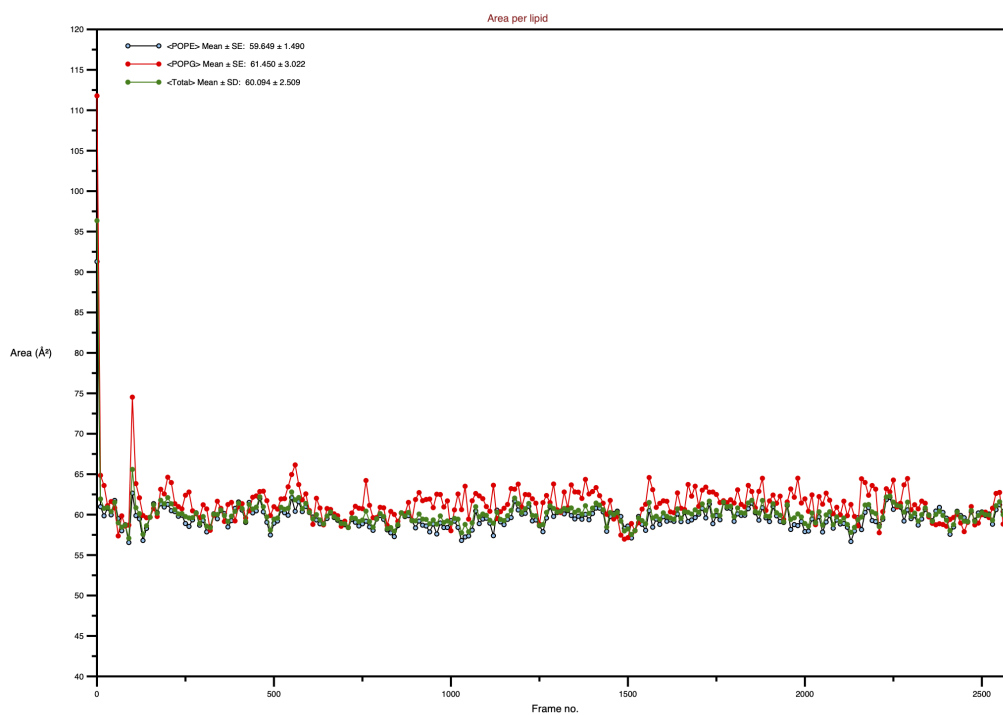
(f) *Parallel 3 of tkbs-013 + membrane*

Figure C.1: *Position of the peptide in the xy -plane for the different peptide-membrane simulations. The overview of the colours corresponding to the time can be seen before the first plot.*

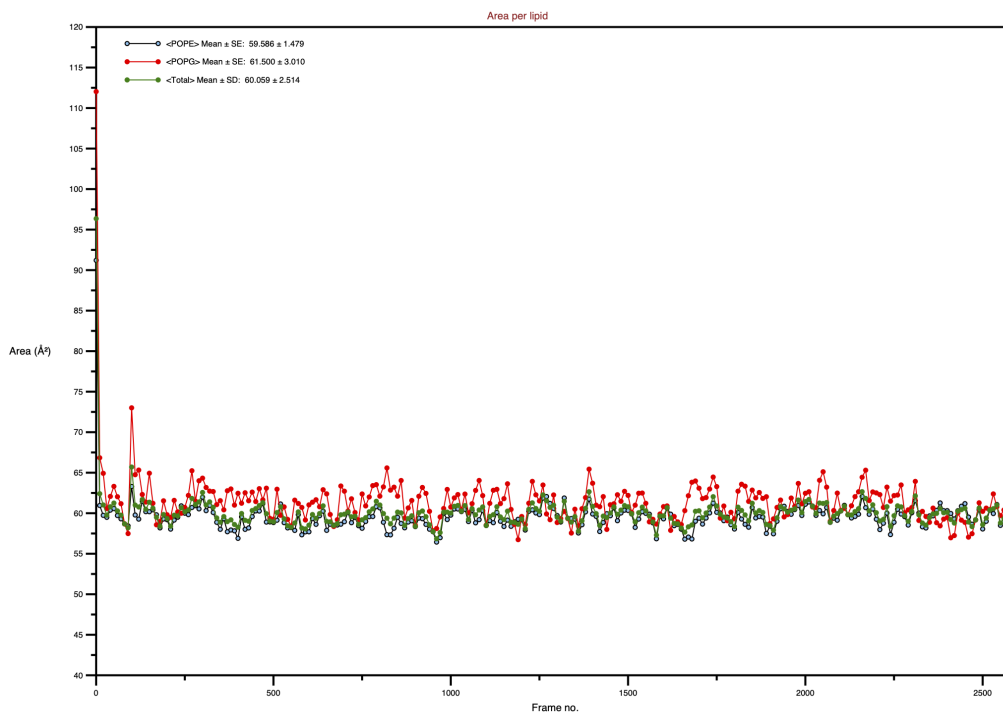
Appendix D

Area per lipid

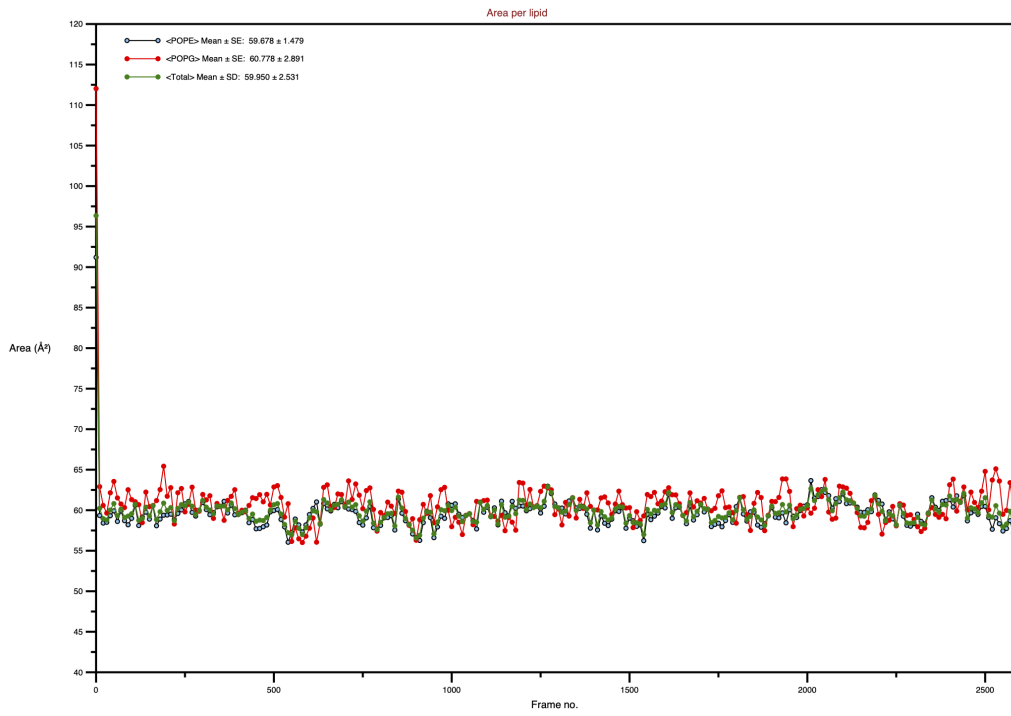
(a) *Parallel 1 of mrs-002 + membrane*(b) *Parallel 2 of mrs-002 + membrane*



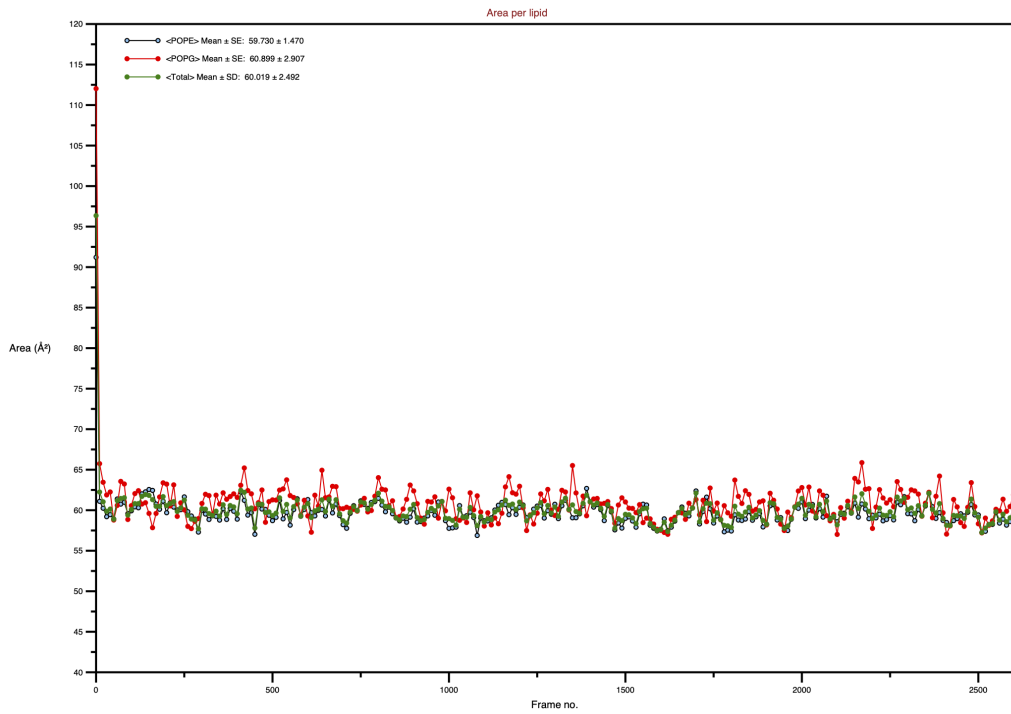
(c) *Parallel 3 of mrs-002 + membrane*



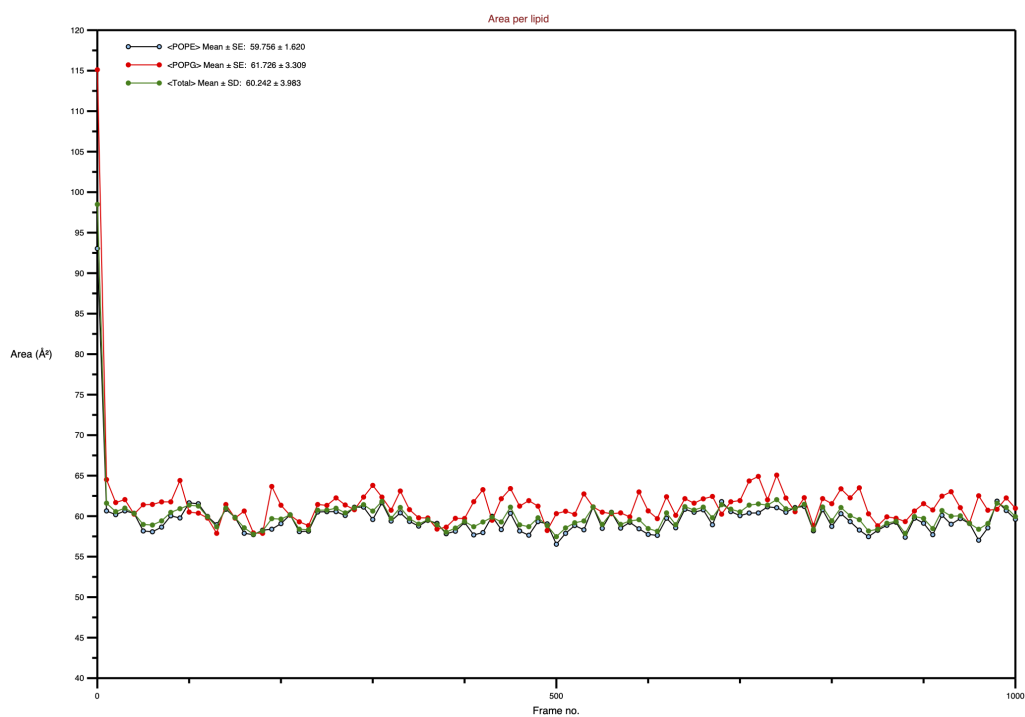
(d) *Parallel 1 of tkbs-013 + membrane*



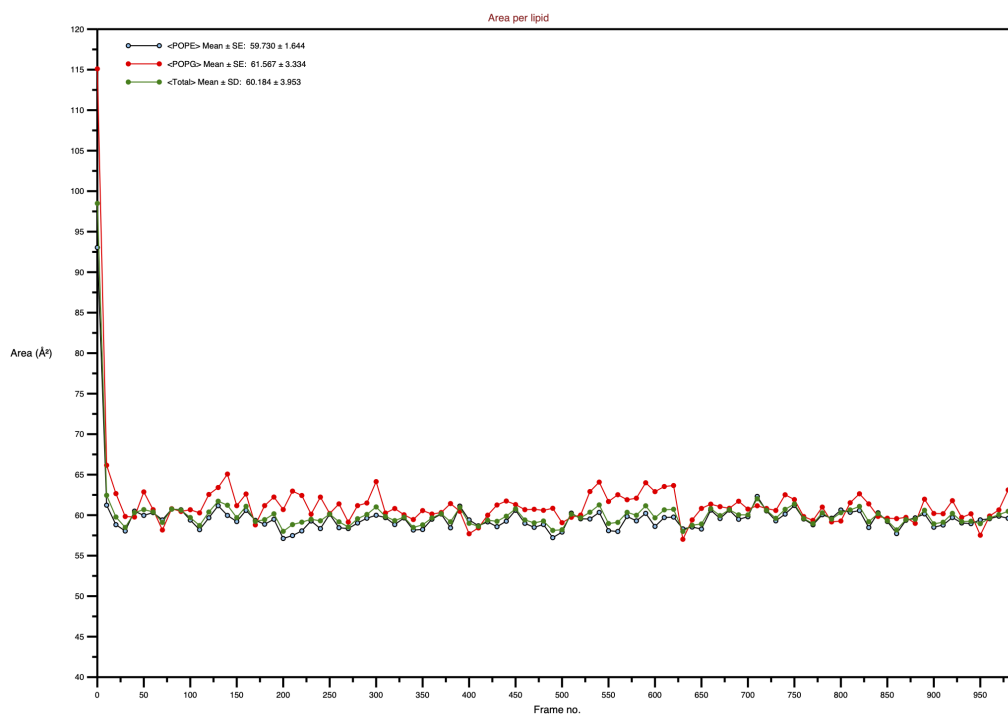
(e) Parallel 2 of tkbs-013 + membrane



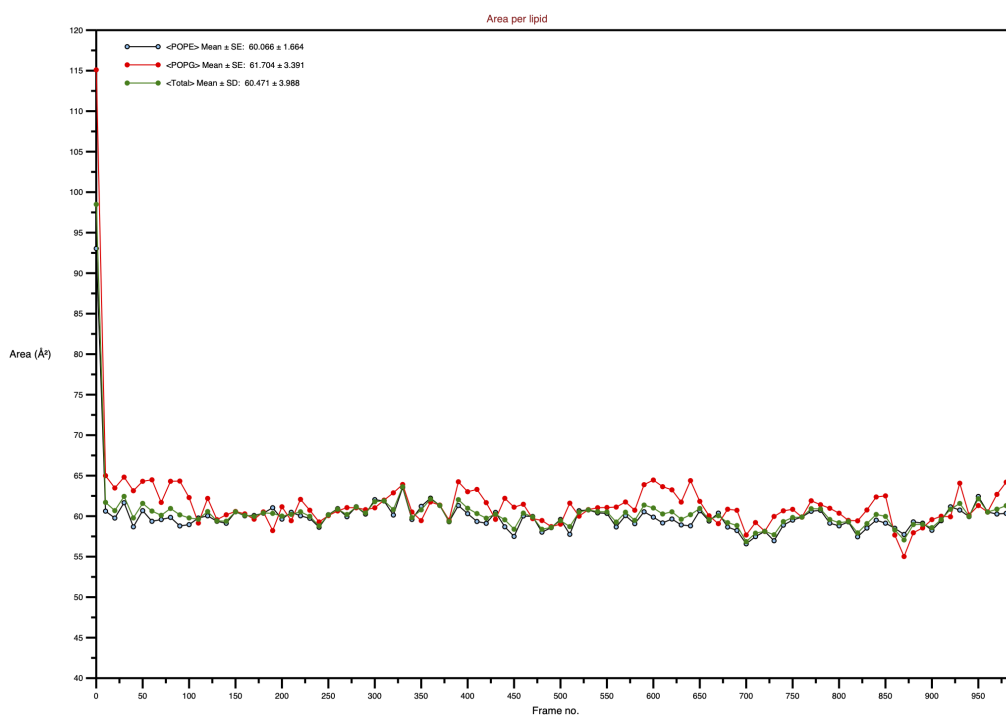
(f) Parallel 3 of tkbs-013 + membrane



(g) *Parallel 1 of membrane-only*



(h) *Parallel 2 of membrane-only*

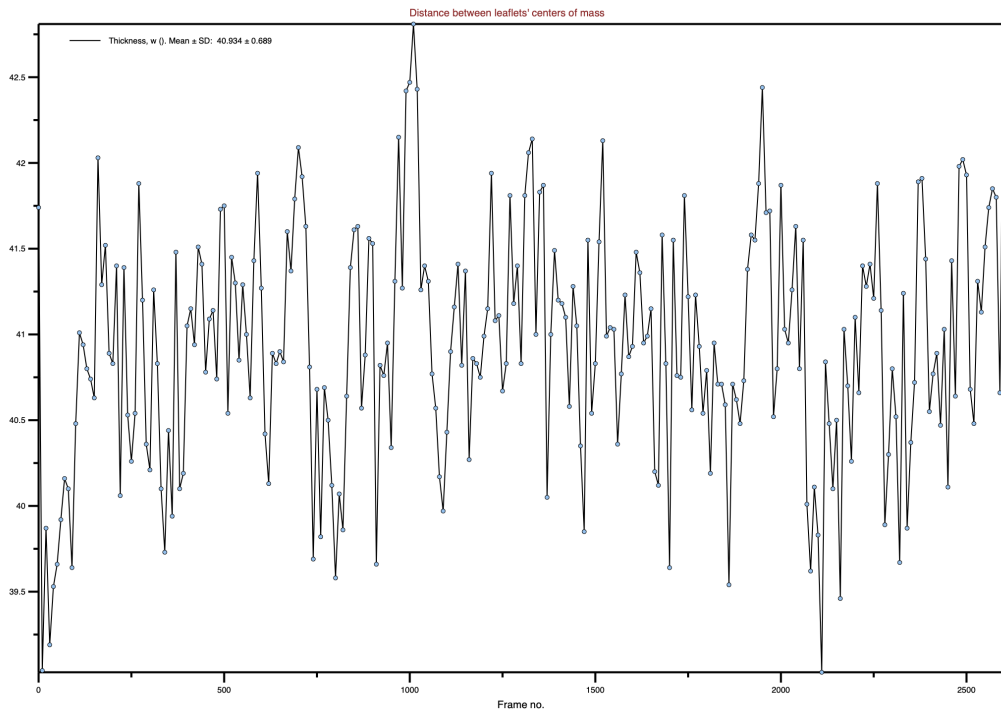
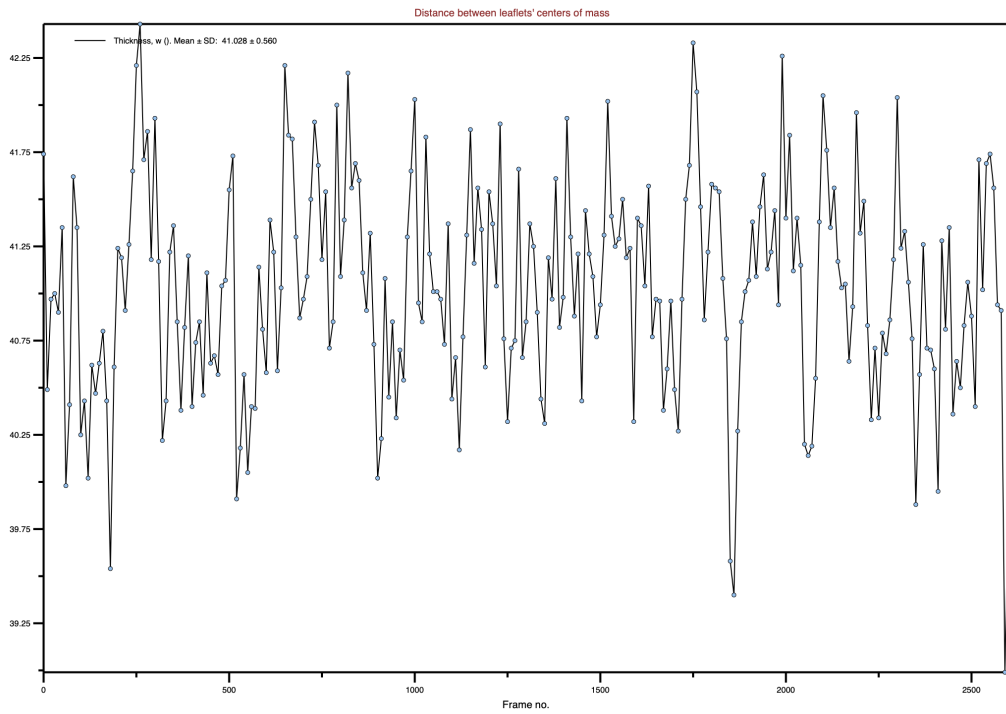


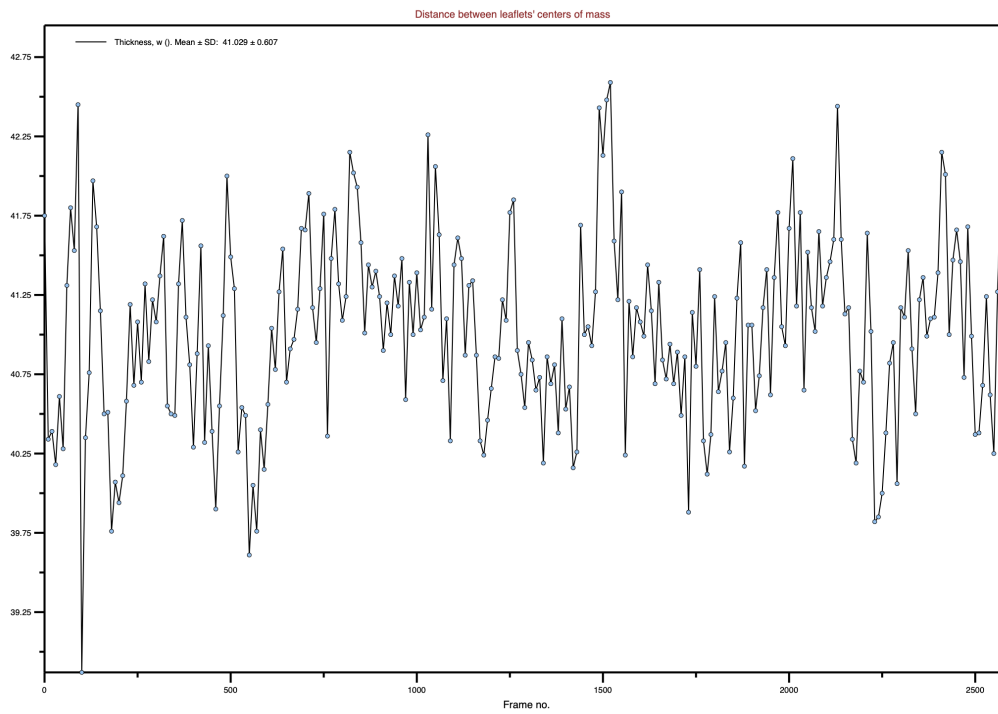
(i) *Parallel 3 of membrane-only*

Figure D.1: *Calculated area per lipid for both peptide+membrane and membrane-only systems. This includes calculations for POPE, POPG and for all lipids in the system over the simulation.*

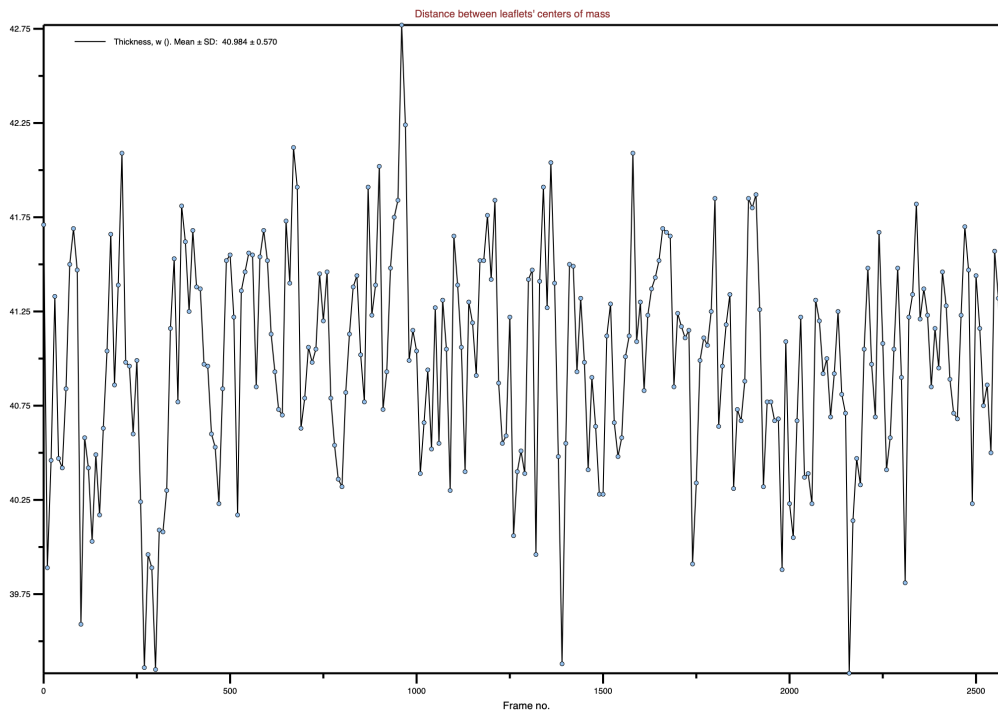
Appendix E

Calculated average membrane thickness during simulation

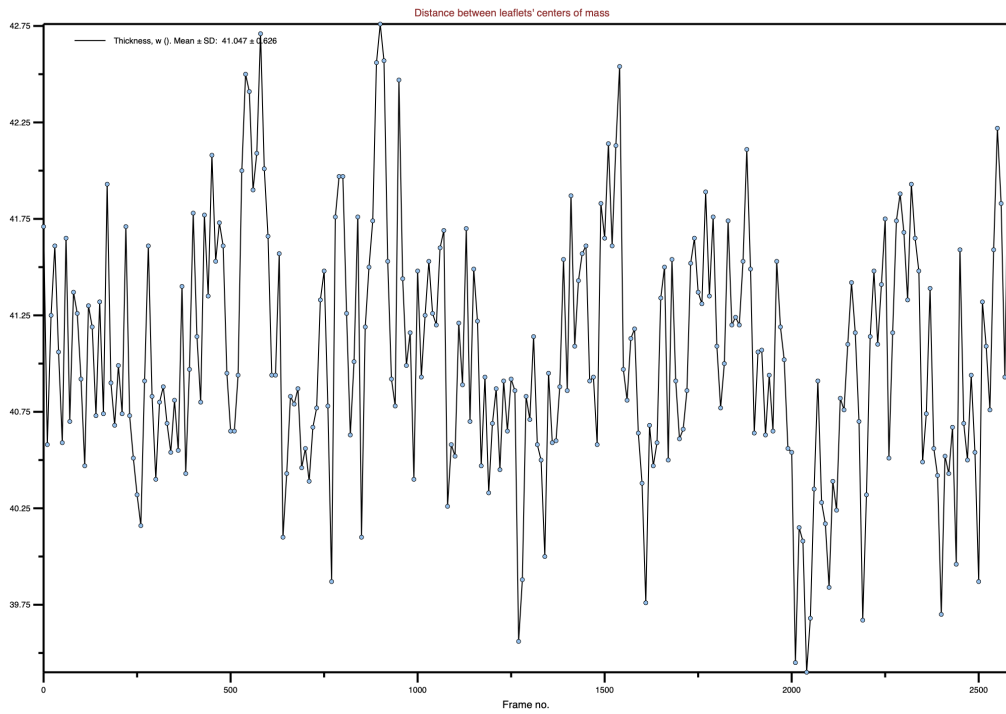
(a) *Parallel 1 of mrs-002 + membrane*(b) *Parallel 2 of mrs-002 + membrane*



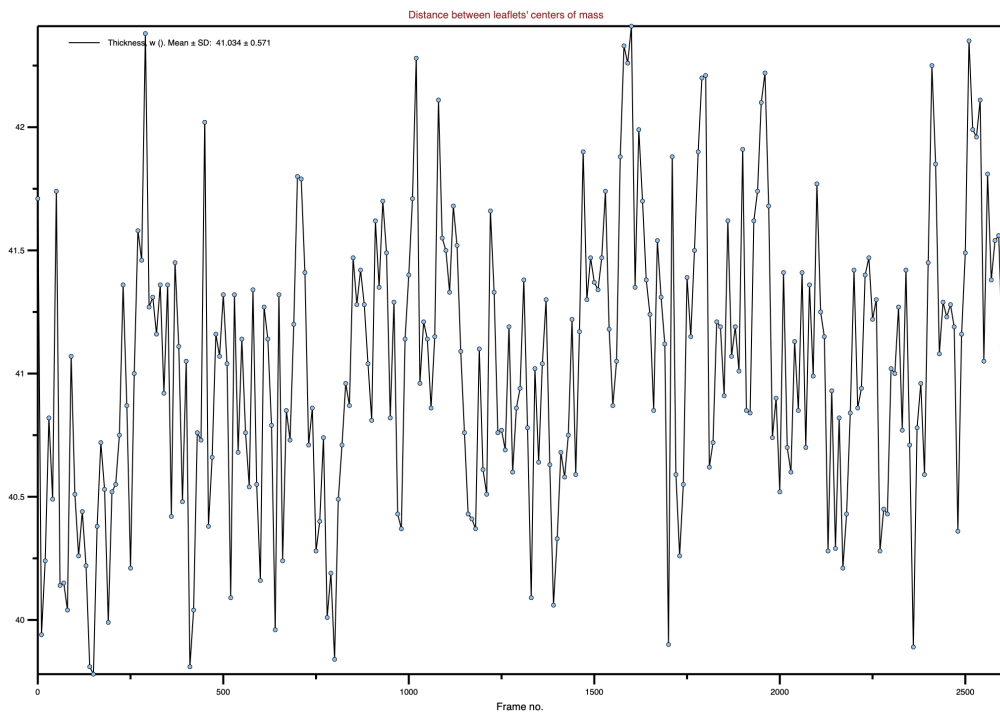
(c) *Parallel 3 of mrs-002 + membrane*



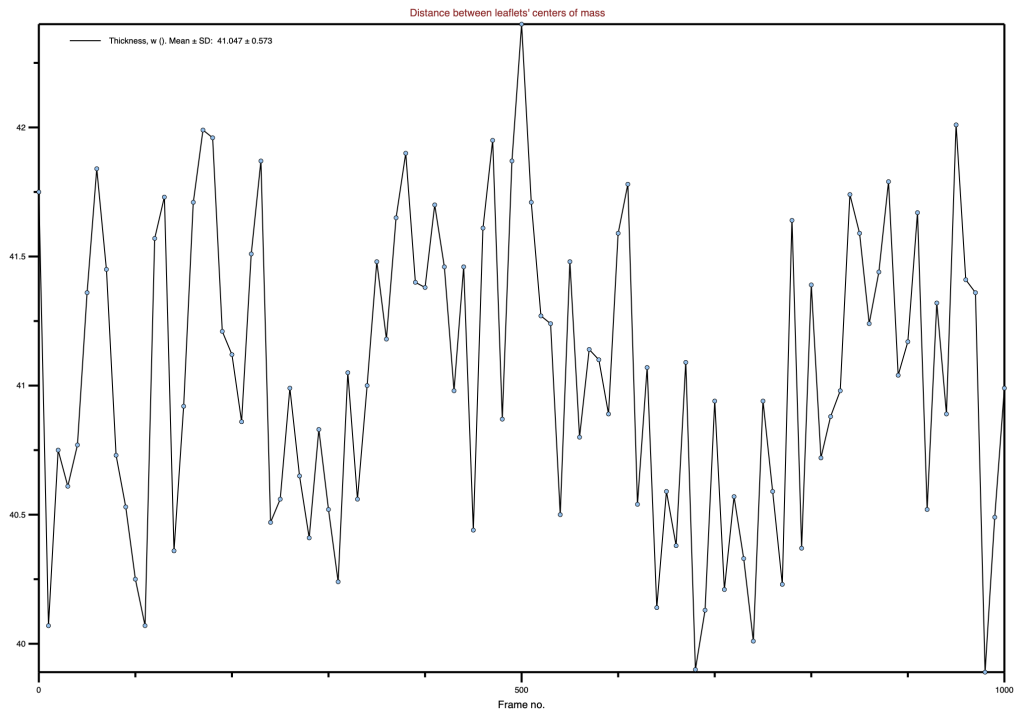
(d) *Parallel 1 of tkbs-013 + membrane*



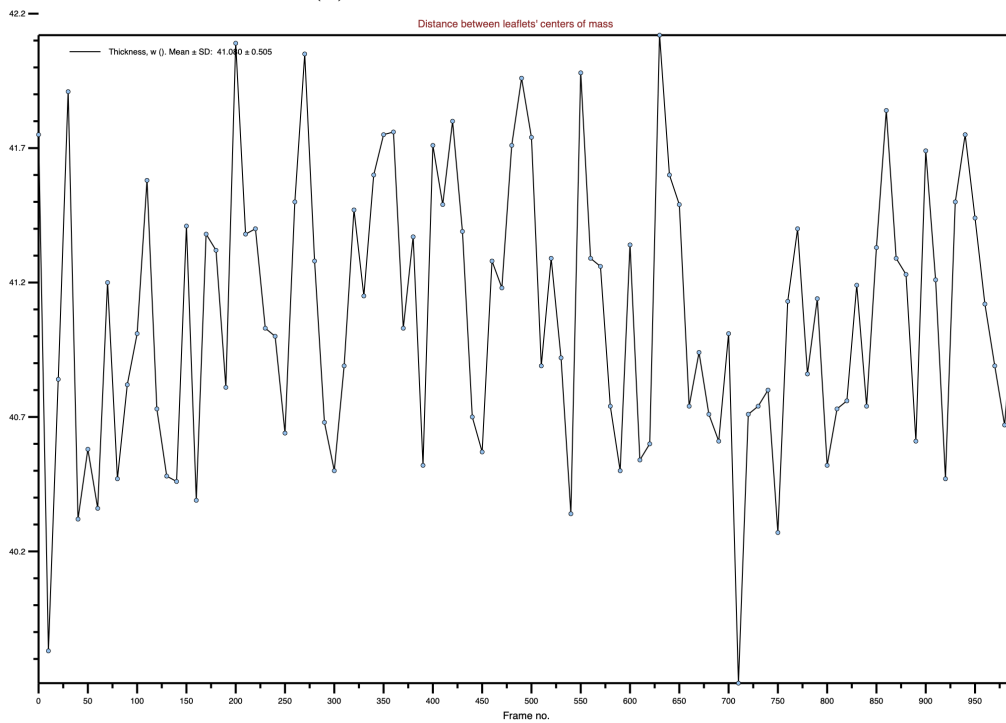
(e) *Parallel 2 of tkbs-013 + membrane*



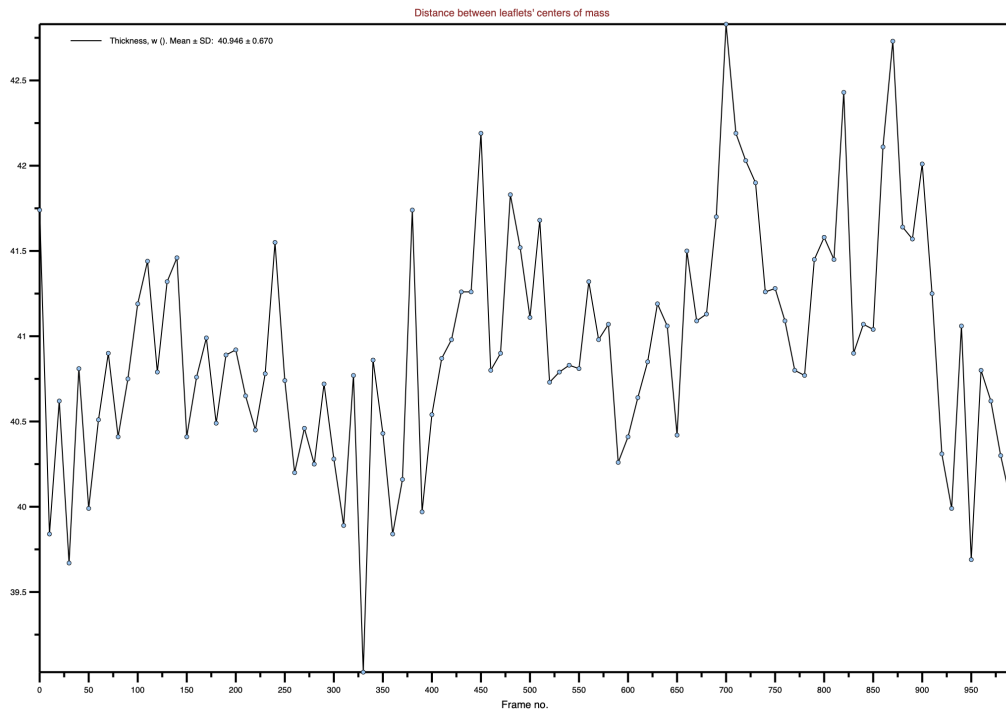
(f) *Parallel 3 of tkbs-013 + membrane*



(g) *Parallel 1 of membrane-only*



(h) *Parallel 2 of membrane-only*

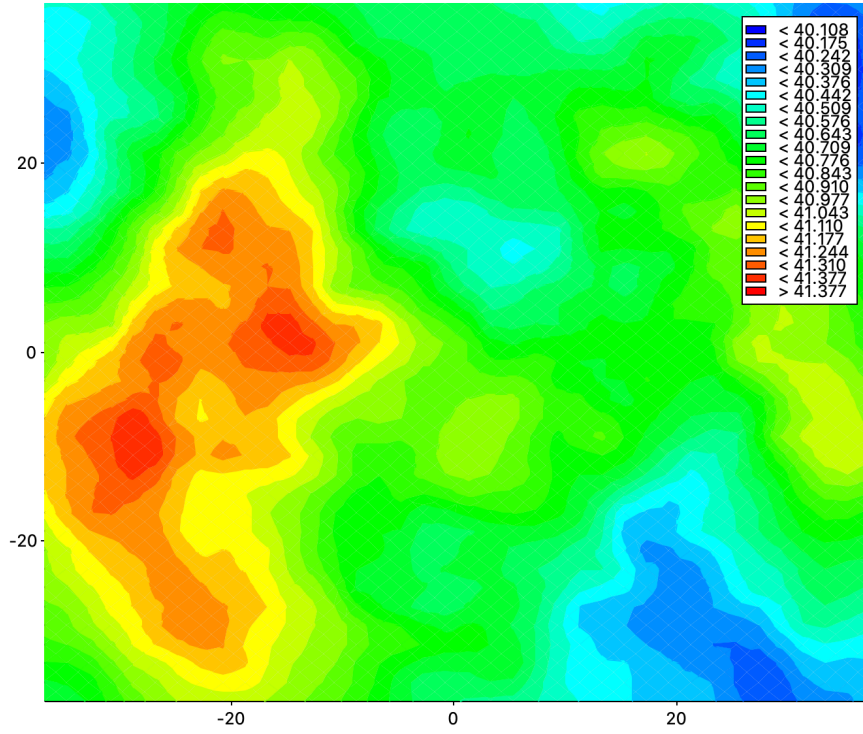
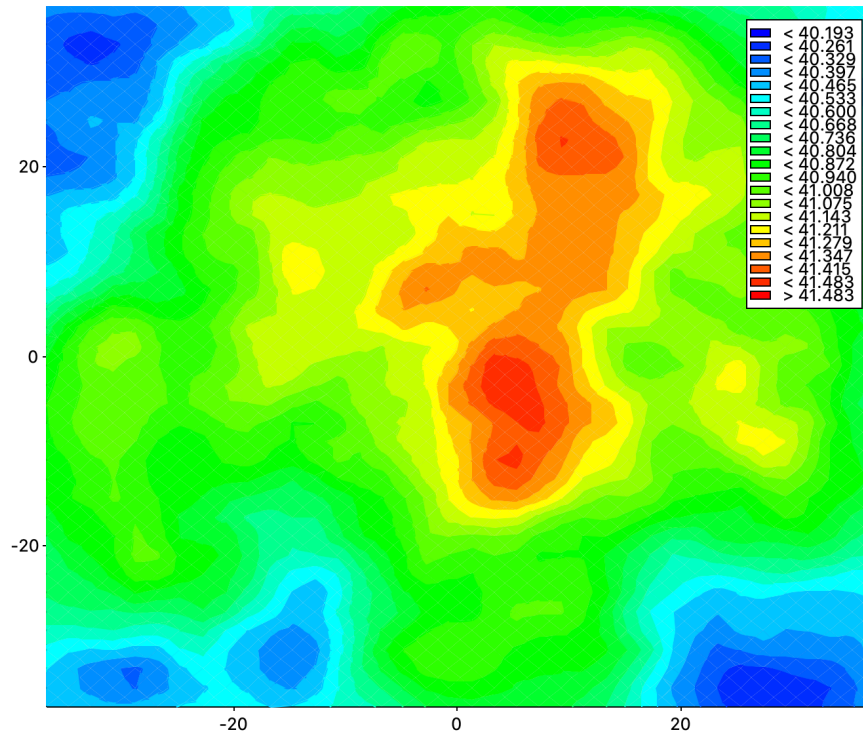


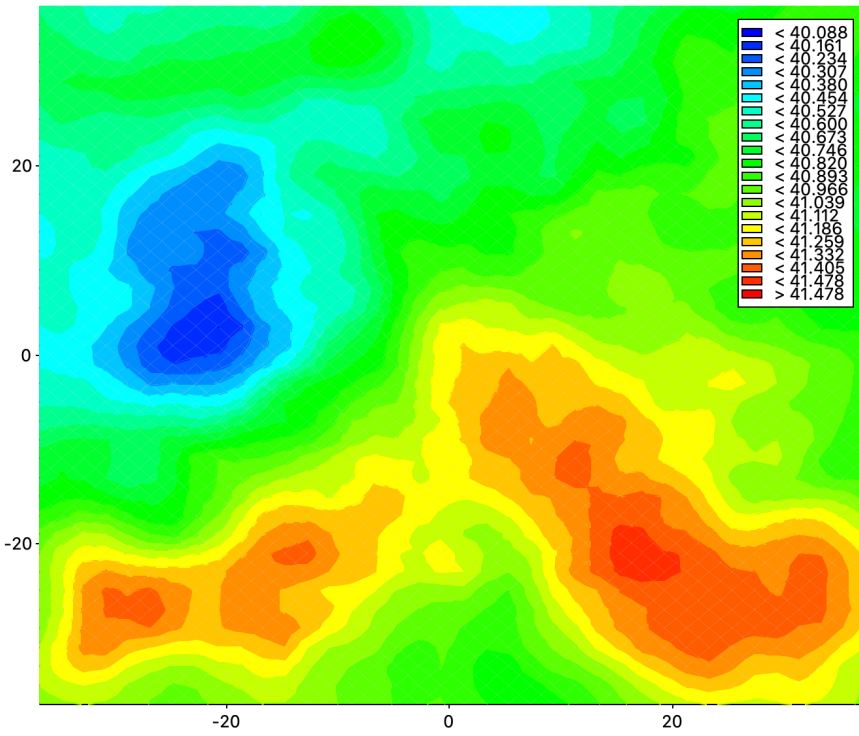
(i) *Parallel 3 of membrane-only*

Figure E.1: *Calculated average thickness of the membrane over the simulation period for peptide+membrane and membrane-only systems.*

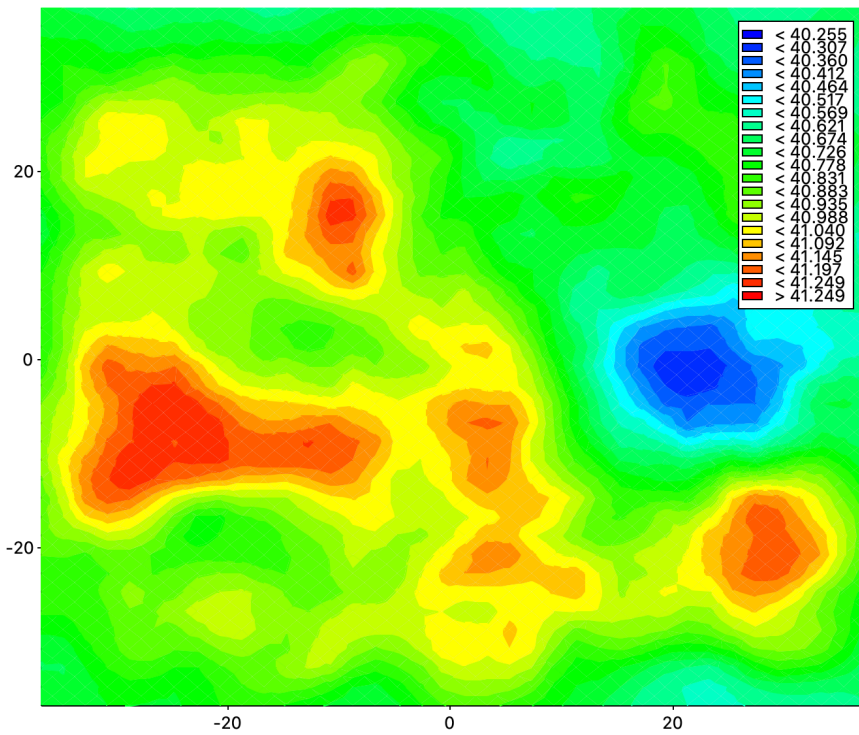
Appendix F

Calculated variance of
membrane thickness for
peptide+membrane and
membrane-only systems.

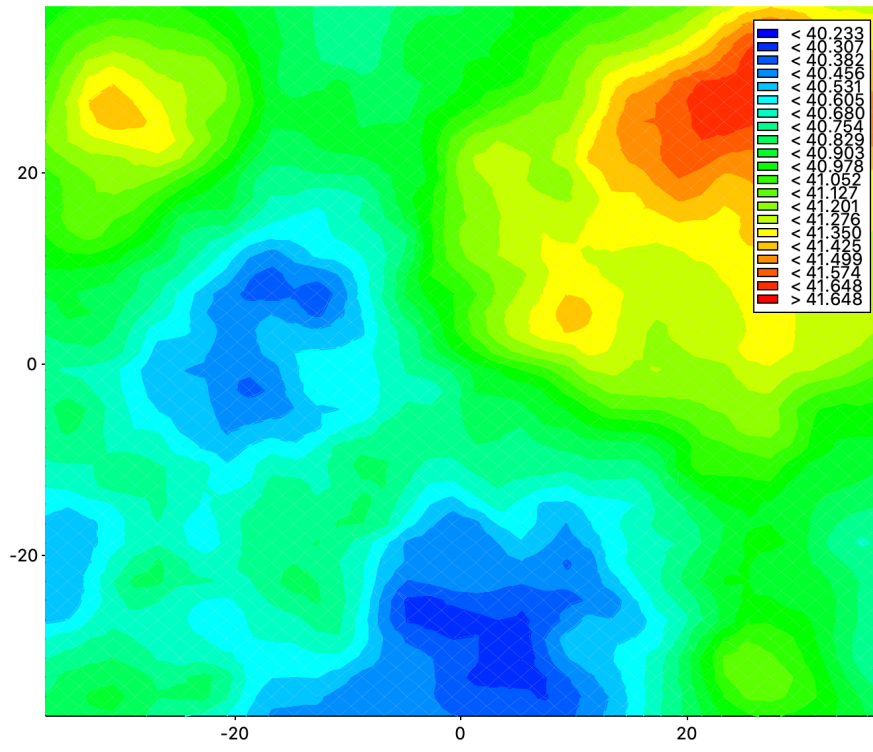
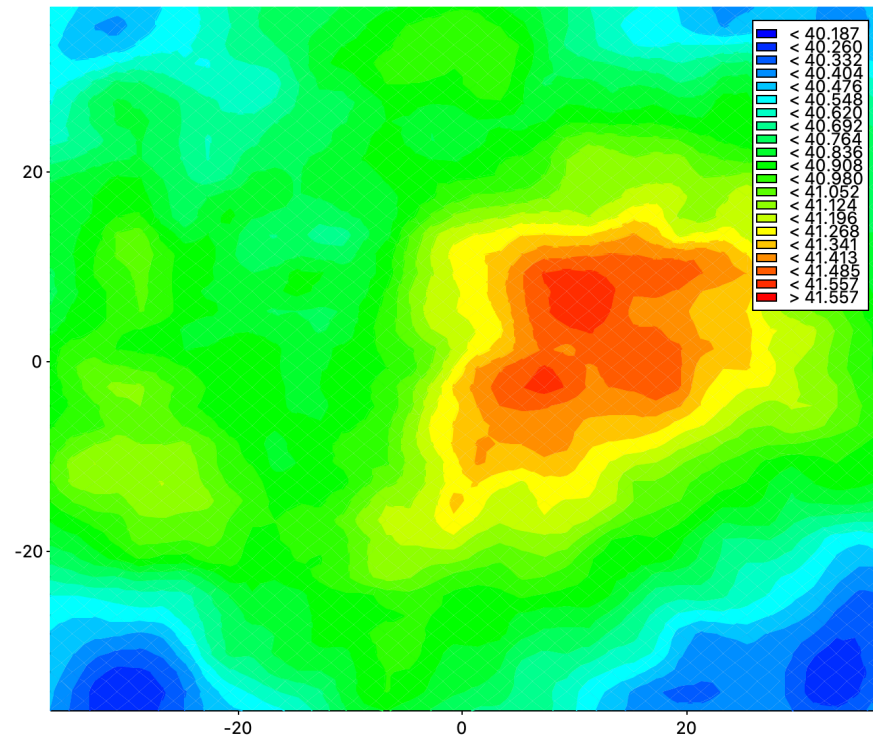
(a) *Parallel 1 of mrs-002 + membrane*(b) *Parallel 2 of mrs-002 + membrane*

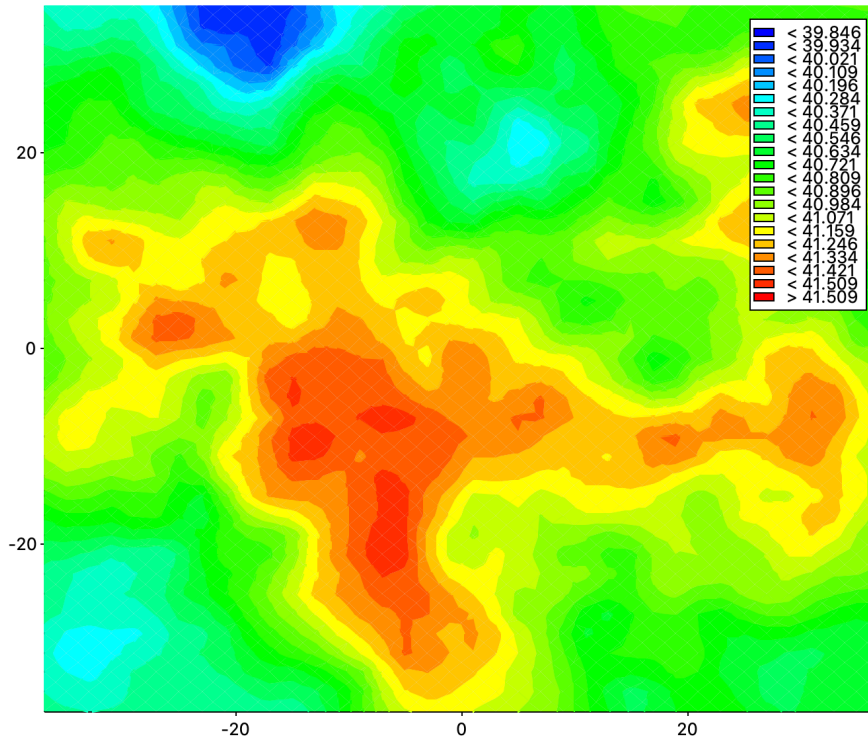


(c) *Parallel 3 of mrs-002 + membrane*

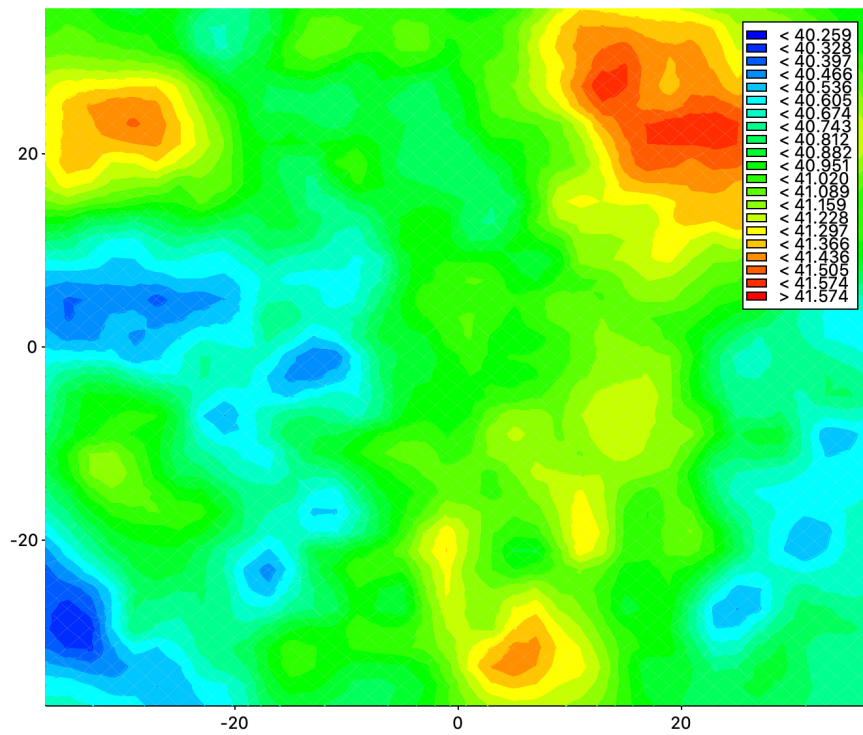


(d) *Parallel 1 of tkbs-013 + membrane*

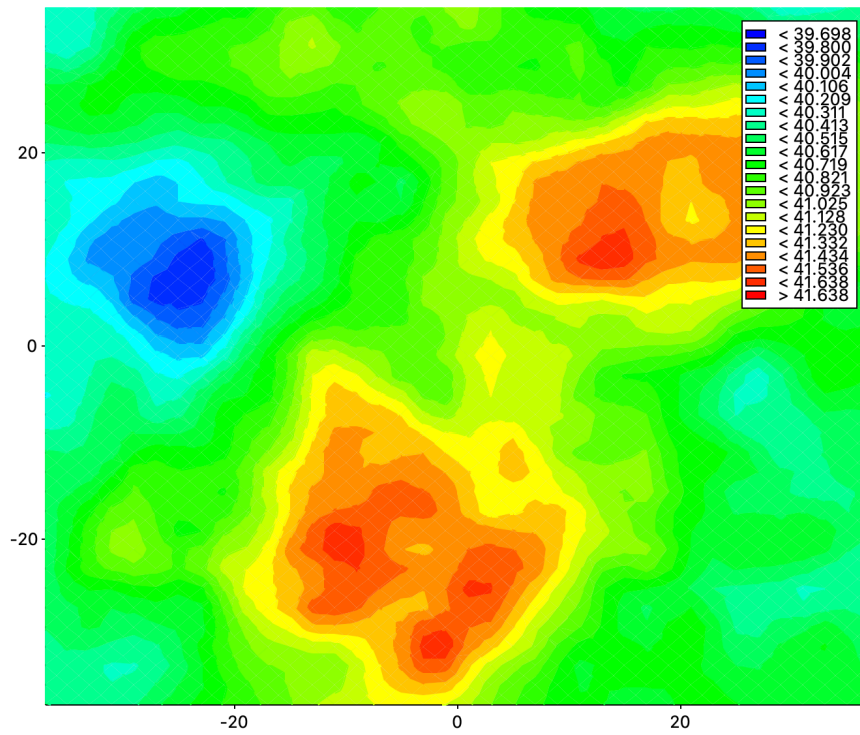
(e) *Parallel 2 of tkbs-013 + membrane*(f) *Parallel 3 of tkbs-013 + membrane*



(g) *Parallel 1 of membrane-only*



(h) *Parallel 2 of membrane-only*

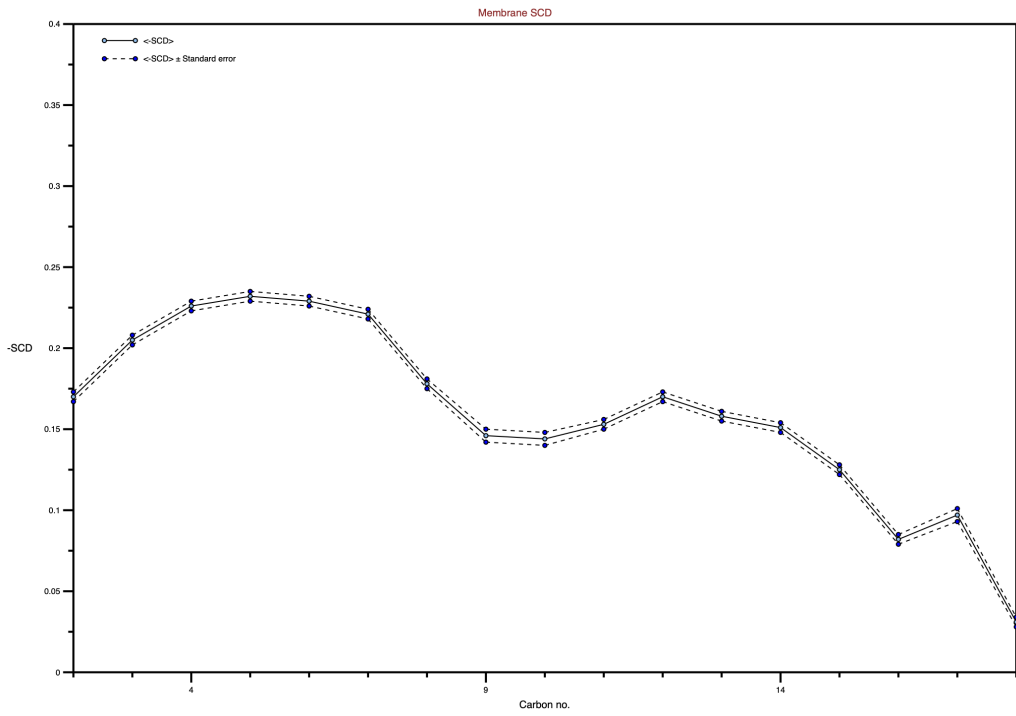
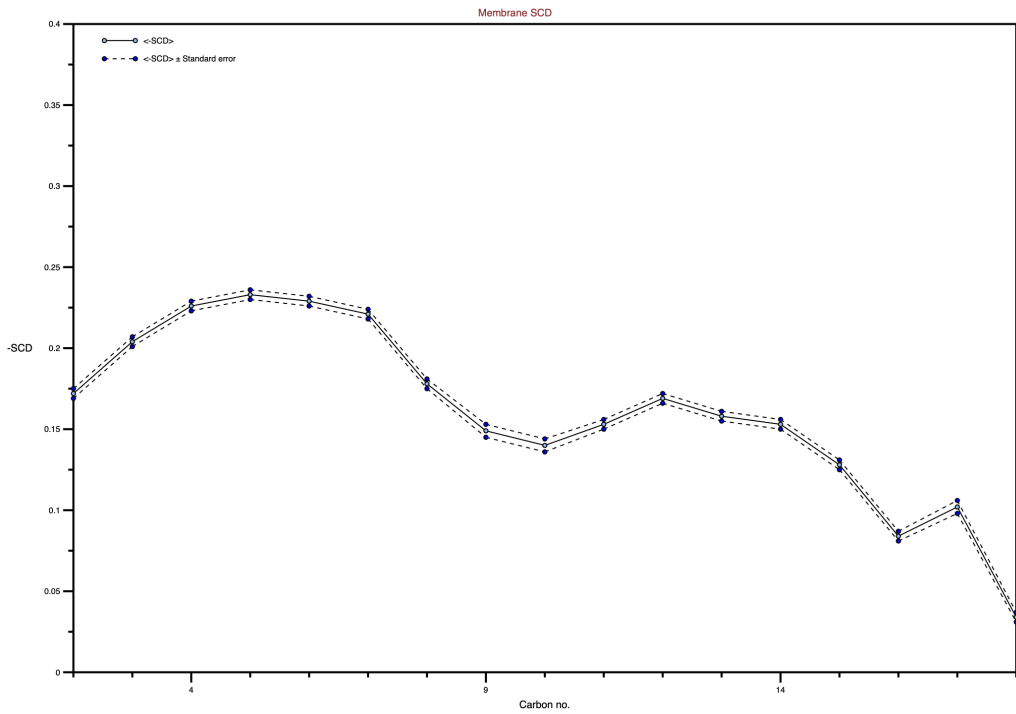


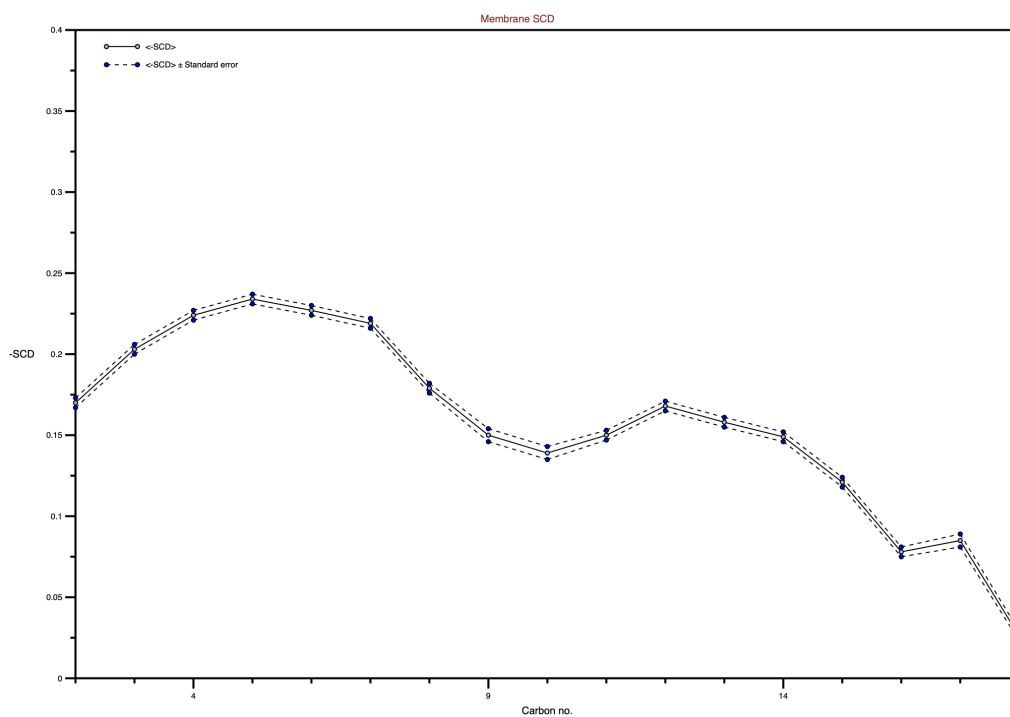
(i) Parallel 3 of membrane-only

Figure F.1: Calculated membrane thickness for simulation period, with variation from average shown in red and blue. The figures are calculated from peptide+membrane and membrane-only system simulations.

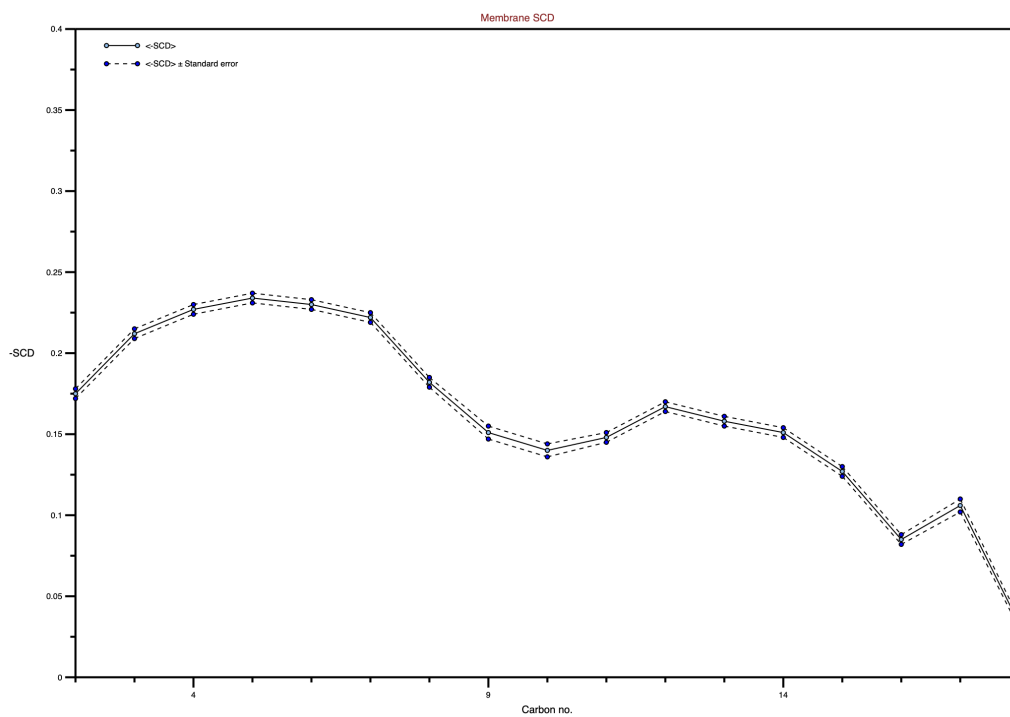
Appendix G

Calculated S_{CD} for
peptide+membrane and
membrane-only systems

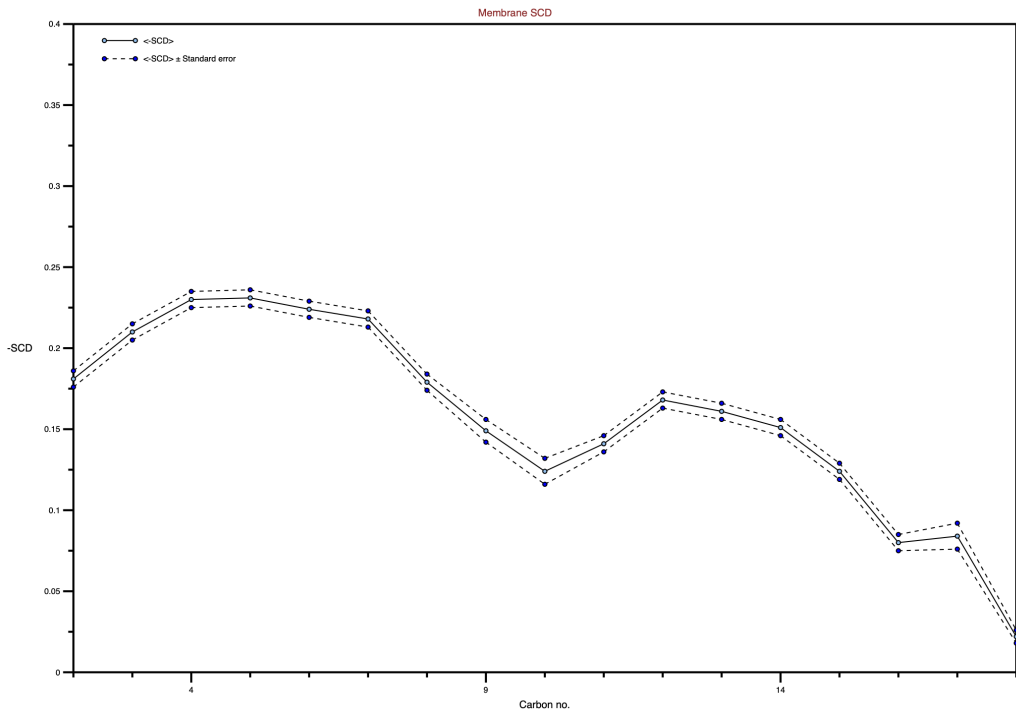
(a) *Parallel 1 of mrs-002 + membrane*(b) *Parallel 2 of mrs-002 + membrane*



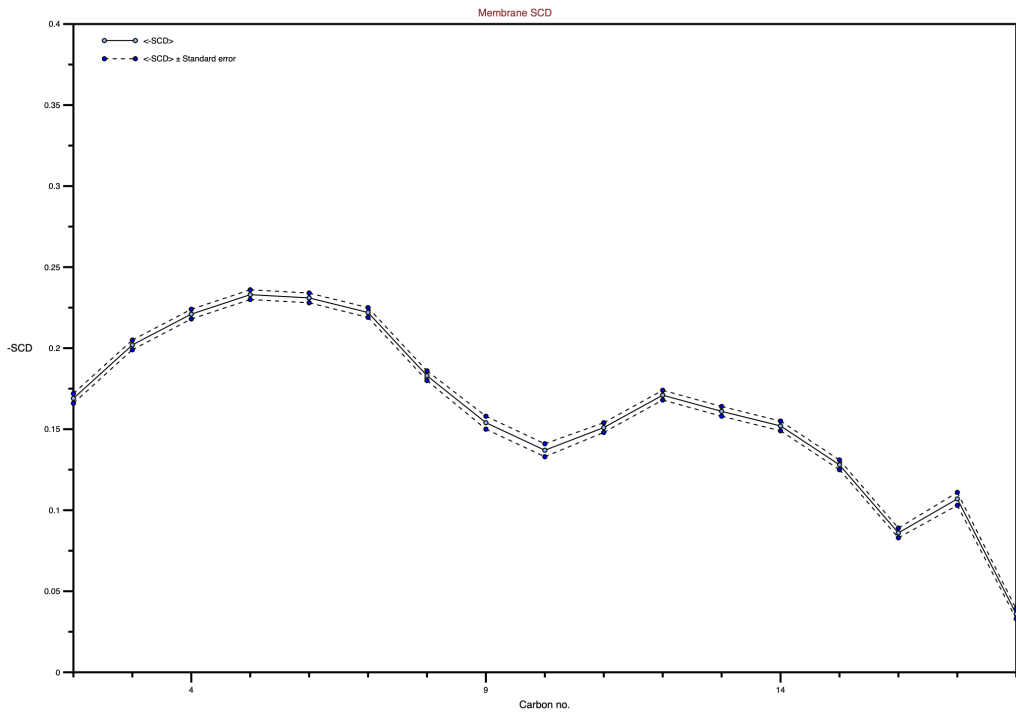
(c) *Parallel 3 of mrs-002 + membrane*



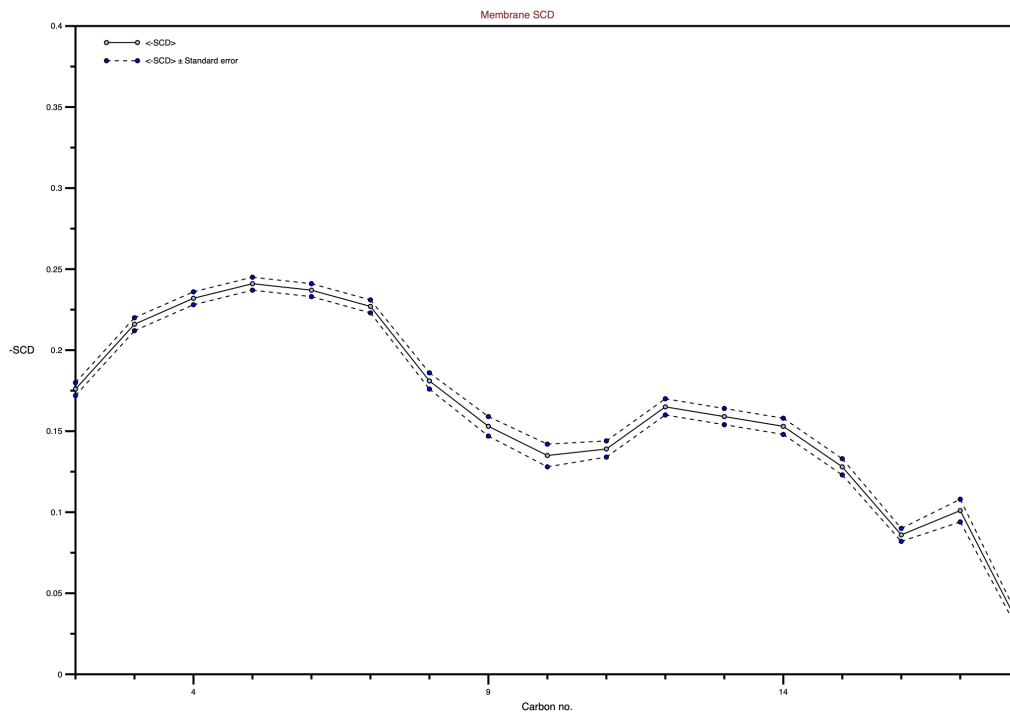
(d) *Parallel 1 of tkbs-013 + membrane*



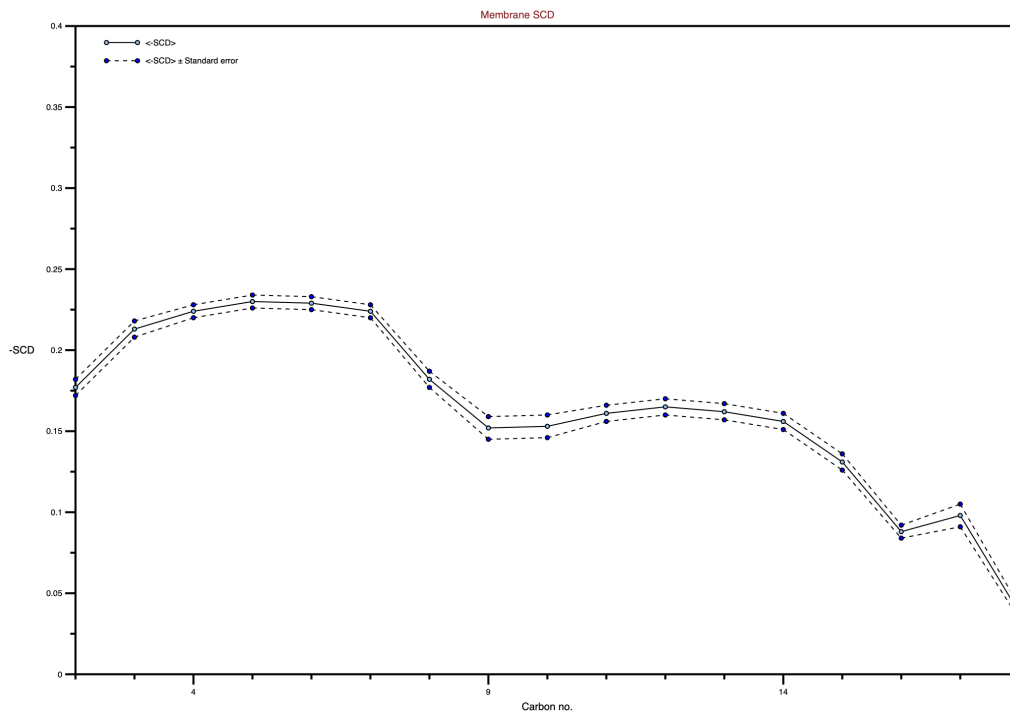
(e) Parallel 2 of tkbs-013 + membrane



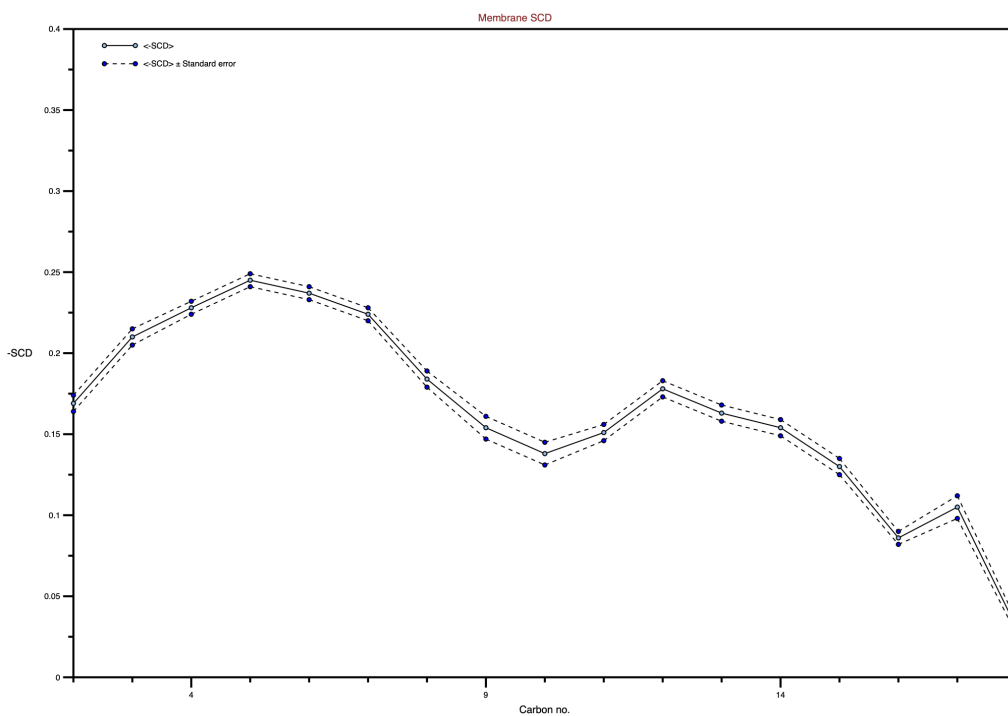
(f) Parallel 3 of tkbs-013 + membrane



(g) *Parallel 1 of membrane-only*

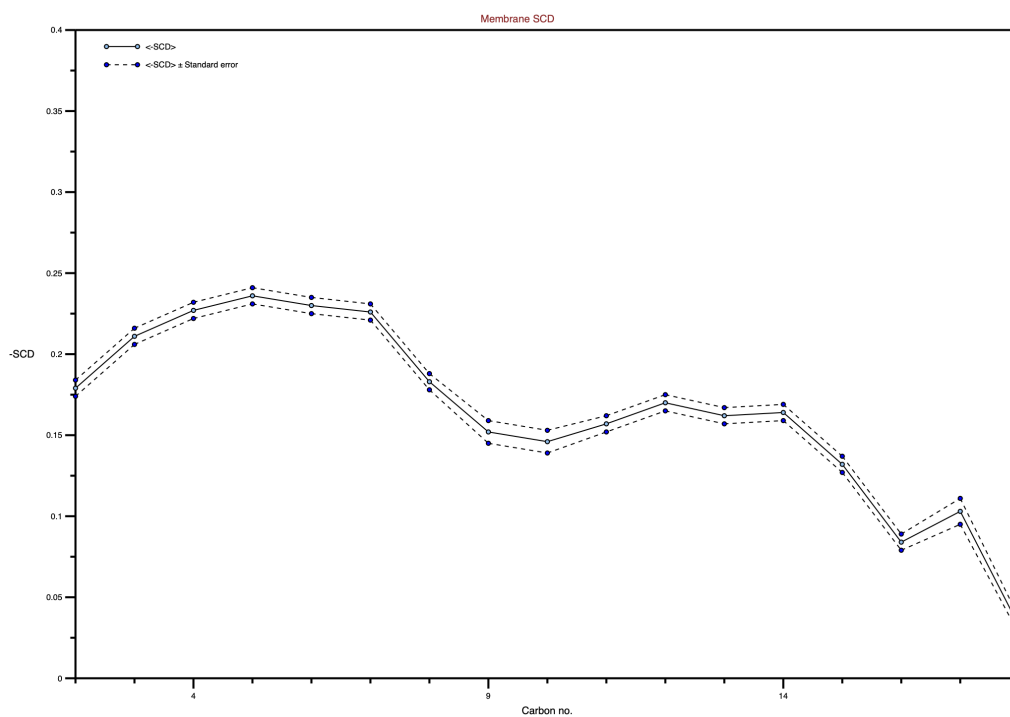
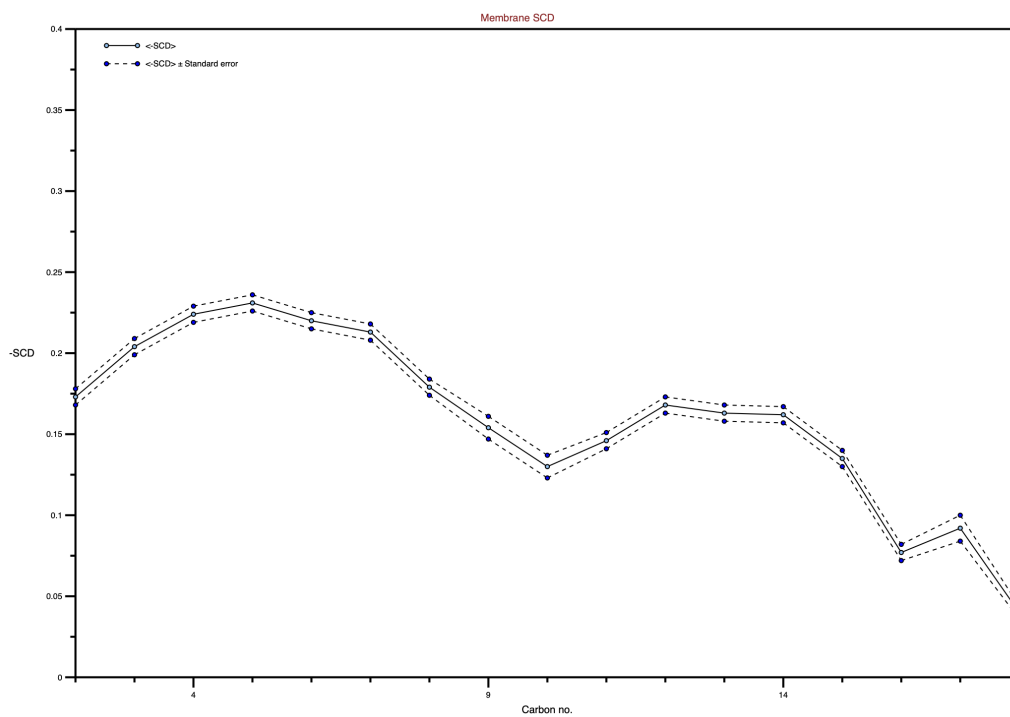


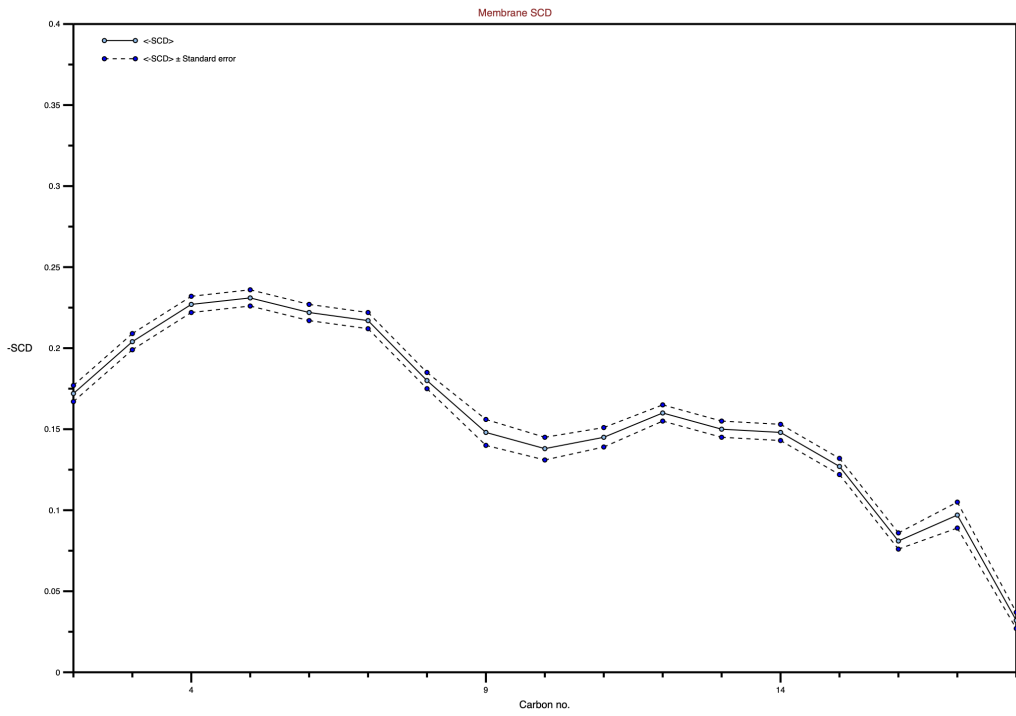
(h) *Parallel 2 of membrane-only*



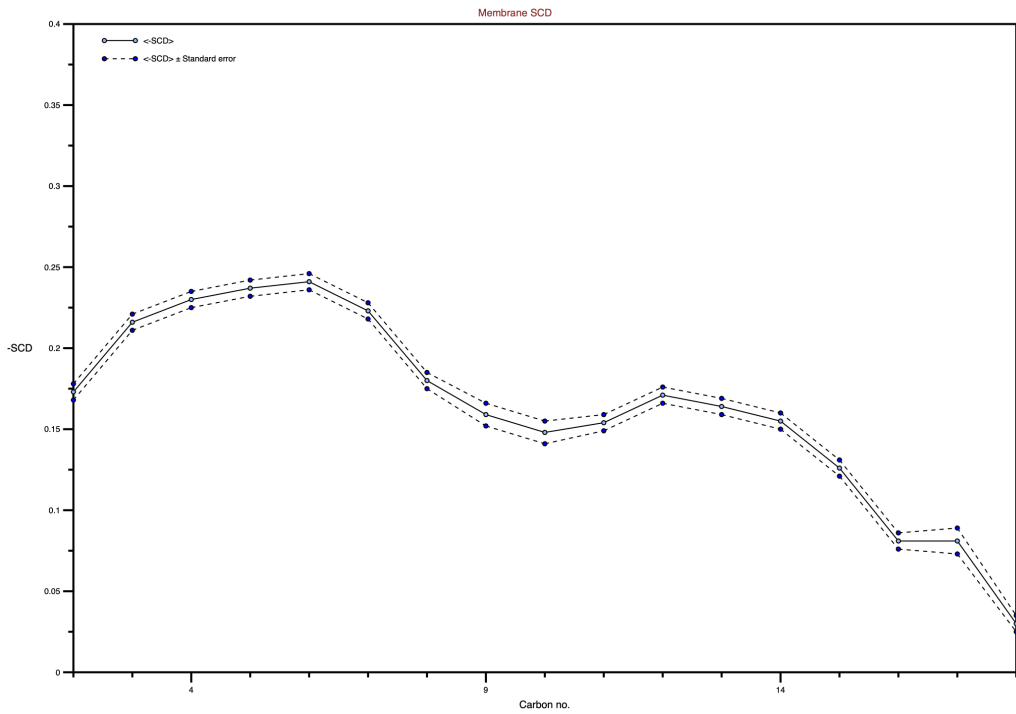
(i) Parallel 3 of membrane-only

Figure G.1: Calculated S_{CD} values for the POPE lipid in the membrane for all peptide+membrane and membrane systems.

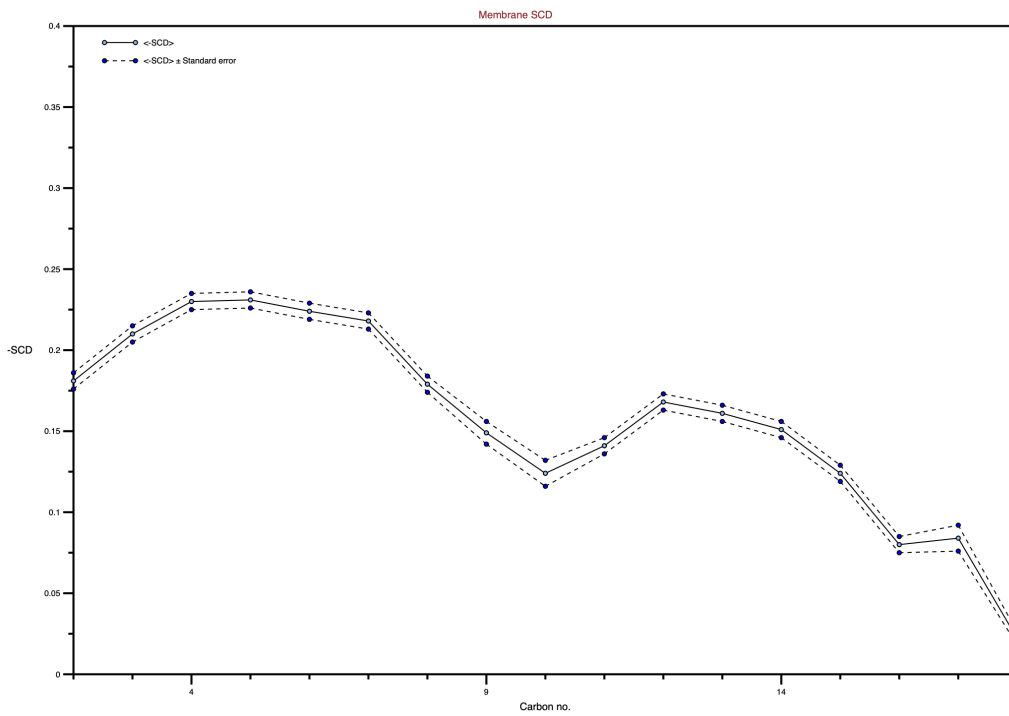
(a) *Parallel 1 of mrs-002 + membrane*(b) *Parallel 2 of mrs-002 + membrane*



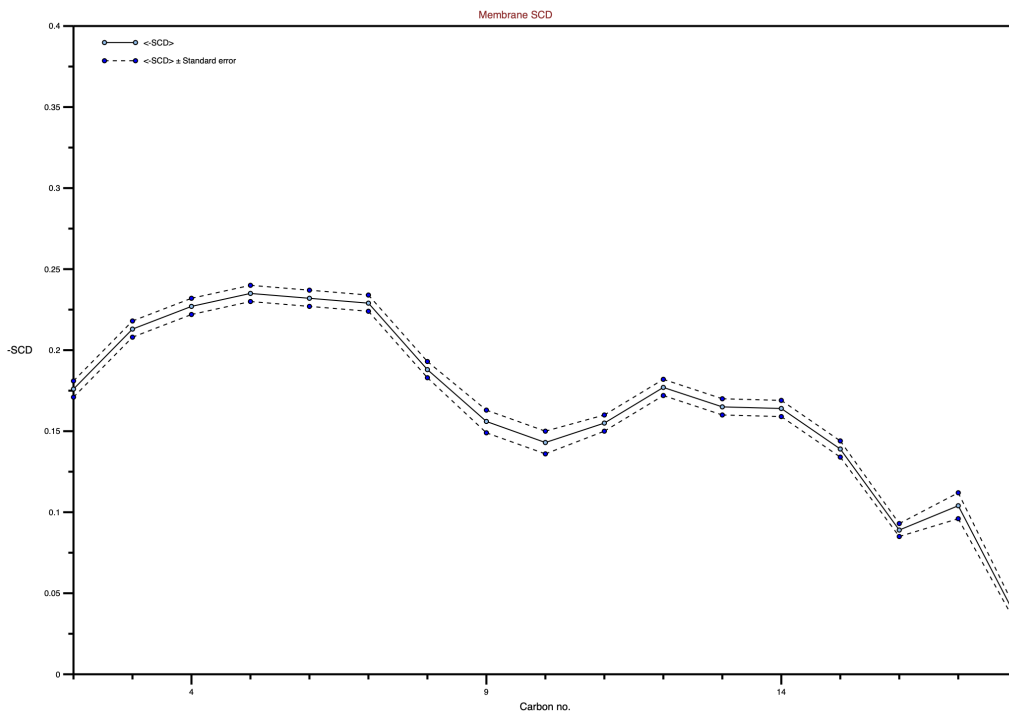
(c) *Parallel 3 of mrs-002 + membrane*



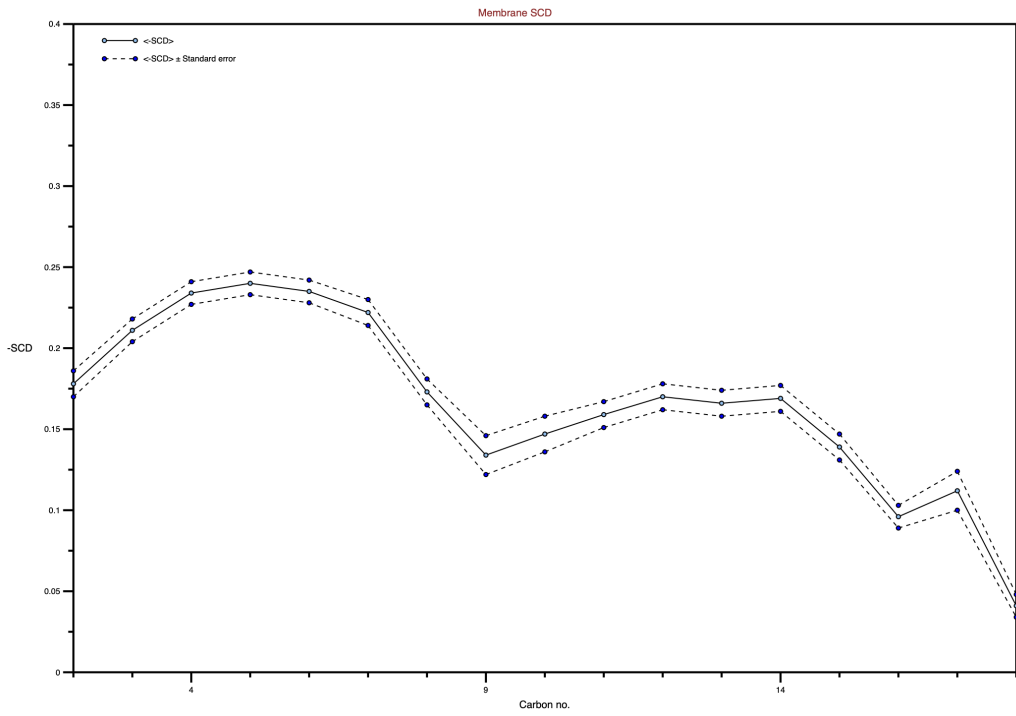
(d) *Parallel 1 of tkbs-013 + membrane*



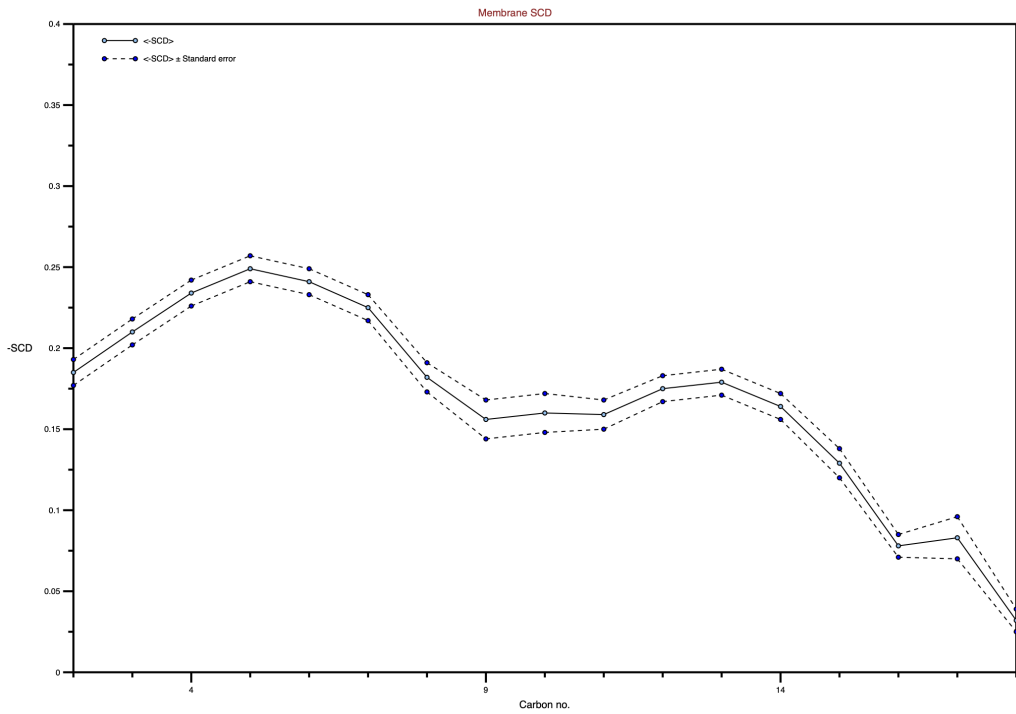
(e) Parallel 2 of tkbs-013 + membrane



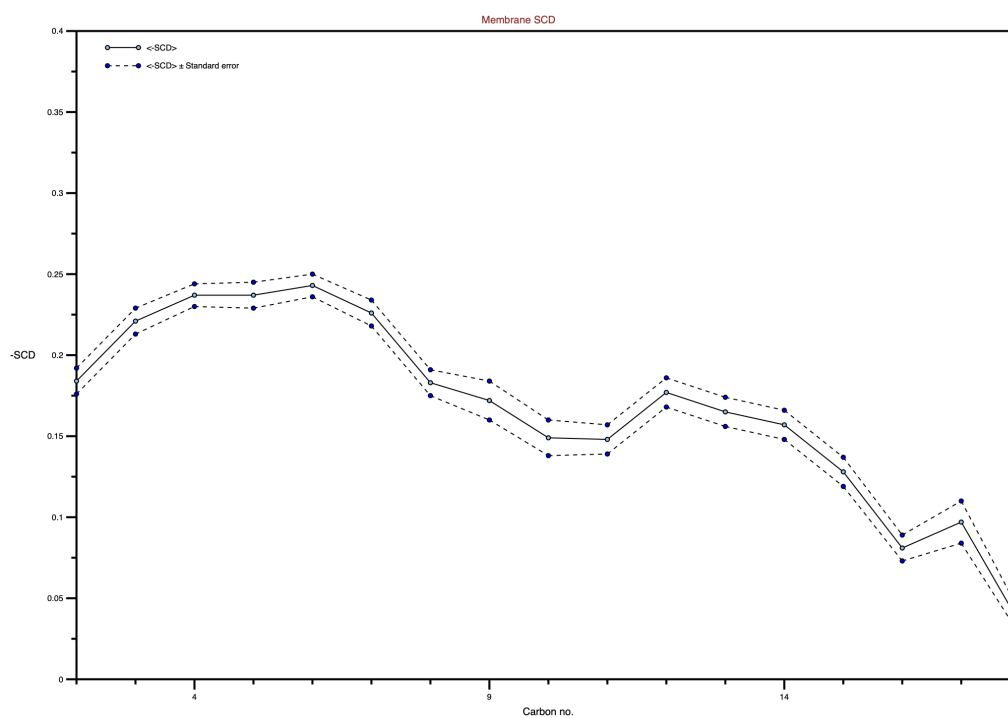
(f) Parallel 3 of tkbs-013 + membrane



(g) *Parallel 1 of membrane-only*

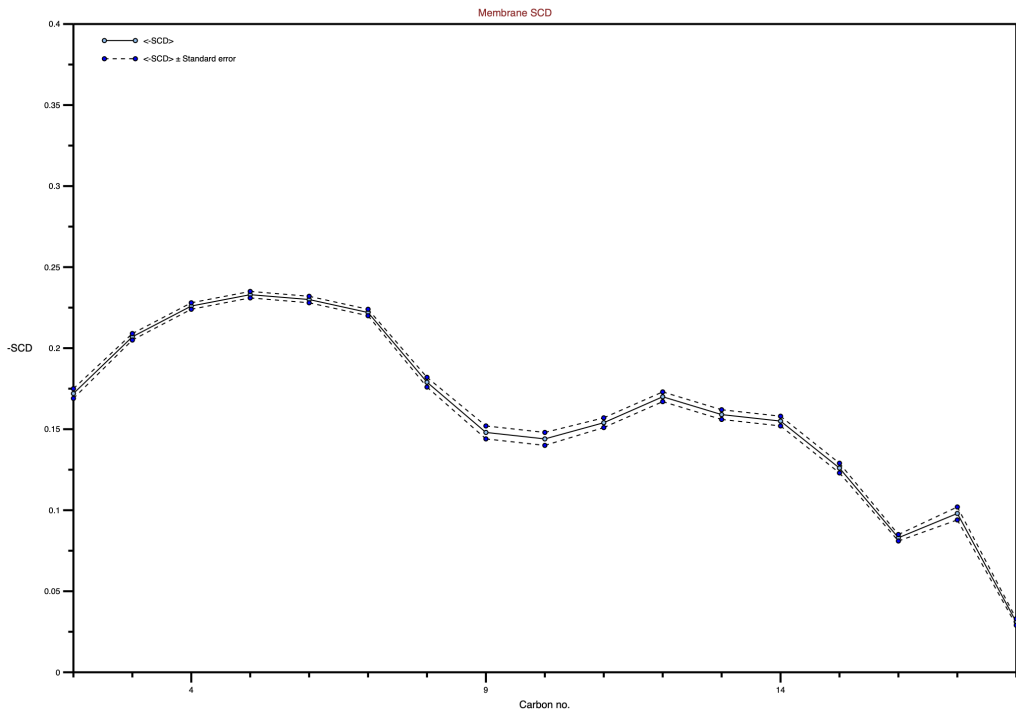
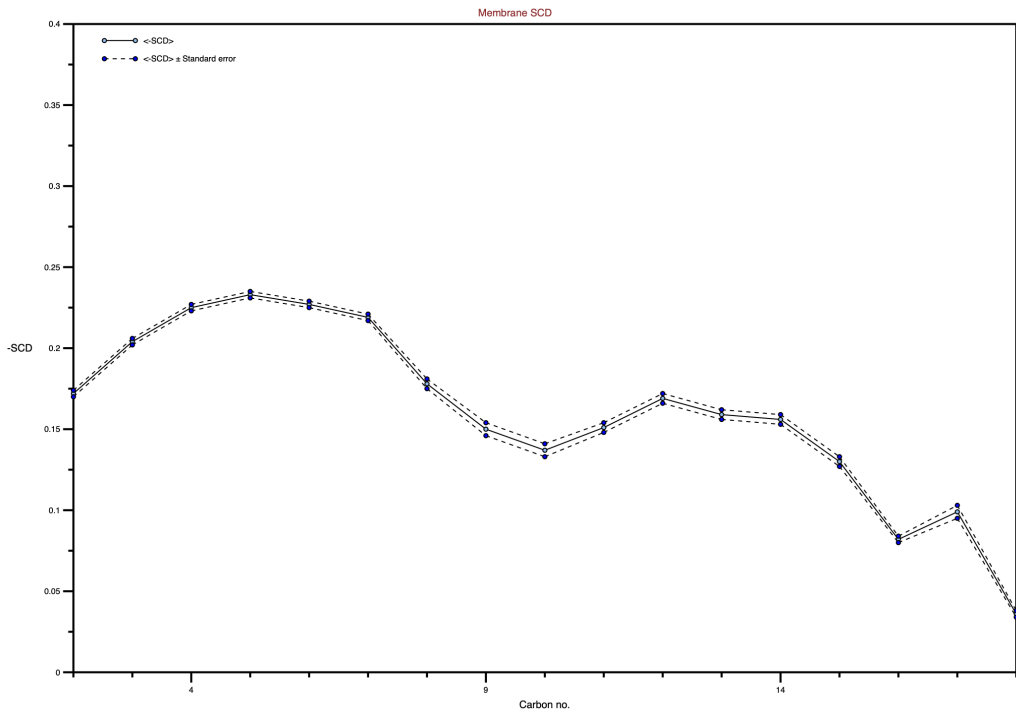


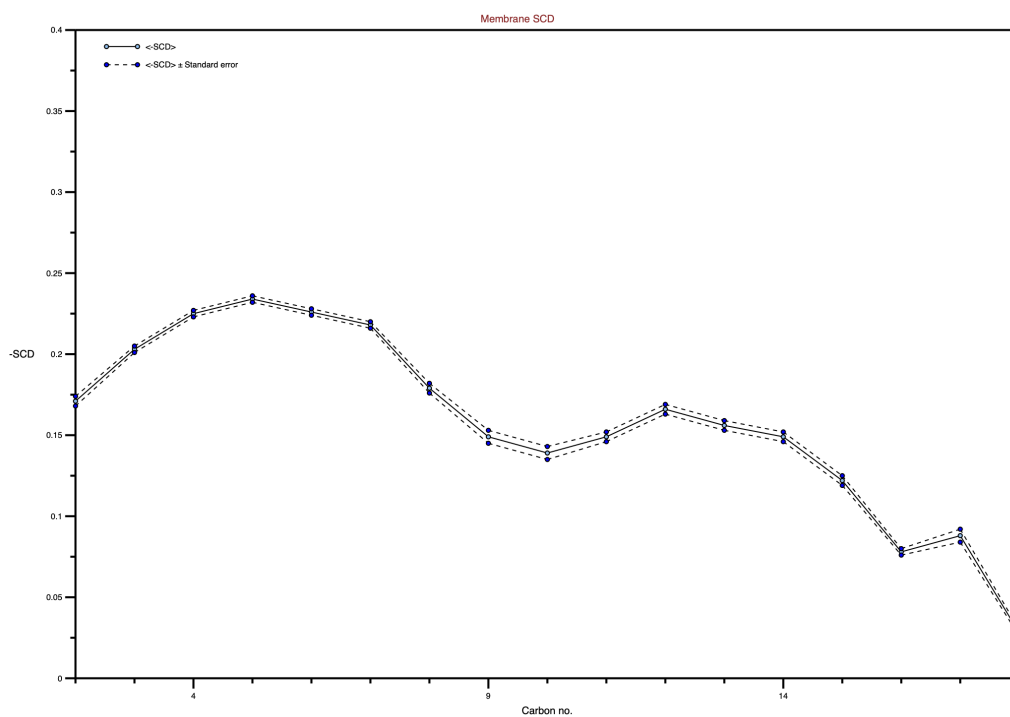
(h) *Parallel 2 of membrane-only*



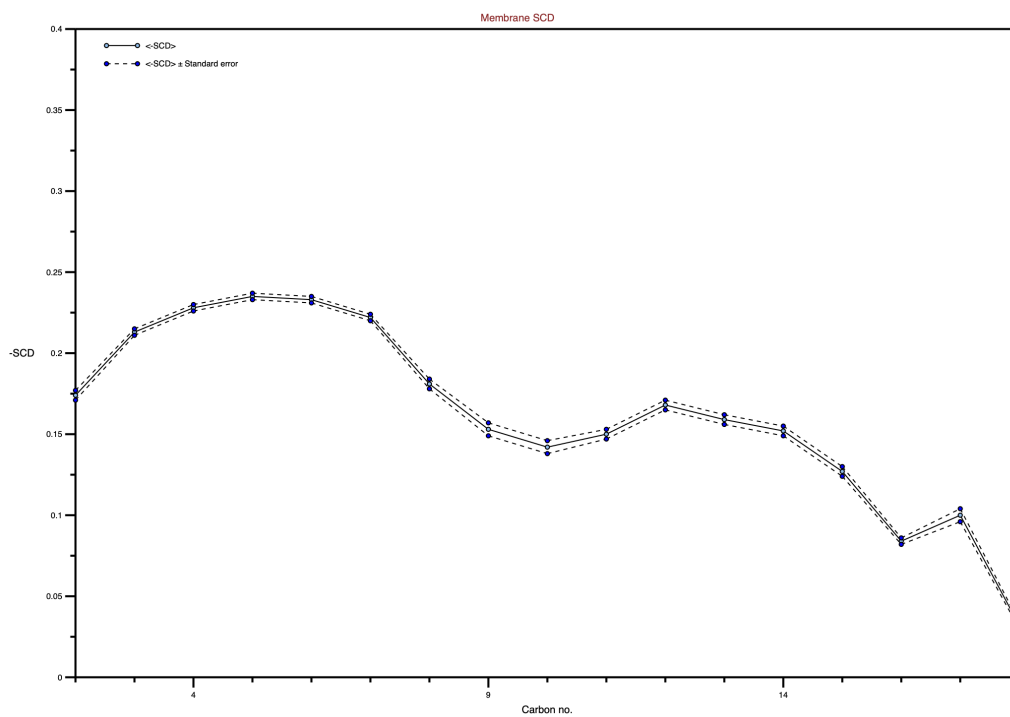
(i) Parallel 3 of membrane-only

Figure G.2: Calculated S_{CD} values for the POPG lipid in the membrane for all peptide+membrane and membrane systems.

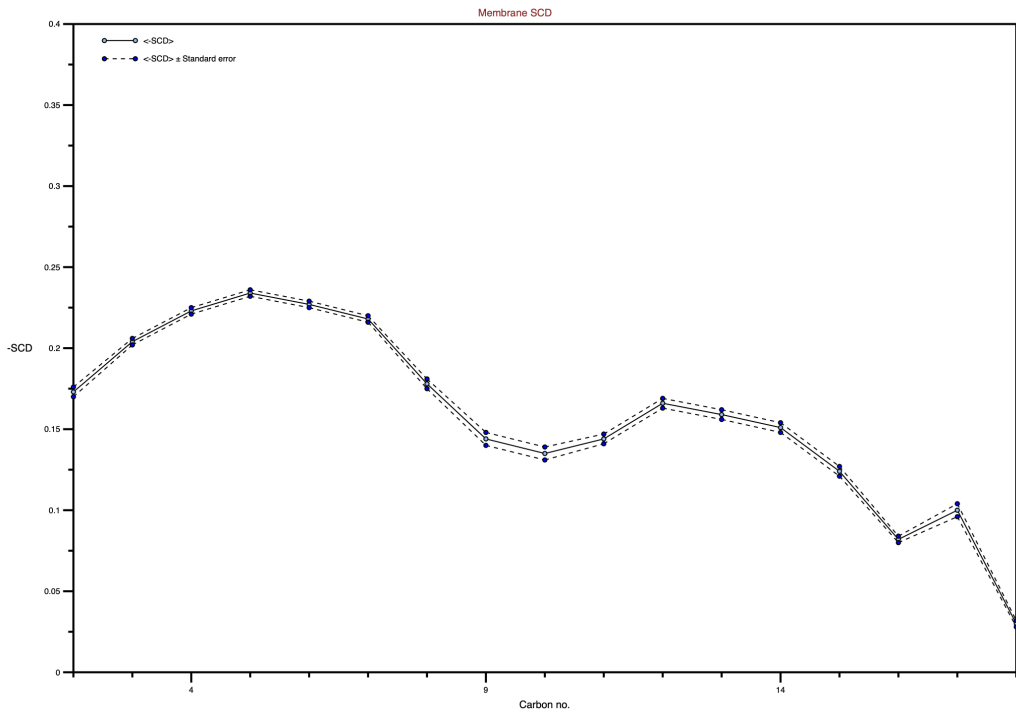
(a) *Parallel 1 of mrs-002 + membrane*(b) *Parallel 2 of mrs-002 + membrane*



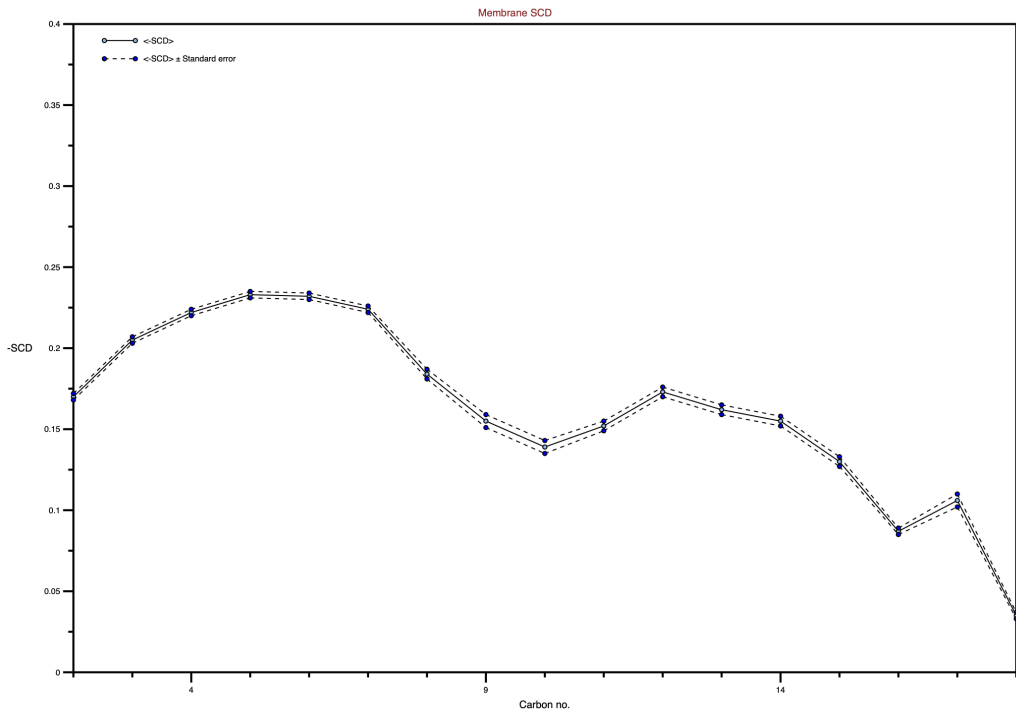
(c) *Parallel 3 of mrs-002 + membrane*



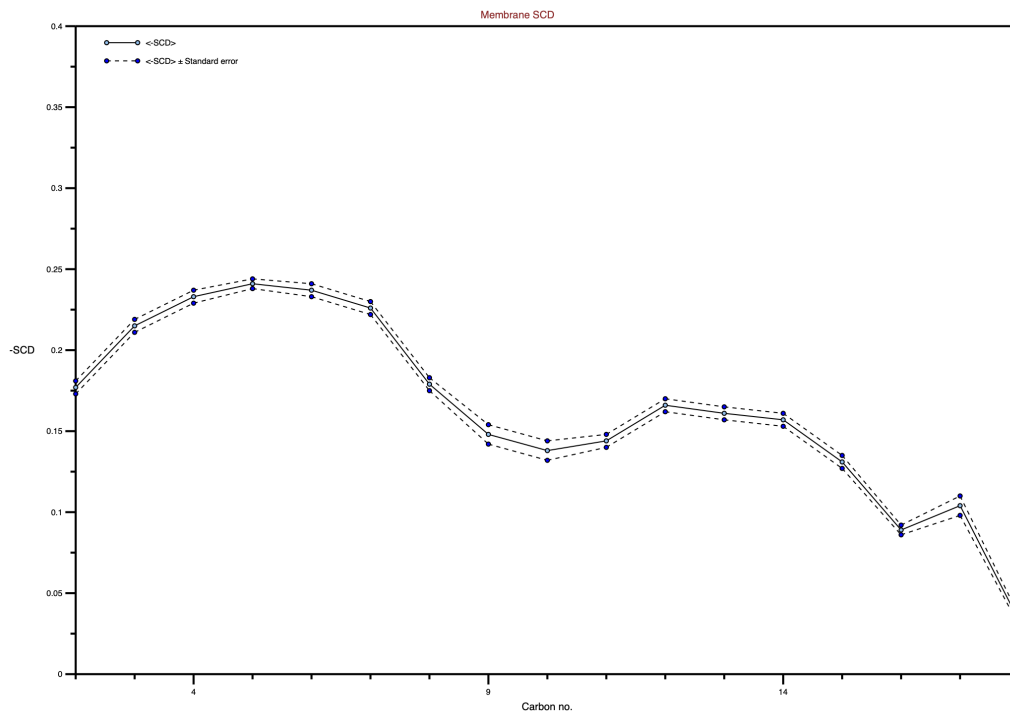
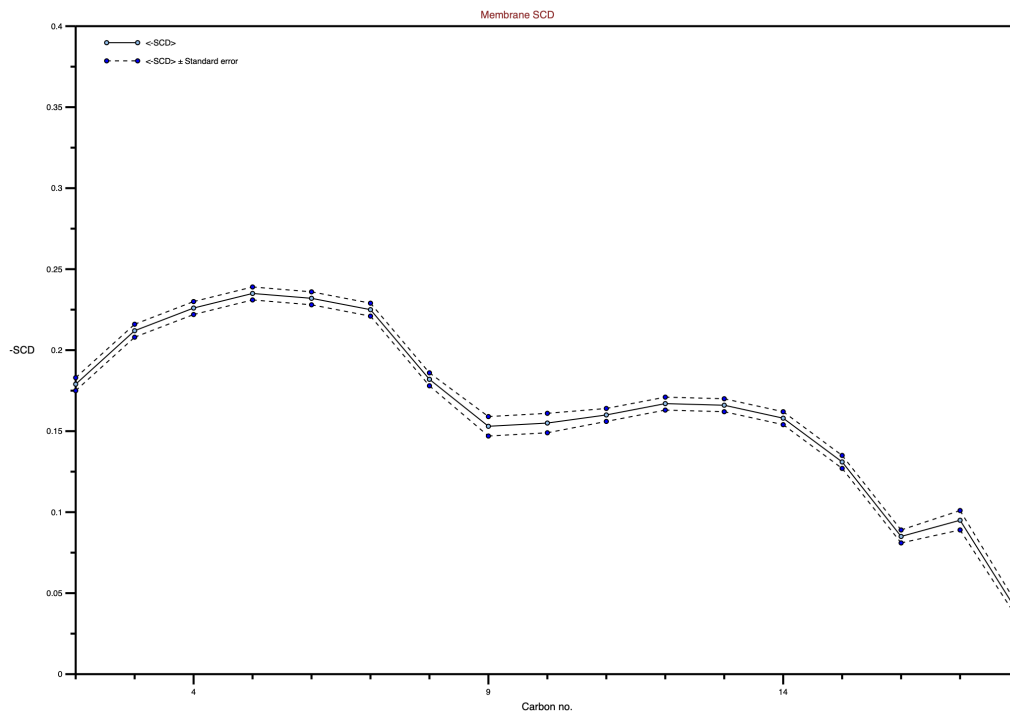
(d) *Parallel 1 of tkbs-013 + membrane*

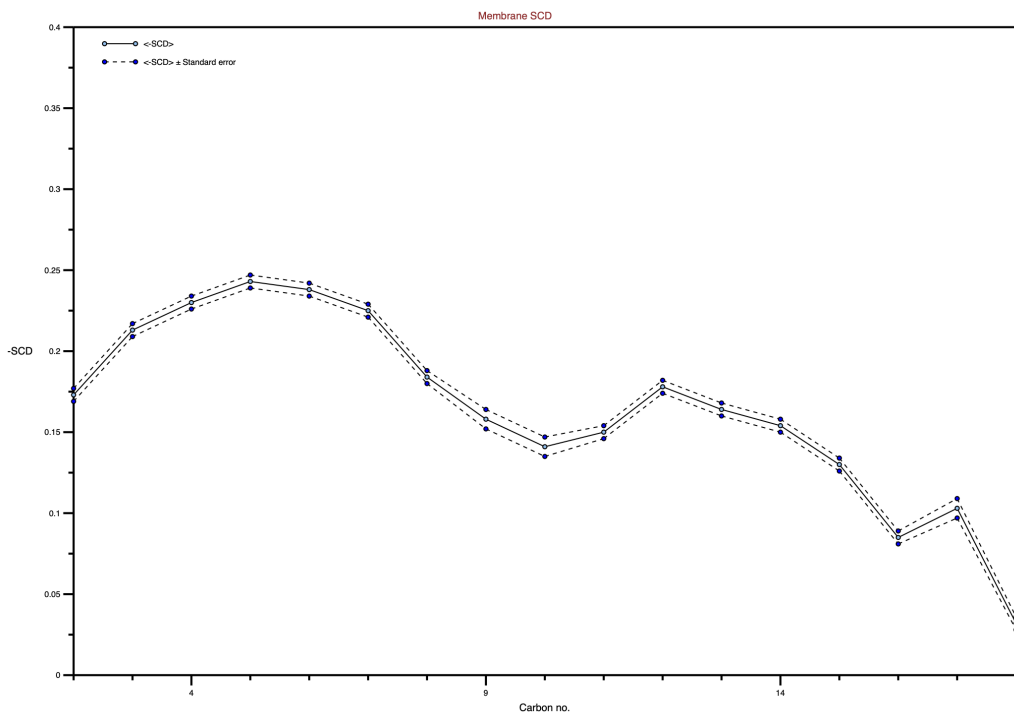


(e) Parallel 2 of tkbs-013 + membrane



(f) Parallel 3 of tkbs-013 + membrane

(g) *Parallel 1 of membrane-only*(h) *Parallel 2 of membrane-only*



(i) Parallel 3 of membrane-only

Figure G.3: Calculated S_{CD} values for all lipids in the membrane for all peptide+membrane and membrane systems.